



**REPUBLIC OF TURKEY
SELÇUK UNIVERSITY
GRADUATE SCHOOL OF NATURAL AND APPLIED SCIENCES**



**INVESTIGATION OF ELECTRICAL CONDUCTIVITY OF
NANOFIBERS (PAN) CONTAINING NANOPARTICLES
(GRAPHENE, COPPER, SILICA) PRODUCED BY
ELECTROSPINNING METHOD**

Olivier Mukongo MPUKUTA

Master of Science Thesis

Department of Mechanical Engineering

**April-2018
KONYA
All rights reserved**

THESIS ACCEPTANCE AND APPROVAL

A thesis study titled as “**Investigation Of Electrical Conductivity Of Nanofibers (PAN) Containing Nanoparticles (Graphene, Copper, Silica) Produced By Electrospinning Method**” was prepared and presented by Olivier Mukongo MPUKUTA. The highlighted thesis study was accepted by unanimity/ majority of votes on 12/04/2018 as a master’s thesis by the following jury and by the department of the mechanical engineering of the Graduate School of Natural and Applied Sciences of the Selcuk University.

Jurors

President

Assoc. Prof. Dr. Mahmut Deniz YILMAZ

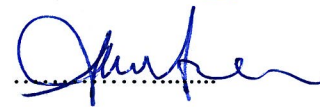
Advisor

Asst. Prof. Dr. Kevser Dincer

Member

Prof. Dr. Ahmet AVCI

Signature



I approve the above result

Prof. Dr. Mustafa YILMAZ
FBE Director


This thesis study was supported by the Scientific Research Projects coordination of the Selcuk University under grant No.17201017.

DECLARATION PAGE

I hereby declare that all information in this document has been obtained and presented in accordance with academic rules and ethical conduct. I also declare that, as required by these rules and conduct, I have fully cited and referenced all material and results that are not original to this work.

TEZ BİLDİRİMİ

Bu tezdeki bütün bilgilerin etik davranış ve akademik kurallar çerçevesinde elde edildiğini ve tez yazım kurallarına uygun olarak hazırlanan bu çalışmada bana ait olmayan her türlü ifade ve bilginin kaynağına eksiksiz atıf yapıldığını bildiririm.



Olivier Mukongo MpuKUTA

ABSTRACT

M.Sc. THESIS

INVESTIGATION OF ELECTRICAL CONDUCTIVITY OF NANOFIBERS (PAN) CONTAINING NANOPARTICLES (GRAPHENE, COPPER, SILICA) PRODUCED BY ELECTROSPINNING METHOD

Olivier Mukongo MPUKUTA

THE GRADUATE SCHOOL OF NATURAL AND APPLIED SCIENCE OF
SELÇUK UNIVERSITY
THE DEGREE OF MASTER OF SCIENCE IN MECHANICAL
ENGINEERING

Advisor: Assoc. Prof. Dr. Kevser Dincer
Co-advisor: Asst. Prof. Dr. Mehmet Okan Erdal

2018, 100 Pages

Jury

Prof. Dr. Ahmet AVCI
Assoc. Prof. Dr. Kevser DINCER
Assoc. Prof. Mahmut deniz YILMAZ
Prof. Dr. Ömer Sinan ŞAHİN
Asst. Prof. Dr. Yusuf ÇAKMAK

In this study, the electrical conductivity of electrospun polyacrylonitrile (PAN) nanofibers containing nanoparticles (graphene, copper, silica) has been investigated as a function of the incorporated nanoparticles content and the applied voltage during the electrospinning process. Different copper, graphene and silica nanoparticles contents (1, 3 and 5 wt. %) were added separately in the electrospinning solutions consisted of PAN and dimethylformamide. In addition, the dynamic viscosity of the obtained solutions was respectively analyzed and its effects on the diameter and electrical conductivity of the as-spun fibers were investigated. Afterwards, further investigations were conducted on the samples that exhibited the highest electrical conductivity values, notably: morphology, crystalline structure, hydrophobicity of the as-spun nanofibers. Taken together, the findings suggested that fibers with low content of nanoparticles led to higher electrical conductivities. When all the results were compared to each other, the highest electrical conductivity values were obtained with 1 wt. % of copper-based fibers and the electrical conductivity values were 1.38×10^{-2} S/cm and 2.83×10^{-2} S/cm for nanofibers produced at 15 kV and 20 kV, respectively. In other words, compared to pure PAN nanofibers, an increase of % 137.52 and % 1636.19 was observed in the electrical conductivity of fibers containing 1 wt. % of copper nanoparticles fabricated at 15 kV and 20 kV, respectively.

Keywords: Copper, Electrical conductivity, Electrospinning process, Electrospun nanofibers, Graphene, Hydrophobicity, Morphology, Nanoparticles, Polyacrylonitrile (PAN) nanofibers, Silica.

ÖZET

YÜKSEK LİSANS TEZİ

ELEKTRO-EĞİRME METODUYLA ÜRETİLEN NANOPARÇACIKLI (GRAFEN, BAKIR, SİLİKA) NANOFİBERLERİN (PAN) ELEKTRİKSEL ELETKENLİKLERİNİN ARAŞTIRILMASI

Olivier Mukongo MPUKUTA

**Selçuk Üniversitesi Fen Bilimleri Enstitüsü
Makine Mühendisliği Anabilim Dalı**

**Danışman: Doç. Dr. Kevser Dincer
İkinci Danışman: Dr. Öğretim üyesi Mehmet Okan Erdal**

2018, 100 Sayfa

Jüri

Prof. Dr. Ahmet AVCI

Doç. Dr. Kevser Dincer

Doç. Dr. Mahmut deniz YILMAZ

Prof. Dr. Ömer Sinan ŞAHİN

Asst. Prof. Dr. Yusuf ÇAKMAK

Bu çalışmada, elektrosprin ile üretilen nano partikül (grafen, bakır, silika)'lü poliakrilonitril (PAN) nanofiberlerin elektriksel iletkenliği, elektrosprin işlemi sırasında uygulanan farklı katkı oranlarındaki nanopartiküllerin ve voltajın bir fonksiyonu olarak araştırılmıştır. Farklı içeriklerdeki bakır, grafen ve silika nano partikül (% ağırlıkça 1, 3 ve 5)'lü, PAN ve dimetilformamidden oluşan elektrosprin solüsyonlarına ayrı ayrı ilave edilmiştir. Buna ilave olarak, elde edilen çözeltilerin dinamik viskozitesi sırasıyla analiz edilmiştir ve üretilmiş nanofiber çapı ve elektrik iletkenliği üzerindeki etkileri araştırılmıştır. Daha sonra, en yüksek elektrik iletkenlik değerlerinde olan numunelerin, özellikle morfoloji, kristal yapı ve hidrofobik/hidrofilik üretilmiş nanopartiküllü nanofiberlerin özellikleri araştırılmıştır. Sonuçlar birlikte değerlendirildiğinde, düşük miktarda nanopartikül içeren nanofiberlerdeki bulgular daha yüksek elektriksel iletkenliklere neden olduğu tespit edilmiştir. Tüm sonuçlar birbiriyle karşılaştırıldığında, en yüksek elektriksel iletkenlik değerleri ağırlıkça oranı % 1 olan bakır esaslı nanofiberin elektriksel iletkenlik değerleri 15 kV'da üretilen nanofiber için $1,38 \times 10^{-2}$ S/cm, 20 kV'da üretilen nanofiber için $2,83 \times 10^{-2}$ S/cm olarak bulunmuştur. Diğer bir deyişle, ağırlıkça % 1 bakır nanopartiküllü nanofiberin 15 kV'da üretilen nanofiberin elektriksel iletkenliği % 137.52, 20 kV'da üretilen nanofiberin elektriksel iletkenliği % 1636.19 olarak yükseldiği tespit edilmiştir.

Anahtar Kelimeler: Bakır, Elektriksel iletkenlik, Elektro-eğirme metodu, Grafen, morfoloji, Nanopartikül, Poliakrilonitril (PAN), Silika.

ACKNOWLEDGEMENTS

First of all, I would like to thank the almighty God for his mercy and wonderment that He has accomplished up to now in my life.

I would like to express my deepest gratitude to my advisor Assoc. Prof. Dr. Kevser Dincer, who gave me the golden opportunity to discover the outstanding properties of nanomaterials, shared her expertise with me very generously and I came to learn so many things on nanomaterials. Thank you for being so patient, and helping me improve. I'm eternally grateful for everything you've taught me.

Thanks are also due to Asst. Prof. Dr. Mehmet Okan Erdal, who is my second advisor and gave me much valuable advice in the early stages of this research.

I am particularly grateful to Assoc. Prof. Dr. Ilkay Özyaytekin for her valuable suggestions, discussions and her ongoing collaboration during this work.

I would like to thank my parents for their invaluable support for helping me to be where I am today. I never thank you enough for guiding me in the right direction.

I am indebted to my uncle Mathieu Sokolo Nkodia for helping me to accomplish my dream of becoming an engineer. You will always remain my mentor.

I owe my deepest gratitude to my love Grâce Kapinga, whose value to me only grows with age. Thank you for your patience.

I would like to express my deepest gratitude to the academic staff and administrative employees of the Selcuk University for their help and services.

Thanks are also due to all the people who helped us and were waiting to see their names be cited in this work, but maybe by inadvertence, we did not mention their names, we are thankful for their aspiring guidance, invaluable constructive criticism, and friendly advice for the success of this long scientist journey.

Thanks are also due to Selcuk University Scientific Research Projects Coordinator for supporting this master thesis financially under the project number 17201017.

Finally, I would like to thank Yurtdışı Türkler ve Akraba Topluluklar Başkanlığı (YTB) for the scholarship they provided throughout my graduate education.

Olivier Mukongo MPUKUTA

KONYA - 2018

TABLE OF CONTENTS

ABSTRACT	vi
ÖZET	vii
ACKNOWLEDGEMENTS	viii
TABLE OF CONTENTS	ix
SYMBOLS AND ABBREVIATIONS	xi
1. INTRODUCTION	1
2. LITERATURE SURVEY	3
3. THEORETICAL BACKGROUND OF ELECTROSPINNING PROCESS	8
3.1. Components and Basic Principles of Electrospinning Setup.....	8
3.2. Electrospinning Parameters	10
3.2.1. Solution parameters	10
3.2.1.1. Polymer molecular weight, concentration and solution viscosity	11
3.2.1.2. Surface tension.....	14
3.2.1.3. Conductivity.....	14
3.2.2. Process parameters.....	14
3.2.2.1. Applied voltage.....	15
3.2.2.2. Feed rate.....	16
3.2.2.3. Tip to collector distance.....	16
3.2.2.4. Diameter of pipette orifice	17
3.2.2.5. Collector effect	17
3.2.3. Ambient parameters	17
3.2.3.1. Humidity	18
3.2.3.2. Type of atmosphere	18
3.2.3.3. Pressure.....	18
3.2.3.4. Temperature	19
3.3. Characterization Techniques.....	19
3.3.1. Morphology characterization	19
3.3.2. Chemical characterization.....	20
3.3.3. Physical characterization	22
3.3.3.1. Four-point probe technique.....	22
4. MATERIALS AND METHODS	24
4.1. Materials	24
4.1.1. Polyacrylonitrile.....	24
4.1.2. Dimethylformamide.....	25
4.1.3. Copper nanoparticles	25
4.1.4. Silica nanoparticles	26
4.1.5. Graphene nanoparticles.....	27
4.2. Parameters Setting and Preparation of Electrospinning Solutions	28

4.2.1. Fabrication of pure PAN nanofibers	29
4.2.2. Morphology of electrospun pure PAN nanofibers.....	32
4.2.3. Fabrication of PAN/ Nanoparticles nanofibers.....	35
4.2.3.1. Fabrication of PAN/CuNPs nanofibers.....	36
4.2.3.2. Fabrication of PAN/Graphene NPs nanofibers.....	39
4.2.3.3. Fabrication of PAN/Silica NPs nanofibers	41
4.3. Viscosity of Electrospinning Solutions.....	43
4.4. Characterization Techniques.....	45
4.4.1. Scanning electron microscopy	45
4.4.2. X-rays diffraction.....	46
4.4.3. Contact angle setup	46
4.4.4. Four-point probe device.....	47
4.4.5. TGA and DSC setup	48
5. RESULTS AND DISCUSSION	50
5.1. Morphology and Diameters of Nanofibers	50
5.1.1. Morphology and diameters of pure PAN nanofibers.....	50
5.1.2. Morphology and diameters of composite nanofibers	51
5.2. Effect of Viscosity on Diameters of Electrospun Nanofibers.....	58
5.3. Electrical Conductivity of Nanofibers	60
5.3.1. Electrical conductivity of nanofibers containing copper nanoparticles.....	61
5.3.2. Electrical conductivity of nanofibers containing graphene nanoparticles	62
5.3.3. Electrical conductivity of nanofibers containing silica nanoparticles	63
5.3.4. Comparison of electrical conductivity of various composite nanofibers	64
5.3.5. Effect of fibers diameter on electrical conductivity.....	67
5.3.6. Effect of solution viscosity on electrical conductivity.....	68
5.3.7. Comparison of electrical conductivity values to the literature studies	70
5.3. Contact Angle Results	72
5.3.1. Contact angle of graphene nanoparticles -based nanofibers.....	72
5.3.2. Contact angle of silica nanoparticles-based nanofibers.....	73
5.3.3. Contact angle of copper nanoparticles-based nanofibers	74
5.4. XRD- Results	75
5.4.1. XRD patterns of pure PAN and Cu/PAN nanofibers	75
5.4.2. XRD patterns of pure PAN and graphene /PAN nanofibers	76
5.4.3. XRD patterns of pure PAN and SiO ₂ /PAN nanofibers	77
5.5. Thermal Analysis.....	78
5.6. Transmission Electron Microscopy	80
6. CONCLUSION AND RECOMMENDATIONS.....	82
6.1. Results.....	82
6.2. Recommendations.....	85
REFERENCES.....	86
CURRICULUM VITAE.....	100

SYMBOLS AND ABBREVIATIONS

Symbols

cm	: Centimeter
g/mol	: Gram per mol
μm	: Micrometer
H ₂ O	: Water
nC	: Nanocoulomb
wt.	: Weight
w/v	: Weight per volume
Fe ₃ O ₄	: Iron oxide
MnO ₂	: Manganese dioxide
N ₂ H ₅ OH	: Hydrazinium Hydroxide
SiO ₂	: Silica
T _p	: Peak derivative temperature, inflection point, °C
T _{onset}	: Onset temperature, °C
$\mu\text{S/cm}$: Micro Siemens per centimeter

Abbreviations

AFM	: Atomic Force Microscopy
AgCl	: Silver chloride
AgNPs	: Silver nanoparticles
ATR-FTIR	: Attenuated Total Reflection - Fourier-transform infrared spectroscopy
CA	: Contact angle
CNTS	: Carbon nanotubes
CS	: Chitosan
CuNPs	: Copper nanoparticles
DSC	: Differential scanning calorimetry
DMF	: Dimethylformamide
DMSO	: Dimethylsulfoxide
DMPC	: Dynamic moisture vapor permeation cell
DNA	: Deoxyribonucleic acid
EMImBr	: Ethyl-3-methylimidazolium bromide
FESEM	: Field emission scanning electron microscopy
Gr.NPs	: Graphene nanoparticles
NMR	: Nuclear magnetic resonance
MWCNT	: Multi-Walled Carbon Nanotubes
PA6	: Polyamide 6
PAN	: Polyacrylonitrile
PEO	: Poly (ethylene oxide)
PLA	: Polylactide
PMSQ	: Polymethylsilsesquixane
PS	: Polystyrene
PU	: Polyurethane
PVA	: Polyvinyl alcohol
PVC	: Polyvinyl chloride

PVP : Polyvinylpyrrolidone
SAXC : Small angle X-ray scattering
SEM : Scanning electron microscopy
SERS : Surface-enhanced Raman spectroscopy
TEM : Transmission electron microscopy
UV : Ultraviolet
WAXD : Wide angle X-ray diffraction
XPS : X-ray photoelectron spectroscopy
XRD : X-rays diffraction



1. INTRODUCTION

Nowadays, nanomaterials have drawn great attention of many researchers due to their outstanding potential properties compared to their bulk counterparts and that they can be used in various areas. Different methods are used in order to produce nanofibers such as drawing, template synthesis, phase separation, self-assembly, Chemical vapor deposition, wet chemical synthesis, electrospinning and so forth (Huang et al., 2003).

Until now electrospinning has been considered to be relatively the simplest process for producing materials at nano-scale. However, it has been stipulated that the physic behind it is not easy to understand since the properties of the electrospun nanofibers can be significantly influenced by many parameters. Electrospun nanofibers present unique properties such as a high surface area to volume ratio, lightweight, high porosity, good thermal, mechanical, electrical and flexibility properties. Materials obtained from electrospinning technique can find a wide range of applications, notably in electronic, medicine, environment protection, energy conversion and storage, and so on.

Over the past few decades, electrospun nanofibers containing nanoparticles are generating considerable interest in terms of features enhancement. The incorporation of nanoparticles into polymers can provide novel or improved performance to the resultant composite fibers (Cavaliere, 2015). Despite this interest, no one to the best of our knowledge has studied the effect of copper NPs, silica NPs and graphene NPs on the electrical conductivity of their respective PAN composite fibers. With this in mind, we tried to investigate the diameter and electrical conductivity of PAN polymer nanofibers containing nanoparticles mentioned above. To do so, 1 wt. %, 3 wt. % and 5 wt. % of each type of nanoparticles were mixed in PAN/DMF solutions.

The aim of this thesis is to produce composite nanofibers (copper NPs, silica NPs and graphene NPs) using electrospinning technique and to examine their electrical conductivity performance using the four-point probe technique.

Nowadays, the mankind is in search of alternative energy sources to prevent various harmful effects caused by the use of fossil fuels. We have to find an emission-free energy source for our Earth. For this reason, new kind of materials are required which will perform the same function with less energy consumption and emission-free than conventional materials. We believe that nanocomposite materials planned to be

produced in this thesis can be find their applications in solar cells (PV) and proton exchange membrane fuel cells (PEMFC).

In the light of previous investigations on electrospinning process, there is considerable concern about electrospinning parameters since they can have a direct effect on the properties of the resultant fibers. In this study, among different parameters: solution concentration, solution viscosity and applied voltage were picked out so as to investigate their effect on the diameter and electrical conductivity properties of the as-spun composite nanofibers.

This current thesis is divided into six chapters. The first chapter is the Introduction which presents the problematic of the study. The second chapter exposes the literature survey of electrospinning process and the resultant fibers properties. The third chapter presents the concept of electrospinning technique, its parameters and the advanced characterization techniques of nanomaterials. The fourth chapter describes the materials and methodology employed in order to fabricate and analyze fibers containing nanoparticles. The fifth chapter reports research findings and results discussion. The sixth chapter presents the key findings of the research and recommendations for the forthcoming researches.

2. LITERATURE SURVEY

There have been many articles published on understanding the basic concepts of electrospinning process and the effects of diverse parameters on the morphology and geometrical properties of electrospun nanofibers and the incorporation of nanoparticles in polymer solutions. Some of them are presented in the following paragraphs.

Zhang et al. (2014) have successfully synthesized a new kind of memory nanocomposite device, consisting of a thermoplastic Nafion polymer and Electrospun polyacrylonitrile-based carbonized membranes of fibers. They found that by calibrating the applied voltage during the fabrication process of the PAN solutions, a significant enhancement of electrical conductivity of the carbon fibers was observed, notably from 7.85 to 12.30 S/cm.

Tapasztó et al. (2011) have investigated the dispersion patterns of graphene and carbon nanotubes in ceramic matrix composites. The experiment results have demonstrated a remarkably different distribution motif for graphene and nanotubes in the ceramic matrix. They observed that a good dispersion was obtained with few-layer graphene flakes. However, carbon nanotubes were chiefly found in the small aggregate structures form.

Levitt et al. (2017) have fabricated twisted assemblies of polyacrylonitrile (PAN), polyvinylidene fluoride trifluoroethylene (PVDF-TrFe), and polycaprolactone (PCL) nanofibers via a modified electrospinning setup, consisting of a rotating cone-shaped copper collector, two syringe pumps, and two high voltage power supplies. They reported that the fiber diameters and twist angles were found to vary as a function of the rotary speed of the collector. In addition, the mechanical testing of the yarns demonstrated that PVDF-TrFe and PCL yarns present a higher strain-to-failure than PAN yarns, reaching 307% for PCL nanoyarns. What is more, for the first time, the porosity of nanofiber yarns was studied as a function of twist angle, the results showed that PAN nanoyarns are more porous than PCL yarns.

Guclu et al. (2016) have studied the pore size and the strengthness of membrane manufactured via simultaneous electrospinning of PAN and polysulfone (PSU). The results of the study showed that polysulfone fibers had higher pore size than PAN fibers membranes. Nevertheless, for polysulfone fibers lower temperatures were sufficient so as to improve mechanical features against fiber rupture. It is of interest to

note that the pore size of PAN fiber membranes was around 0.8 μm and 185°C was sufficient to improve the strength of polysulfone fibers against rupture.

Khan et al. (2017) have evaluated thermal behaviors of electrospun polyacrylonitrile (PAN) fibers incorporated with graphene nanoplatelets and multiwall carbon nanotubes (MWCNTs) using DSC and TGA. They have found that pristine PAN fiber presented a glass transition temperature (T_g) of 104.09°C. Their findings revealed that the glass transition temperatures of the composite fibers increased with an increase of nanoparticles contents (both for graphene and MWCNTs). But a further increase in nanoparticles contents led to the decrease of glass transition temperatures.

Tai et al. (2015) in their work have fabricated a lightweight and compressible sponge made of carbon-silica nanofibers via electrospinning process. Their experiment revealed that the fabricated sponge had high porosity ($> 99\%$) and presented ultra-hydrophobicity and superoleophilicity, as results the fabricated materials have been found to be favorable to be used as oil adsorbent.

Pant et al. (2011) have studied the effect of polymer molecular weight on the fiber morphology of electrospun mats. It was found that the prepared fibers were smooth and uniform in diameter along their lengths. In addition, their results revealed an increase in the wettability, mechanical strength and in the BET area as well as a decrease of the pore size in the electrospun mats. These phenomena were due to the presence of the double layer of two distinct fibers in the mats.

Cramariuc et al. (2013) examined the fiber diameter in electrospinning process. In their work, they have controlled two process parameters, namely applied voltage and polymer solution flow rate to reach the predetermined fiber diameters. At greater distances from the tip, the diameter of the fiber can be carried out as function of the density of the solution, the flow rate of the solution, the applied voltage and the distance from the tip. However, near the collector, the fiber diameter can be carried out as function of the surface tension of the electrospinning solution, the dielectric permittivity, the solution flow rate as well as the intensity of the electric current.

Ráčová et al. (2014) have studied the influence of copper ions on mechanical properties of PVA-based nanofiber textiles fabricated by electrospinning process. According to the results of their experiment, they have that the addition of copper ions caused an increase of the strength and stiffness of the resultant nanofibers.

It has been reported that the selection of a desirable solvent or solvent system as the carrier of a particular polymer is fundamental for the optimization of

electrospinning. Luo et al. (2010) have developed a novel method of selecting solvents for polymer electrospinning. To do so, 28 solvents diversely positioned on the Teas graph were examined for the solubility and electrospinnability or making polymethylsilsesquixane (PMSQ) solutions. According to the results of their study, it was observed that suitable electrospinning solutions cannot be necessarily obtained by using solvents with high solubility. The results revealed that for a PMSQ solutions of the same concentration, the solution were found to present a good spinnability in a solvent with partial solubility than in solvent with high solubility.

There have been many attempts made by researchers to incorporate the metal nanoparticles whether in the solutions which will be electrospun or in the electrospun nanofibers in order to reach some required characteristics of materials in different fields of science.

Adding conductive additives to electrospinning solutions has been proven to increase the conductivity of electrospun membranes. Savest et al. (2016), they have investigated the effect of ionic liquids on the conductivity of electrospun polyacrylonitrile membranes. In their study three different ionic liquids namely BMImCl, EMImBr and EMImTFSI were used as additives in PAN solutions wherein the DMF and DMSO were used as solvents. They reported that with small increasing of the concentration of ionic liquids the membrane conductivity has significantly increased comparing to the membranes obtained from the pure PAN in DMF and PAN in DMSO solutions.

Heikkilä and Harlin (2009) examined the effect of the salt as conductive additive and CNTs as filler on the electrospinning process with polyacrylonitrile. They tried to vary some electrospinning parameters such as voltage, distance and nozzle size then they analyzed the quality of the electrospun web and fibers, as well as the functioning of the process. They reported that although the PAN and PAN/Salt solution presented nearly the same viscosity range but the PAN/Salt solution produced slightly larger fibers because the increased conductivity has an effect of enhancing the mass flow rate. In addition, they observed that the higher conductivity of the PAN/Salt solution increased the instabilities in the electrospinning process. Moreover, compared to the conductivity of PAN/CNT solution, the PAN/Salt solution presented a higher viscosity.

Zhang et al. (2009) have made an investigation on fabrication and property analysis of electrospun polyacrylonitrile nanocomposite fibers reinforced with Fe₃O₄ nanoparticles. The experiments results demonstrated that slight changes in operating

parameters may lead in considerable changes in the fiber morphology. From SEM analysis they concluded that the beads can be avoid either by rising the solution concentration, distance and applied voltage to a certain level or by the reduction of the flow rate. The incorporation of Fe₃O₄ nanoparticles into the polymer matrix has a significant effect on the crystallinity of PAN and a strong interference between PAN and Fe₃O₄.

Crosslinked electrospun polyvinyl alcohol nanofibers coated by antibacterial copper nanoparticles were prepared and investigated by Rezaee and Moghbeli (2014). In their study, the poly (vinyl alcohol) nanofibers were prepared via electrospinning of concentrated PVA solutions. Then, in order to enhance their resistance against the moisture the nanofibers were crosslinked using glutaraldehyde as crosslinking agent in the presence of hydrochloride acid. In addition, the crosslinked nanofibers were coated by copper nanoparticles using electrospraying technique. The effect of the stabilizer concentration (0.001 and 0.005 M) and reduction temperature (25 and 75°C) were investigated on the copper nanoparticle dispersion in the media using UV-visible spectroscopy. They reported that UV spectra exhibited the most stable copper nanoparticle dispersion prepared using PVA stabilizer at higher reduction temperature (70°C) and the lower salt concentration (0.001M). This colloidal dispersion with 70 nm mean size was used to cover the crosslinked nanofibers via electrospraying process.

The effect of silver nitrate quantity on the morphology, conductivity and mechanical properties of PAN/AgNPs composite nanofibers were investigated by Demirsoy et al. (2015). They reported that bead-free and uniform composite fibers with diameters ranging from 499-515 nm were successfully electrospun. The results of the investigation revealed that the bursting stress and bursting elongation of the neat PAN nanofibers were lower than the PAN/Ag composite nanofibers. Moreover, the conductivity of the produced nanowebs was enhanced up to around 10⁻⁸ S/cm when the silver nanoparticles were dispersed in the solution.

An investigation on the preparation and characterization of gelatin nanofibers containing silver nanoparticles was done by Jeong and Park (2014). In their research, the gelatin nanofibers containing AgNPs were prepared by electrospinning process. After examination, the average diameters of the gelatin nanofibers was 166.52 ± 32.72 nm, which decreased with AgNO₃.

Ji and Zhang (2008), worked on ultrafine polyacrylonitrile/silica composite fibers via electrospinning technique. Techniques such as SEM, TEM, ATR-FTIR, and

DSC were used to analyze the produced fibers. They reported that beads were formed and at silica contents higher than 2 wt. %, agglomeration of silica was observed in nanofibers. Furthermore, they observed that the addition of silica nanoparticles also changes the thermal properties of PAN/silica nanofibers.

The electrical conductivity and morphology of MWCNT-MnO₂ within PVA nanofiber were investigated by Zamri et al. (2011). It was reported that the presence of MWCNT-MnO₂ nanocomposites inside the PVA nanofiber was detected by TEM images. They discovered that the sizes of the pores of the nanofiber composite were smaller compared to those in the neat PVA nanofiber. Moreover, they highlighted that the PVA/MWCNT-MnO₂ nanofiber composites showed an enhanced electrical conductivity of $6.99 \times 10^{-6} \text{ Scm}^{-1}$ compared to $5.26316 \times 10^{-6} \text{ Scm}^{-1}$ for PVA/ MWCNT without MnO₂ and $1.25 \times 10^{-15} \text{ Scm}^{-1}$ for neat PVA.

Dung et al. (2016) have conducted research on the effect of copper salt concentration on electrospun CuO nanofibers for gas sensing application. They highlighted that the 12 g-device shows the best response to ethanol and LPG meanwhile the 6 g-device shows the best response to hydrogen. The devices show a good selectivity to hydrogen at both working temperatures of 350 and 400 °C. The best device shows a percentage response of 170 % to 1000 ppm hydrogen at 250 °C.

3. THEORETICAL BACKGROUND OF ELECTROSPINNING PROCESS

Contrary to conventional fiber spinning processes (wet spinning, dry spinning, melt spinning, and gel spinning) which can produce polymers fibers with diameters down to micrometer range, electrospinning technique is a process that is used to produce polymer fibers with diameter in the nanometer range (Frenot and Chronakis, 2003).

Electrospinning technique is considered as a variant of the electrostatic spraying (or electrospraying) process, as both methods use high-voltage to induce the formation of liquid jets. In electrospraying process, small droplets or particles are produced as a consequence of the break-up of the electrified jet, whereas a solid fiber is collected as the electrified jet is stretched in electrospinning (Karakas, 2015).

Electrospinning is recognized as a novel and efficient production process that can be employed to piece together fibrous polymer mats consisted of fiber diameters ranging from several microns down to fibers with diameter lower than 100 nm (Frenot and Chronakis, 2003). So far, the electrospinning process is considered to be the only process that can be further promoted for mass fabrication of one-by-one continuous nanofibers from different types of polymers (Huang et al., 2003).

3.1. Components and Basic Principles of Electrospinning Setup

A simple electrospinning setup consists of three major components: a high-voltage power supply, a collector, and a spinneret (Ding and Yu, 2014). A basic setup of electrospinning process is illustrated in Figure 3.1 below.

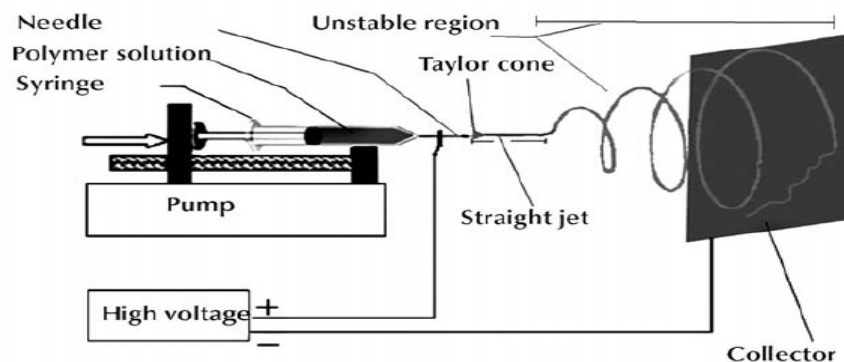


Figure 3.1. Electrospinning setup (Haghi, 2011)

Although the setup for electrospinning seems to be simple, it has been reported that the physics behind it is extremely intricate and very new to researchers and requires the understanding of electro-statics, fluid rheology, and polymer solution properties (Ding and Yu, 2014).

The electrospinning technique is basically different from air or other mechanically governed spinning processes by the fact that the extrusion force is caused by the interference between an externally applied electric field and the charged polymer fluid. A higher applied voltage corresponds to a highly charged polymer solution. Therefore, two predominant forces (the electrostatic repulsion force and surface tension) come across the solution droplet at the tip.

Undergoing these electrostatic solicitations, a cone referred to the Taylor cone is observed when the intensity of the applied voltage increases up to a threshold where the hemispherical surface of the solution starts to elongate (Huang et al. (2003); Ding and Yu (2014)). An additional increase of the electric field leads the repulse electrostatic force to overpower the surface tension as results the charged jet of the solution is ejected from the tip of the Taylor cone (Huang et al. (2003); Frenot and Chronakis (2003); Karakaş (2015)).

The demeanor of the as-spun jet comprehends three main regions: the occurrence of the Taylor cone, the kicking out of the straight jet and the unstable whipping region. The Figure 3.2 shows the behavior of the electrospun jet. A Taylor cone is a consequence of the interference of electrical charges on the polymer solution with external electric field. Since the Taylor cone undergoes a high applied voltage, an instability is created in the droplet and leading to the creation of single fluid jet. Beyond the straight path, the thrown fluid jet reaches the unstable region which is referred to whipping jet (Karakaş, 2015).

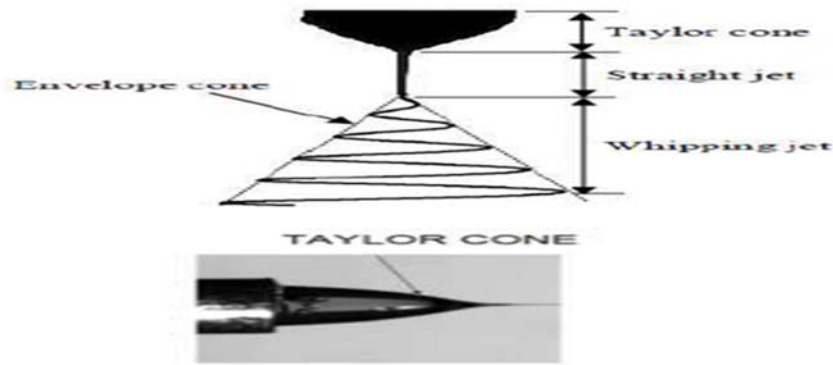


Figure 3. 2. Behavior of the electrospun jet (Huang et al., 2003)

3.2. Electrospinning Parameters

The electrospinning process is controlled by several parameters, which can affect the processing of polymer solutions into nanofibers. These parameters are basically regrouped into three categories: solutions parameters, governing variables, and ambient parameters. Solution parameters encompass viscosity, molecular weight, conductivity, molecular weight distribution, elasticity, and surface tension, and process parameters encompass electric field at the capillary tip, hydrostatic pressure in the capillary tube, feed rate and concentration, and the gap (distance between the tip and the collecting screen), and ambient parameters include temperature, humidity, and the air velocity in the electrospinning chamber (Huang et al. (2003); Frenot and Chronakis (2003); Ding and Yu (2014)). Since all these parameters significantly affect the morphology and structure of the electrospun nanofibers, it is possible to obtain nanofibers with the desired diameters and morphologies by controlling those parameters (Karakas, 2015).

In recent years, the spinnability of different polymers in solution form or molten form was investigated by many researchers. Therefore, the electrospinning parameters and their various effects on the nanofiber morphology and structure are summarized below.

3.2.1. Solution parameters

The electrospinning process and its resultant fiber features are mainly affected by the properties of the polymer solution. For instance, the surface tension can influence

the occurrence of beads along the fiber length. The solution viscosity play a significant role in extending the elongation of the solution. This will in turn have an effect on the diameter of resultant electrospun fibers (Ramakrishna, 2005).

3.2.1.1. Polymer molecular weight, concentration and solution viscosity

The molecular weight is among the different parameters that affect the solution viscosity. It has generally reported that a polymer of high molecular weight disbanded in a solvent presents a higher viscosity than a solution of the same polymer having a low molecular weight (Ramakrishna, 2005). A polymer with a good enough molecular weight and a solution having a sufficient viscosity are generally required in order to produce fibers via electrospinning technique (Ramakrishna, 2005). As shown in Figure 3.3, for the same concentration, when a polymer with low molecular weight is used, the production of beads occurs instead of fibers. An increase in the molecular weight leads to smooth fibers, meanwhile fibers with a considerable diameter are obtained for a polymer with high molecular weight (Karakaş, 2015).

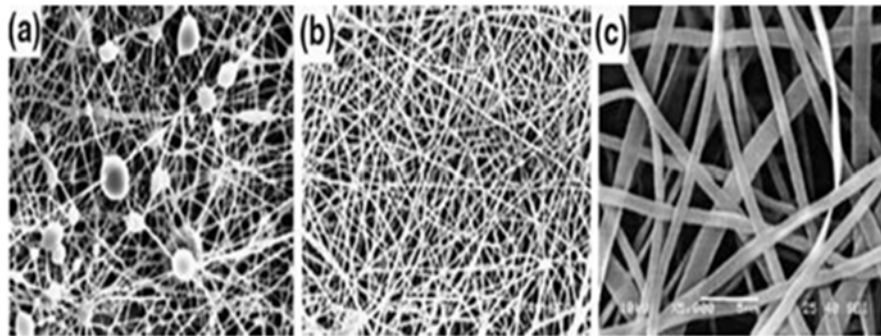


Figure 3.3. SEM photographs showing typical structure in the electrospun polymer for various molecular weights a) 9.000-10.999 g/mol, b) 13.000-23.000 g/mol, c) 31.000- 50.000 g/mol (solution concentration 25 wt. % (Koski et al., 2004)

The fiber diameter is recognized to be related to the electrospinning process. It has been reported that fibers diameter depends on the jet size and on the content of the polymer in the jets. It has been reported that during the traveling of a solution jet from the pipette onto the metal collector, the primary jet may or may not be split into multiple jets, resulting in different fiber diameters as can be observed in Figure 3.4. As long as no splitting is involved, the solution viscosity was found to be one of the most significant parameters influencing the fiber diameter. The higher the polymer

concentration the larger the resulting nanofiber diameters will be. In fact, Deitzel et al. (2001) mentioned that a rise in the polymer concentration leads to a rise in the fiber diameter according to a power law relationship.

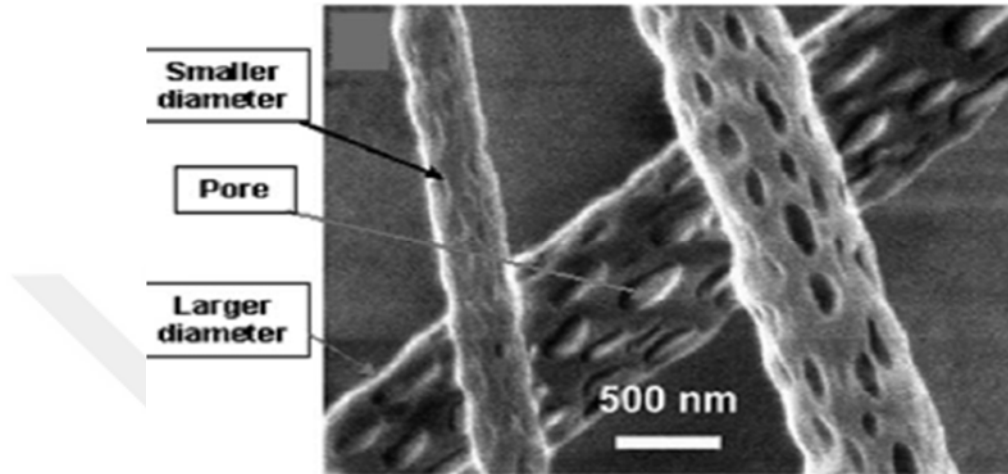


Figure 3.4. PLLA nanofibers with different diameters and pores (Huang et al., 2003)

Defects such as pores and beads may occur in electrospun polymer nanofibers. It has been found that the polymer concentration also affects the formation of the beads (Jaeger et al., 1996). Fong et al. (1999) stated from their experiment that higher polymer concentration led to the formation of fibers with fewer beads. In addition, they have reported how the morphology of the fiber membranes has been altered by increasing the polymer concentration and therefore the solution viscosity. Figure 3.5 and Figure 3.6 show the effect of polymer concentration and the solution viscosity on the electrospun fibers.

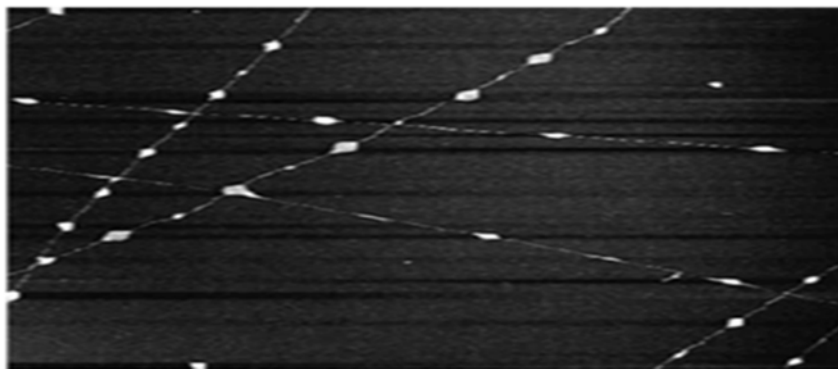


Figure 3.5. AFM image of electrospun PEO nanofibers with beads (Fong et al., 1999; Huang et al., 2003)

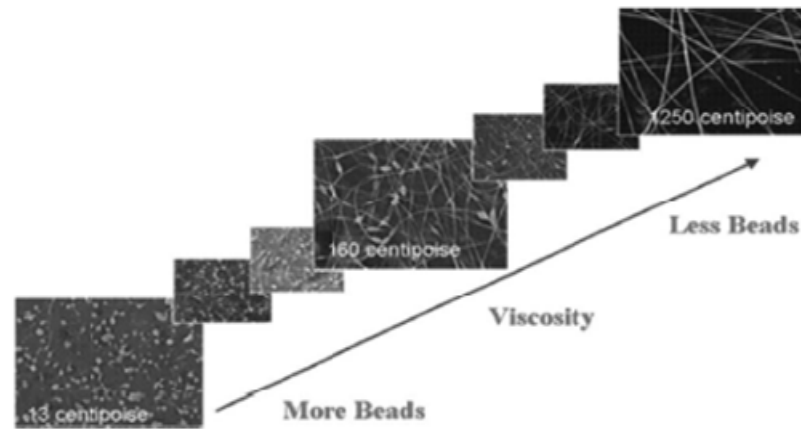


Figure 3.6. SEM photographs of electrospun nanofibers from different polymer concentration solutions (Fong et al., 1999)

It was reported that solution concentration and fiber diameter are linked in a power-law relationship. Hence, a rise in solution concentration leads to an increase in fiber diameter as can be observed in Figure 3.7 (Ding and Yu, 2014). Similar results have also been reported about other polymer fibers such as polyurethane (Cramariuc et al. (2013)), polylactide (Savest et al. (2016)), polyvinyl chloride (PVC), polyamide 6 (PA6), and chitosan (CS) (Ding and Yu, 2014), which indicated the significant role of polymer concentration and viscosity in controlling the structure of electrospun fibers.

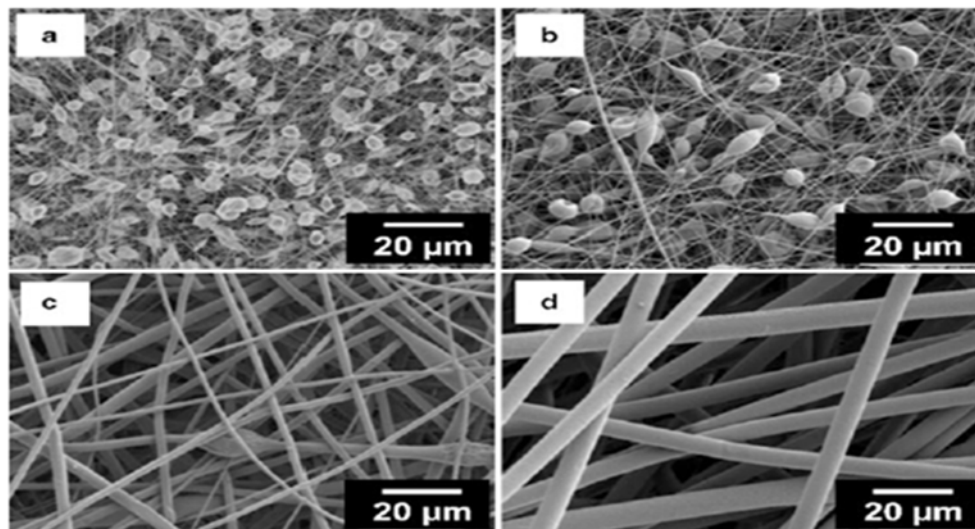


Figure 3.7. FE-SEM images of electrospun PS fibers from various concentrations of (a) 5 wt. %, (b) 10 wt. %, (c) 20 wt. %, and (d) 30 wt. % (Ding and Yu, 2014)

3.2.1.2. Surface tension

Surface tension was recognized to be very important in the electrospinning process. Therefore, attention must be paid when selecting a solvent to be used in the solution preparation, due to the fact that the surface tension is solvent composition dependent. A charged solution is needed so as the electrospinning process to take place (Ding and Yu, 2014). Generally speaking, a solution with a high surface tension impedes the process of electrospinning to occur. That is to say, a solution with a high surface tension leads to the instability of the jets as well as the creation of sprayed droplets.

The surface tension of the solution is a very important parameter due to the fact that the production of droplets, beads, and nanofibers is linked to it. It was reported that a solution having a lower surface tension allows the fabrication of fibers at a lower electric field. Such phenomena were encountered during the fabrication of PS, CS, PEO and PVC. In summary, keeping all variables unchanged, the surface tension delimits the range values in the electrospinning process (Ding and Yu, 2014).

3.2.1.3. Conductivity

A solution with a sufficient charge helps the repulsive forces within the solution to overthrow its surface tension and therefore to commence the electrospinning process. The facility of the solution to convey charges determines the outcomes of the electrospinning process that may be an eventual stretching or a drawing of the solution jet (Ding and Yu, 2014). Typically, fibers with smaller diameter are formed by increasing the electrical conductivity of the solution. Notwithstanding, uniform fibers with or without beads may be obtained by using solution with a low electrical conductivity (Ding and Yu, 2014). The existence of ionic salts in the solution, the types of polymer and solvent used in the solution preparation are the very important parameters that affect the conductivity of the electrospinning solution (Karakaş, 2015).

3.2.2. Process parameters

External factors that influence the stability of the solution jet in electrospinning process are referred as process parameters. This category encompasses the applied

voltage, the temperature of the solution, the shape of the collector, the inner diameter of the needle, the feed rate and the gap between the needle tip and the collector. It was reported that the effects of these parameters on the morphology of the electrospun fibers are less significant than that of the solution parameters (Ramakrishna, 2005).

3.2.2.1. Applied voltage

Applied voltage is an important parameter in the electrospinning process. The use of high voltage allows the motion of the necessary charges, together with the external electric field will trigger the electrospinning process once the surface tension is overcome by the electrostatic force (Ding and Yu, 2014).

It has been reported that applied voltage and the resulting electric field both act on the jet acceleration and on the way of stretching the solution jet. Researchers have reported that higher voltage leads to the formation of fibers with smaller diameters and helps the solvent to evaporate quickly, therefore, resulting in drier fibers (Buchko et al. (1999); Megelski et al. (2002)). Electrospinning of low viscosity solution at higher voltage may encourage the occurrence of secondary jets. In consequence, fostering the decrease of fiber diameters (Demir et al., 2002).

The flight time of the electrospinning jet may have also an influence on the diameter of the as-spun nanofibers. When the flight time is long, fibers take more time to stretch and elongate before it is deposited on the collector. Researchs have demonstrated that the flying time of the solution jet rises when a lower applied voltage and weaker electric field are used during the production of fibers. In this case, (Yang et al., 2004) reported that a voltage close to the critical voltage for electrospinning may be favorable to obtain finer fibers.

It is of interest to note that not only the high voltage may affect the physical appearance of the as-spun polymer nanofibers but also its crystallinity. The crystallinity of the fibers can be improved by using a high electrostatic field, which results in more ordered molecules during the electrospinning process. However, above a certain voltage, the crystallinity of the fiber can be reduced. Furthermore, given sufficient flight time, the fabrication of fibers at higher voltage enhances the crystallinity of the electrospun fibers (Ramakrishna, 2005). In addition, it should be noted that the diameter of the fibers can be influenced by the applied voltage. However, the level of diameter

change depends also on parameters such as the concentration of the solution as well as the distance that separates the needle from the collector.

3.2.2.2. Feed rate

The feed rate is recognized to be among the key parameters in the electrospinning process due to the fact that a sufficient flow rate is required in order to maintain the stability of the Taylor cone (Ding and Yu, 2014). It was reported that the increase of the feed rate leads to an increase of fiber diameter or beads size (Ramakrishna, 2005). However, it was pointed out that there is a limit to the increase in the diameter of the fiber due to higher feed rate (Rutledge et al., 2000).

A higher flow rate is not recommended during the electrospinning process. This can be justified by the long time that takes the solution jet to dry (Ramakrishna, 2005). In order to give the solvent more time to evaporate a lower feed rate is more desirable (Yuan et al., 2004).

3.2.2.3. Tip to collector distance

As we have seen from the previous section, the flight time of the jet in electrospinning is a very important aspect to consider. Parameters such as flight time and the intensity of the electric field influence on the electrospinning process as well as on the resulting fibers. The flight time and the intensity of the electric field are directly affected by the change of the tip-collector distance. (Ding and Yu, 2014). Hence, an optimum gap between the needle tip and the collector is required. This statement may be justified by firstly allowing the fibers to have a sufficient time to dry and secondly to avoid the formation of beads when either the needle tip is too close or too far to the collector (Min et al., 2004).

On the other and, fibers with bigger diameters may be collected by using longer distance between the tip and collector. This phenomenon was explained as consequence of the diminution of the strength of the electrostatic field, which leads to poor stretching of the fibers (Bhardwaj and Kundu, 2010). Therefore, it clear to keep in mind that there is an optimum tip-collector distance which favors the evaporation of solvent for each electrospinning process (Ramakrishna, 2005).

3.2.2.4. Diameter of pipette orifice

It has been reported that even though electrospinning technique is simple but the technique behind it is not easy to understand due to the fact that the resultant fibers are influenced by many parameters. Like other work parameters, it was observed that fibers with a few number of beads were produced by using a needle with a smaller inner diameter (Mo et al., 2004). It was also reported that the decrease in the internal diameter of the needle was also found to reduce the diameter of the electrospun fibers. Nonetheless, a needle with an extremely small inner diameter do not allow the solution droplet to be extruded from the tip of the needle (Ramakrishna, 2005).

3.2.2.5. Collector effect

In order to initiate the electrospinning process an electric field is required between the source and the collector. It was reported that collector should be fashioned with conductive materials so as to guarantee that the potential difference between the supplier apparatus and the collector can be maintained constant during the electrospinning process (Ramakrishna, 2005). It has been proved that a conductive collector helps to efficiently dissipate the charges on the fibers and therefore to allow a good distribution of the fibers on the collector (Liu and Hsieh, 2002).

Whether or not the collector is static or moving also have an effect on the electrospinning process. Where a rotating collector was used it was observed that the solvent took more time to evaporate and also helped to increase the rate of evaporation of the solvents on the fibers. As results, the morphology of the fibers was enhanced where distinct fibers were required (Wannatong et al., 2004).

3.2.3. Ambient parameters

The influence of ambient parameters on the electrospinning process was not widely examined by several researchers. Any interaction between the surrounding and the polymer solution may result in changing the morphology of the electrospun fiber. It is well known that the fabrication of fibers via electrospinning process is also affected by the external electric field. Whence, any changes around the electrospinning device may disturb the electrospinning process (Ramakrishna, 2005).

3.2.3.1. Humidity

The humidity of the electrospinning vicinity may have an influence on the polymer solution during electrospinning. It was reported that at high humidity, it is likely that water condenses on the surface of the fiber when electrospinning is carried out under normal atmosphere (Ding and Yu, 2014). As a result, this may have an influence on the fiber morphology especially polymer dissolved in volatile solvents (Megelski et al., 2002). It is clearly showed from the open literature that increasing the humidity of the electrospinning vicinity enhances widely the porous structure. Further increasing the humidity, the depth, diameter, and number of the pores start to saturate. (Casper et al., 2004). Moreover, the humidity has an effective effect on the evaporation of the solvent since it determines the rate of evaporation of the solvent in the solution. When a volatile solvent is used at an extremely low humidity, the electrospinning process lasts only for a few minutes before the orifice tip is clogged. This phenomenon can be induced by a fast evaporation rate of the solvent compared to the time made to leave the tip of the orifice (Ding and Yu, 2014).

3.2.3.2. Type of atmosphere

The air composition in the electrospinning vicinity affects the fabrication of fibers. Researchs have revealed that gases behave in a different manner in the presence of high electrostatic field. For instance, from the open literature it was found that a gas such as helium breaks down. In such conditions, the electrospinning of the polymer solution becomes impossible. However, it was shown that when a gas with higher breakdown voltage is used such as Freon 12, the resultant fibers have twice the diameter of those electrospun in air keeping all other conditions unchanged (Baumgarten, 1971).

3.2.3.3. Pressure

It has been demonstrated that when the pressure is below atmospheric pressure, the polymer solution in the syringe will have a greater tendency to flow out of the needle and therefore causing unstable jet initiation. Generally, lowering pressure neighboring the solution jet does not ameliorate the electrospinning process. It has been

reported that with a very low pressure, the fabrication of fibers via electrospinning is not possible as a consequence of the direct discharge of the electrical charges (Ramakrishna, 2005).

3.2.3.4. Temperature

The viscosity of the solution decreases with the increase of the temperature while the increase of the temperature improves the rate of evaporation of the solvent (Demir et al., 2002). It is of interest to note that the use of a high temperature can result in a loss of functionality of the substance when biological substances such as enzymes and proteins are added to the solution for the electrospinning operation (Ramakrishna, 2005).

3.3. Characterization Techniques

Nowadays, there are many characterization techniques which help scientist and researchers to examine in depth the properties of nanomaterials. Some of them will be presented in the following sections.

3.3.1. Morphology characterization

In order to characterize the geometric properties of nanofibers such as fiber diameter, diameter distribution, fiber orientation and fiber morphology (e.g. cross-section shape, density and surface roughness) numerous techniques can be used, namely Scanning Electron Microscopy (SEM), Field Emission Scanning Electron microscopy (FESEM), Transmission Electron Microscopy (TEM) and Atomic Force Microscopy (AFM) (Huang et al., 2003). However, it is necessary to bear in mind that each microscopy has its own unique pros and cons. Among different geometrical characterization techniques mentioned above, SEM, and TEM will be set forth in following paragraphs.

3.3.1.1. Scanning electron microscopy (SEM)

A focused beam of high level energy is employed in SEM setup so as to beget images of a sample by generating several signals on its surface. SEM technique has an advantage of possessing the ability of magnifying objects about 10 times up to 300 000 times with high resolution. Great information (such as crystalline structure, morphology, and chemical composition) concerning the sample are provided by the signals.

Scanning electron microscopy is an apparatus that is employed to investigate materials with size ranging from 1 micron to 1 nanometer. Contrary to the light microscopy which can generate images up to 200 nm as the best resolution, SEM can characterize materials with about 10 nm as high resolution (<https://bioaccent.org>).

3.3.1.2. Transmission electron microscopy (TEM)

Transmission electron microscopy is recognized as a powerful tool for characterizing several types of materials. Transmission electron microscopy has great advantages over other microscopy techniques, in that its ultrahigh imaging resolution can reach several angstroms on modern instrument, or even sub-angstrom level but also structural information since the electrons penetrate through the thin samples, and chemical compositional information due to the interaction of high-energy electrons with core electrons of the sample (Luo, 2015). In addition, the use of TEM does not require the sample in a dry state as that of SEM. Hence, electrospun nanofibers from a polymer solution can be directly observed under TEM (Ramakrishna, 2005). Compared to other microscopy techniques, however, the samples for transmission electron microscopy must to be thin enough, typically thinner than 100 nm, so as to be penetrate by electrons, while there is no such requirement for other microscopies (Luo, 2015).

3.3.2. Chemical characterization

Techniques such as Nuclear Magnetic Resonance (NMR) and Fourier Transform Infra-Red (FTIR) are commonly used to investigate the molecular structure of nanofibers (Huang et al., 2003).

Supramolecular structure describes the architecture of the macromolecules in a nanofibers, and can be analyzed by Optical birefringence , Wide Angle X-ray Diffraction (WAXD), Small Angle X-ray Scattering (SAXC) as well as Differential Scanning Calorimeter (DSC) (Ramakrishna, 2005) .

Generally, techniques such as XPS, FTIR-ATR analyses, and Water Contact Angle measurement are used to examine the chemical properties of nanofibers surfaces. What is more, the hydrophilicity of the nanofibers surface helps to investigate the chemical properties of nanofibers (Huang et al., 2003).

Among different chemical characterization techniques mentioned above, contact angle will be presented in following section since it will be used in this thesis.

3.3.2.1. Water contact angle analysis

A wetting surface is analyzed by the contact angle (CA) technique. A contact angle is defined as the angle between the tangent to the liquid-fluid interface and the tangent to the solid surface at the contact line between the three phases (Mittal, 2006). Small contact angles ($< 90^\circ$) correspond to hydrophilicity, while large contact angles ($> 90^\circ$) correspond to hydrophobicity (Yuan and Lee, 2013). More specifically, a contact angle less than 90° means that surface is well wetted by the liquid (hydrophilic solid surface), and the fluid tends to have an important contact with the surface. However, contact angles higher than 90° generally indicate that the fluid tends to lessen its contact with the surface and form a compact liquid droplet. In other words the surface of the solid is hydrophobic.

A super-hydrophilic state is reached when complete wetting occurs, in other words when the contact angle is 0° , as the droplet turns into a flat puddle. Contact angles higher than 150° lead to surfaces referred as superhydrophobic surfaces. Under these conditions, the system presents almost no contact between the liquid drop and the surface. The so-called lotus effect is observed in this range of contact angles (Lafuma and Quéré, 2003).

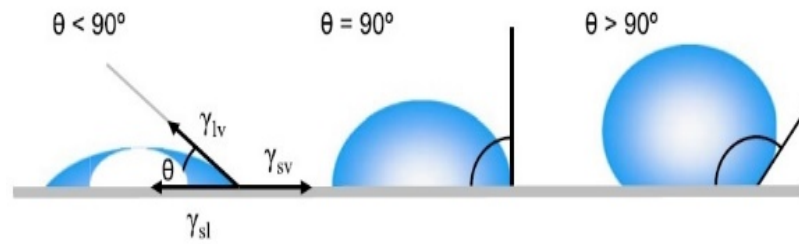


Figure 3.9. Illustration of contact angles formed by sessile liquid drops on a smooth homogeneous solid surface (Yuan and Lee, 2013)

3.3.3. Physical characterization

The ability of the electrospun nanofibers of favoring air and vapor transportation is commonly measured by a device called DMPC (Dynamic Moisture Vapor Permeation Cell) (Huang et al., 2003).

Electrical transport properties of electrospun nanofibers can be characterized by various techniques such as two-point probe technique, four-point probe technique, and interdigitated electrodes.

Four-point probe technique will be presented in the following section since will be used in this thesis to investigate the electrical conductivity of the electrospun nanofibers.

3.3.3.1. Four-point probe technique

As can be seen in Figure 3.10 the four point probe setup consists of four equally spaced tungsten metal tips with finite radius. The four tips are designed in such way to be in contact with the sample under test.

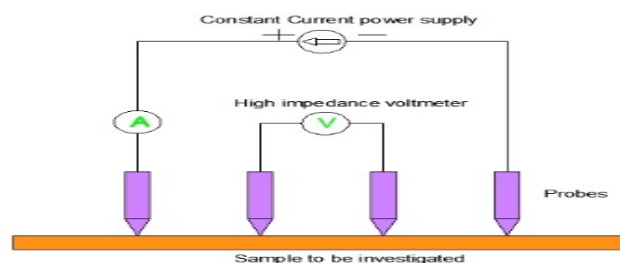


Figure 3.10. Four point probe setup

Each tip is supported by springs on the end to underrate the sample damage during probing. The four metallic tips are part of an auto-mechanical apparatus, which moves up and down during the measurement process. A use of a high impedance current is required so as to supply a current through the outer two tips while the differential potential is measured between the two inner tips, ideally without drawing any current (<http://www.sardarsinghsir.com>).



4. MATERIALS AND METHODS

The main objective of this study is to investigate the electrical conductivity of electrospun nanofibers containing nanoparticles. The influences of applied voltage, the content of nanoparticles (Copper, Graphene and Silica) on morphology, diameter of nanofibers as well as electrical conductivity were characterized. In order to achieve this goal, specific objectives were settled as:

- To find suitable processing parameters and beadless nanofibers;
- To test different nanoparticle contents;
- To analyze the viscosity solutions changes for each type of nanoparticles;
- Characterization of the produced nanofibers by SEM, XRD, TEM, Contact angle techniques, TGA and DSC;
- The four-point probe technique was used to investigate the electrical conductivity of the obtained nanofibers.

4.1. Materials

In this work, polyacrylonitrile (PAN) and dimethylformamide (DMF) were picked out as polymer and solvent, respectively. Copper, graphene nanoplatelet and silica were selected as nanoparticles to be dispersed in the PAN/DMF solutions. The following sections present the products specification and /or the application fields.

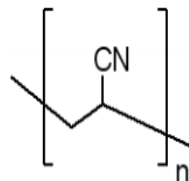
4.1.1. Polyacrylonitrile

Polyacrylonitrile is a synthetic, semi-crystalline organic polymer resin, with the linear formula $(C_3H_3N)_n$. Though it is thermoplastic, it does not melt under normal conditions. It degrades before melting. It melts above 300 °C if the heating rates are 50 degrees per minute or above. It is a versatile polymer used to produce large variety of products including ultra -filtration membranes, hollow fibers for reverse osmosis, fibers for textiles, oxidized PAN fibers (Gupta et al., 1998). PAN has properties involving low density, thermal stability, high strength and modulus of elasticity. These unique properties have made PAN an essential polymer in high tech.

Product Specification

Product Name:
Polyacrylonitrile - average Mw 150,000 (Typical)

Product Number: 181315
CAS Number: 25014-41-9
MDL: MFCD00084395
Formula: C₃H₃N



TEST	Specification
Appearance (Color)	White to Yellow
Appearance (Form)	Conforms to Requirements
Powder and Chunks	
Infrared spectrum	Conforms to Structure

Figure 4. 1. PAN specification (Sigma Aldrich Co.)

4.1.2. Dimethylformamide

N, N-Dimethylformamide (DMF) is among the most used solvent in the electrospinning process. DMF is used in many applications such as in the isolation of chlorophyll from plant tissues, reagent inorganic synthesis, a reducing agent, dehydrating agent, catalyst and so forth. (www.sigmaaldrich.com).

Product Specification

Product Name:
N,N-Dimethylformamide - anhydrous, 99.8%

Product Number: 227056
CAS Number: 68-12-2
MDL: MFCD00003284
Formula: C₃H₇NO
Formula Weight: 73.09 g/mol

$$\begin{array}{c} \text{O} \\ \parallel \\ \text{H}-\text{C}-\text{N}-\text{CH}_3 \\ | \\ \text{CH}_3 \end{array}$$

TEST	Specification
Appearance (Clarity)	Clear
Appearance (Color)	Colorless
Appearance (Form)	Liquid
Infrared spectrum	Conforms to Structure
Purity (GC)	> 99.75 %
Water (by Karl Fischer)	≤ 0.005 %
Residue on Evaporation	≤ 0.0005 %

Specification: PRD.5.ZQ5.10000004536

Figure 4. 2. DMF specification (Sigma Aldrich Co)

4.1.3. Copper nanoparticles

Copper nanoparticles are known for their high electrical conductivity. It is mainly used in electronics industry. It can be used in conducting coatings, inks and

pastes, raw material for electronic parts, catalysis for reactions such as methanol production, microelectronic devices, additive for lubricants, for wear resistant coatings, sintering additives etc. Technical properties of copper nanoparticles used in this work are as follows:

- Cu purity (%): ≥ 99.8 (partially passivated by coating nanoparticles with 0.8 wt. % Oxygen for only safe shipping);
- Bulk density (g/cm^3): 0.2 - 0.4;
- True density (g/cm^3): 8.9;
- Color : dark brown;
- Shape : spherical;
- Crystal structure : cubic;
- Average particle size(nm): 25;
- Specific surface area (m^2/g) : 35 – 55;

Cu(Copper) Nanoparticles Partially
Passivated, 99.85%, 22nm

29
Cu
Copper
63.546



Figure 4. 3. Copper nanoparticles specification (Nanografi)

4.1.4. Silica nanoparticles

The properties of nanoparticles are as follows:

- Purity (%) : 99.8;
- Specific surface area : 175-225 m^2/g ;
- Loss on ignition: typically 2-16 %;
- Appearance (form): powder;
- Appearance (color): White.

Product Specification

Product Name:
Silica - 99.8%

Product Number: **381276**
CAS Number: 112945-52-5
MDL: MFCD00011232
Formula: O₂Si
Formula Weight: 60.08 g/mol

SiO₂

TEST	Specification
Appearance (Color)	White
Appearance (Form)	Powder
Loss on Ignition	Typically 2 - 10%
Surface Area	175 - 225 m ² /g
ICP Major Analysis	Conforms
Confirms Silicon Component	
Purity	Conforms
99.8% Based on Trace Metals Analysis	
Trace Metal Analysis	≤ 2500.0 ppm

Specification: PRD.1.ZQ5.10000008023



Figure 4. 4. Silica nanoparticles specification (Sigma- Aldrich Co)

4.1.5. Graphene nanoparticles

The addition of Graphene to different composites show improvements in their physical properties. These improvements include electrical conductivity, thermal conductivity, hardness, strength, viscosity etc. Technical properties of graphene nanoparticles used in this study are as follows:

- Purity 99.5% ;
- Thickness (nm) : 6;
- Diameter (μm): 5;
- Specific surface area (m²/g): 150;
- Conductivity (S/m): 1100 – 1600;
- Color : Grey



Graphene

Nanoplatelet, 99.5+%, 6 nm, S.A: 150 m²/g, Dia: 5 μm

**Graphene Nanoplatelet,
99.5+%, 6 nm, S.A:150m²/g
Dia: 5μm**



Figure 4. 5. Graphene specification (Nanografi)

The equipment and chemicals used in this study for the preparation of the solutions, production and characterization of nanofibers are listed in the Table 4.1. In this project, all chemicals were used as- received without further purification.

Table 4. 1. List of materials

Equipments or chemicals	Description
Polyacronitrile (PAN)	150,000g/mol of (Mw)
N, N- Dimethylformamide anhydrous, 99.8%	From the Sigma Aldrich Co.
Copper	From Nanografi, nanopowder 25nm %99.9
Graphene	From Nanografi, Specific surface area 150m ² /g
Silica	From the Sigma Aldrich Co.
Collector	Covered by the aluminum foil
Digital balance	
High voltage power supply	
Magnetic stirrer	
Magnetic fish	
Syringe pump	
Stainless steel needles	with 0.8ml as inner diameter.
SEM	
XRD	
TEM	
Contact angle device	
Four-point probe device	
Gloves	
masks	
Scissors	

4.2. Parameters Setting and Preparation of Electrospinning Solutions

Setting of electrospinning parameters was recognized by many researchers as a crucial factor to the success of the process. Therefore, in this study some effective parameters ranges suggested by experts were used. Notably, $15 \text{ kV} \leq V \leq 25 \text{ kV}$ was selected to be the desired domain for applied voltage and $10 \text{ cm} \leq d \leq 20 \text{ cm}$ was considered as the effective range for spinning distance (Haghi, 2011). The electrospinning parameters used in this study are mentioned in the Table 4.2

Table 4.2. Electrospinning parameters for pure PAN electrospinning process

Sample (% wt. of PAN)	Processing parameters			
	Feed rate (mL/hr.)	Tip to collector (cm)	Collector Rotational speed(rpm)	Applied voltage (kV)
8	2.5	12	112.5	10
				15
				20
9	2.5	12	112.5	15
				20
10	2.5	12	112.5	15
				20
11	2.5	12	112.5	15
				20

According to our main objective, in this project two types of solutions were prepared. The first type refers to solutions prepared without nanoparticles and will be referred as pure PAN solutions in this document. The second type encompasses all solutions containing nanoparticles. In the following pages, the procedure used in order to prepare those solutions will be presented.

4.2.1. Fabrication of pure PAN nanofibers

A polyacronitrile (PAN) with an average molecular weight (Mw) of 150,000 g/mol and N, N-Dimethylformamide anhydrous, 99.8% were purchased from the Sigma Aldrich Co. all the materials were used as- received without further purification.

Different PAN/ DMF solutions with polymer content of 8 wt. %, 9 wt. %, 10 wt. % and 11 wt. % by mass were prepared. Two samples of PAN electrospinning solutions were prepared for each polymer Content highlighted above. For each electrospinning solution, the composition of its chemicals in terms of mass was summarized in the following Table.

Table 4.3. Composition of electrospinning solution

Samples		PAN (gr)	DMF (gr)	Solution (gr)
Number	(% wt. of PAN)			
1	8	0.200	2.300	2.5
2	9	0.225	2.275	2.5
3	10	0.250	2.250	2.5
4	11	0.275	2.225	2.5

In order to prepare the electrospinning solutions, the amount of each polyacrylonitrile sample was dissolved in its DMF solvent quantity, respectively. Then, each solution sample was stirred using a magnetic stirrer device at 85°C and 1200 rpm for an hour so as to obtain a homogeneous electrospinning solution. A total of 9 solution samples were prepared under the same conditions. It is important to realize that after the homogenization process, in each case the solution sample was brought to the room temperature. After reaching the room temperature, the prepared electrospinning solutions were poured into a 2.5 mL syringe pump with 0.8 mm as inner diameter in order to proceed with the electrospinning setup. The following Figures (from Figure 4.6 to Figure 4.10) illustrate the procedure of the electrospinning solutions preparation.

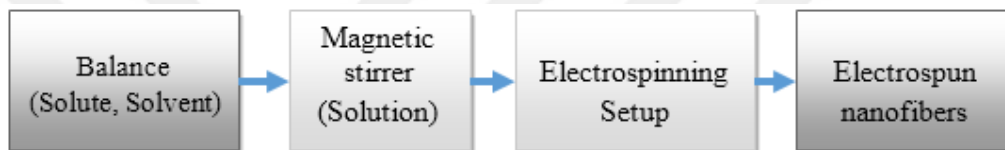


Figure 4. 6. Main steps followed in electrospun nanofibers fabrication



Figure 4.7. Preparation and electrospinning process of 8 wt. % PAN polymer content solution. (a) 0.20 gr of PAN, (b) 2.300 gr of DMF, (c) solution of PAN and DMF on the magnetic stirrer, (d) electrospinning process



Figure 4.8. Preparation and electrospinning process of 9 wt. % PAN polymer content solution. (a) 0.225 gr of PAN, (b) 2.275 gr of DMF, (c) solution of PAN and DMF on the magnetic stirrer, (d) electrospinning process



Figure 4.9. Preparation and electrospinning process of 10 wt. % PAN polymer content solution. (a) 0.250 gr of PAN, (b) 2.250 gr of DMF, (c) solution of PAN and DMF on the magnetic stirrer, (d) electrospinning process



Figure 4.10. Preparation and electrospinning process of 11 wt. % PAN polymer content solution. (a) 0.275 gr of PAN, (b) 2.225 gr of DMF, (c) solution of PAN and DMF on the magnetic stirrer, (d) electrospinning process

The experimental setup consisted of a syringe pump, sample collector and a high – voltage power supply, as shown in Figure 4.11 below. The spinning solution was held in a horizontal syringe with a stainless steel needle. The needle was electrically connected to a positive high voltage power supply. Whereas, the metallic disc used as collector was electrically connected to a negative high voltage power supply. The rotational speed of the collector during electrospinning was setup at 112.5 rpm (displayed as 15% of the maximum rotational speed of the collector on the electrospinning setup). The needle to the collector distance was 12 cm and the solution flow rate maintained at 2.5 mL/hr. using a digitally controlled syringe pump.

For each PAN polymer content at least two samples of nanofibers were produced at three different applied voltages (10 kV, 15 kV and 20 kV) keeping all the highlighted variables constant. The electrospinning process was carried out in a closed environment inside a transparent box at a room temperature as it can be seen from the Figure below.



Figure 4.11. Electrospinning setup

Under the setting parameters, the samples of the obtained nanofibers are shown in the following pictures.

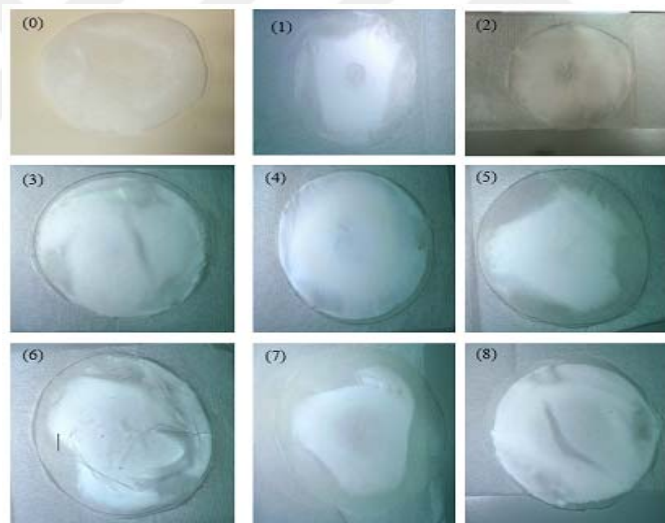


Figure 4.12. Pictures of pure PAN electrospun nanofibers. (0) 8wt. % PAN and 10kV, (1) 8wt. % PAN and 15kV, (2) 8wt. % PAN and 20kV, (3) 9wt. % PAN and 15kV, (4) 9wt. % PAN and 20kV, (5) 10wt. % PAN and 15kV, (6) 10wt. % PAN and 20kV, (7) 11wt. % PAN and 15kV, (8) 11wt. % PAN and 20kV. All the other variables remained constant

4.2.2. Morphology of electrospun pure PAN nanofibers

The nanofibers' morphology has been reported as a main factor that affects the performance of electrospun nanofibers. Numerous electrospinning process parameters as well as polymer solution properties considerably affect the nanofibers' morphology. In this project only the concentration and applied voltage parameters were considered while other electrospinning parameters were kept constant. Although such assumption

has been done, the possibility that some small variation in the charge density occurs as a result of charge dissipation from the tip into the atmosphere cannot be dismissed entirely.

Morphological characterization was conducted with Zeiss Evo LS10 Scanning electron microscopy (SEM) of the advanced research center (Iltak) of the Selçuk University. Since a conductive coating is recommended to prevent charging of specimen with an electron beam in conventional Scanning Electron Microscopy technique, the obtained electrospun nanofibers were brought in a sputter machine (Cressington Sputter Coater) in order to cover specimens with a thin layer of conducting material and therefore to increase the sample conductivity. Then, the coated nanofibers were characterized using SEM. The morphology and the diameter ranges of pure PAN nanofibers are presented from the Figure 4.13 to Figure 4.16 below.

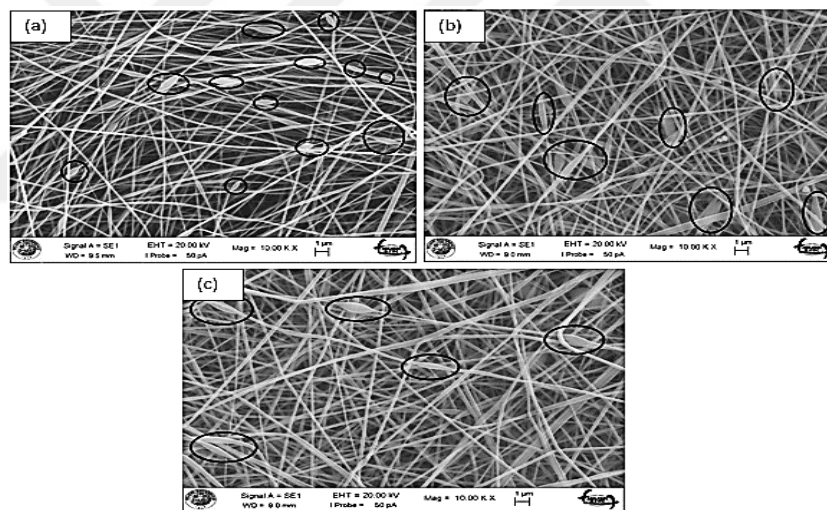


Figure 4.13. SEM images of electrospun pure PAN nanofibers from various applied voltages and 8 wt. % PAN Polymer content. (a) Morphology at 10 kV, (b) Morphology at 15 kV, (c) Morphology at 20 kV

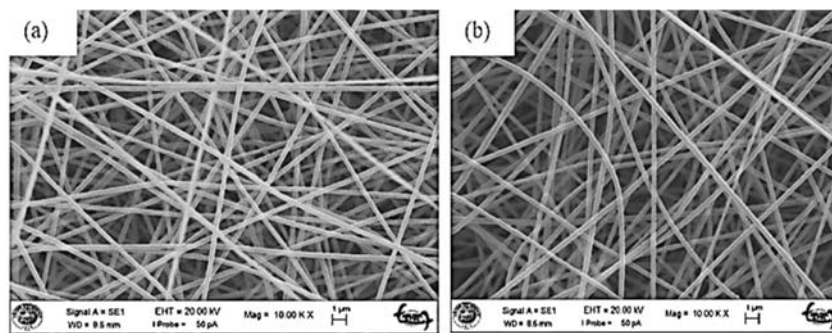


Figure 4.14. SEM images of electrospun pure PAN nanofibers from various applied voltages and 9 wt. % PAN Polymer content. (a) Morphology at 15 kV, (2) Morphology at 20 kV

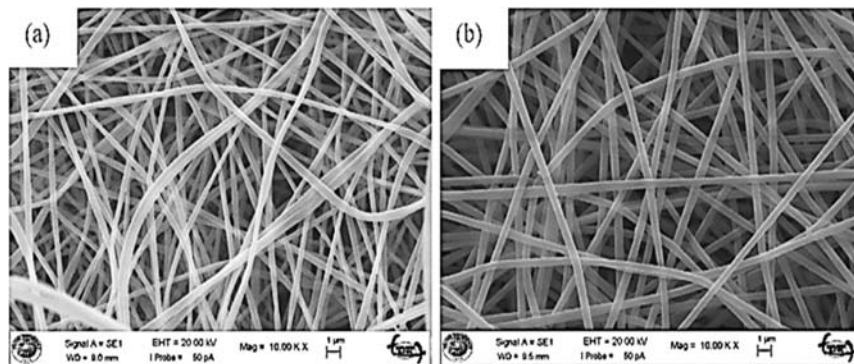


Figure 4.15. SEM images of electrospun pure PAN nanofibers from various applied voltages and 10 wt. % PAN Polymer content. (a) Morphology at 15 kV, (b) Morphology at 20 kV

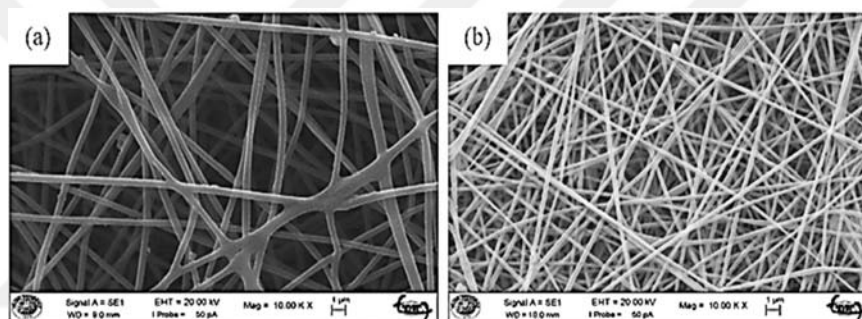


Figure 4.16. SEM images of electrospun pure PAN nanofibers from various applied voltages and 11 wt. % PAN Polymer content. (a) Morphology and diameter range for 15 kV, (b) Morphology and diameter range for 20 kV

The concentration effect on the fiber morphology and geometry has been reported by numerous researchers. The main effect pointed out was the presence of beads in the electrospun fibers which can affect its unusual properties, as an illustration a decreased specific area (Zhang et al., 2009). Hence, it is important to realize that PAN polymer concentration can be handled in order to produce beads-free electrospun nanofibers. To do so, in this work, different electrospun pure PAN nanofibers with 8 wt. %, 9 wt. %, 10 wt. % and 11 wt. % of polymer contents dissolved in DMF were produced respectively. The samples of the obtained electrospun fibers were investigated by SEM. The resulting SEM images were illustrated above from Figure 4.13 to Figure 4.16. According to the SEM images, it can be seen that PAN polymer solutions with lower concentration led to nanofibers with more beads than polymer solution with higher concentration. In other words, straight and bead-free nanofibers with a smooth

surface were observed when the concentration of the polymer in the solution was brought from 8 wt. % to 11 wt. %.

4.2.3. Fabrication of PAN/ Nanoparticles nanofibers

The main motivation of testing different PAN polymer contents in the previous section was in order to determine the content which will exhibit both the best morphology and bead-free nanofibers. Therefore, after analyzing the previous pure PAN nanofiber samples using Scanning Electron Microscopy technique, the solution containing 9 wt. % of PAN was chosen because of its good diameter range and beads-free nanofibers.

Bearing in mind that all the electrospinning solutions containing nanoparticles were prepared in the same way, the used procedure can be presented as follows:

- i. Weigh the required amount of chemicals (PAN and DMF) using the digital balance;
- ii. Homogenization of PAN/DMF mixture using magnetic stirrer for an hour;
- iii. Once the second step is successfully achieved, weigh the mass of the obtained homogeneous solution using again the digital balance;
- iv. According to the quantity of mass obtained in the third step, calculate the required amount of nanoparticles in relation to their respective percentage which must be introduced in the previous PAN/DMF solution;
- v. Pour the required amount of nanoparticles in the PAN/DMF solution;
- vi. Homogenization of the new PAN/DMF/NPs mixture using magnetic stirrer for an hour;
- vii. Once the sixth step is successfully achieved then, withdraw the solution from the magnetic stirrer until it reaches the room temperature;
- viii. The last step is pouring the solution in the syringe.

4.2.3.1. Fabrication of PAN/CuNPs nanofibers

After adopting 9 wt. % as the adequate amount of PAN polymer content for the electrospinning solution, the next step was the preparation of different solutions containing copper nanoparticles (CuNPs). The preparation of PAN/DMF/CuNPs solutions was conducted by following the steps mentioned above.

The pure PAN electrospinning solution preparation procedure was explained in the previous section. In the same fashion, three samples of solution containing 9 wt. % of PAN and % 91 of DMF as solvent were prepared under the same conditions and stirred in the similar conditions as it was done for each previous solution. The next step was the weighing of the homogeneous PAN/DMF solutions on the digital balance so as to determine its mass. Once the mass of the homogeneous solution was known for each sample, an amount of copper nanoparticles in reference to its required content (%1, % 3 or % 5) was thoroughly added in each solution sample, respectively. Then, in order to get a homogeneous solution, the new mixture was brought again on the magnetic stirrer for an hour at 85°C and 1200 rpm. Table 4.4 summarizes the composition of chemicals in terms of mass in each solution sample. All steps involved in the preparation of solutions are illustrated from the Figure 4.17 to Figure 4.19.

Once the homogenization process ended, the solution samples were brought to the room temperature. After reaching the room temperature, the prepared electrospinning solutions were poured into a 2.5 mL syringes with 0.8 mm as inner diameter in order to proceed with the electrospinning setup.

From the open literature, it has been reported that many parameters can affect the results of electrospinning process. In this project only the effect of applied voltage was investigated, all other parameters considered invariable.

Table 4.4. Composition of PAN/DMF/CuNPs solution samples

Sample		9wt.	DMF(gr.)	(DMF+PAN)(gr.)	(DMF+PAN) (gr.)	Cu NPs(gr.)
N°	% of Cu	% of PAN (gr.)		Before Stirring	After stirring	
1	1	3	30.333	33.333	31.520	0.315
2	3	3	30.333	33.333	29.777	0.893
3	5	3	30.333	33.333	31.871	1.593

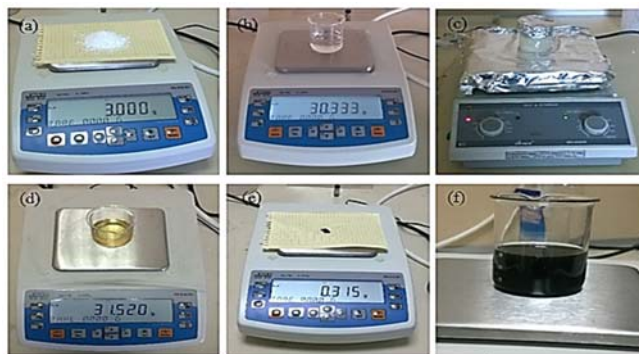


Figure 4.17. Weighing of chemicals and preparation of electrospinning solution containing 1 wt. % of CuNPs. (a) 3.00 gr of PAN, (b) 30.333 gr of DMF, (c) Steering of PAN/DMF mixture. (d) Mass of the PAN/DMF solution (31.520 gr) after steering, (e) 0.315 gr of CuNPs, (f) Mixture of PAN/DMF/CuNPs after steering process

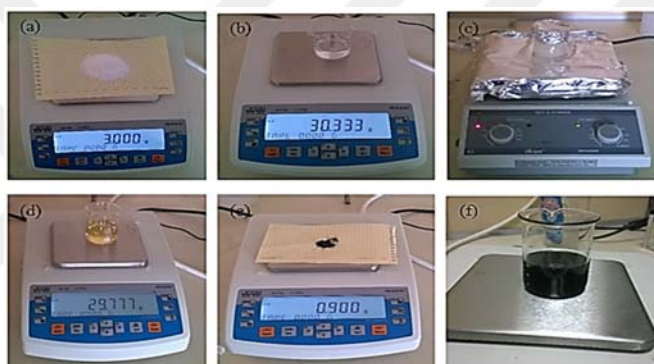


Figure 4.18. Weighing of chemicals and preparation of electrospinning solution containing 3 wt. % of CuNPs. (a) 3.000 gr of PAN, (b) 30.333 gr of DMF, (c) Steering of PAN/DMF mixture (d) 29.777 gr of mass of the PAN/DMF solution after steering, (e) 0.893 gr of CuNPs, (f) Mixture of PAN/DMF/CuNPs after steering process

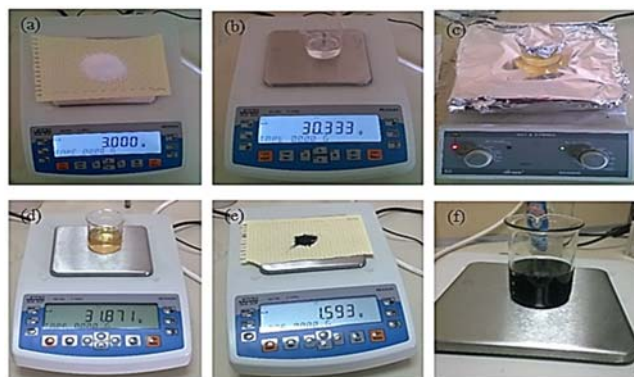


Figure 4.19. Weighing of chemicals and preparation of electrospinning solution containing 5 wt. % of CuNPs. (a) 3.000 gr of PAN, (b) 30.333 gr of DMF, (c) Steering of PAN/DMF mixture (d) 31.871 gr of mass of the PAN/DMF solution after steering, (e) 1.593 gr of CuNPs, (f) Mixture of PAN/DMF/CuNPs after steering process

For each copper content in solutions two samples of nanofibers were produced at two different applied voltage (15 kV and 20 kV), keeping all other electrospinning parameters unchanged. The electrospinning process was carried out in a closed environment inside a transparent box having similar conditions as in the fabrication of pure PAN nanofibers described above.

The electrospinning process was conducted under the conditions specified in the Table 4.5 and the obtained samples of electrospun nanofibers are shown in the Figure 4.20 below.

Table 4.5. Electrospinning parameters for PAN/DMF/NPs electrospinning process.

Sample (% wt. of NPs)	Processing parameters			
	Feed rate (mL/hr.)	Tip to collector (cm)	Collector Rotational speed(rpm)	Applied voltage (kV)
1	2.5	12	112.5	15
				20
3	2.5	12	112.5	15
				20
5	2.5	12	112.5	15
				20

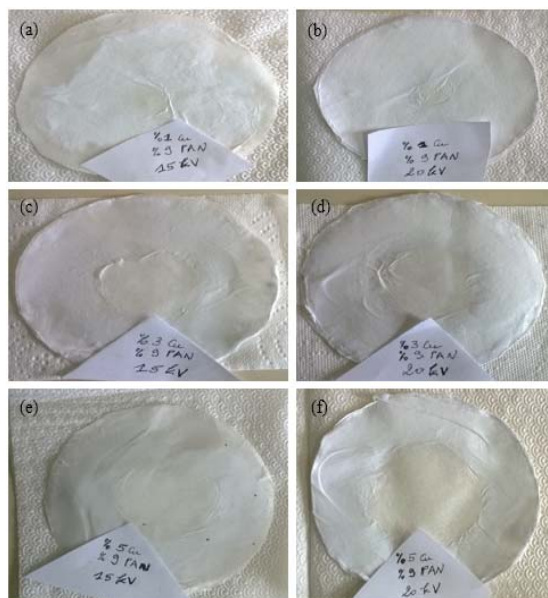


Figure 4.20. Pictures of pure PAN/DMF/CuNPs electrospun nanofibers. (a) 1 wt. % CuNPs and 15 kV, (b) 1 wt. % CuNPs and 20 kV, (c) 3 wt. % CuNPs and 15 kV, (d) 3wt. % CuNPs and 20 kV, (e) 5wt. % CuNPs and 15 kV, (f) 5wt. % CuNPs and 20 kV. All the other variables remained constant

4.2.3.2. Fabrication of PAN/Graphene NPs nanofibers

As it was highlighted in the previous section, all our nanofibers containing nanoparticles were prepared under the same conditions (from the preparation of solutions to the electrospinning process). In this section the solutions' preparation and fabrication of PAN/graphene nanoparticles nanofibers will be reported.

In the same way, three samples of solution containing 9 wt. % of PAN and 91% of DMF as solvent were prepared under the same conditions and stirred in the similar conditions as it was done for each previous solution. The next step was the weighing of the homogeneous PAN/DMF solutions on the digital balance so as to determine its mass. Once the mass of the homogeneous solution was known for each sample, an amount of graphene nanoparticles in reference to its required content (%1, %3 or % 5) was thoroughly added in each solution sample respectively. Then, in order to get a homogeneous solution, the new mixture was brought again on the magnetic stirrer for an hour at 85°C and 1200 rpm. The Table 4.6 summarizes the composition of chemicals in terms of mass in each solution sample. All steps involved in the preparation of solutions are illustrated from the Figure 4.21 to Figure 4.23.

Once the homogenization process ended, the solution samples were brought to the room temperature. It must be remembered that as for the copper nanoparticles, three solution samples were prepared at different nanoparticles contents: 1%, 3% and 5wt. %, respectively. In order to proceed with the electrospinning setup, each solution sample was poured into two syringes of 2.5 mL and 0.8 mm as inner diameter.

Table 4. 6. Composition of PAN/DMF/Graphene NPs solution samples

Sample		9 wt. % of PAN (gr)	DMF(gr)	(DMF+PAN) (gr.) Before Stirring	(DMF+PAN) (gr.) After stirring	Graphene NPs (gr)
N°	% of Graphene					
1	1	3	30.333	33.333	32.017	0.320
2	3	3	30.333	33.333	30.640	0.918
3	5	2.3	23.25	25.55	21.328	1.066



Figure 4.21. Weighing of chemicals and preparation of electrospinning solution containing 1 wt. % of graphene NPs. (a) 3.00 gr of PAN, (b) 30.333 gr of DMF, (c) Steering of PAN/DMF mixture. (d) 32.017 gr of PAN/DMF solution after steering, (e) 0.32 gr of graphene NPs, (f) Mixture of PAN/DMF/graphene NPs after steering process

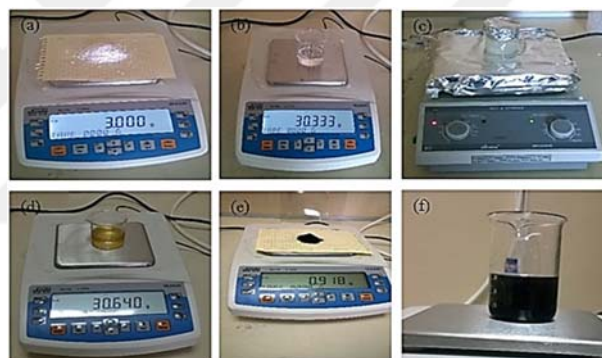


Figure 4.22. Weighing of chemicals and preparation of electrospinning solution containing 3 wt. % of graphene NPs. (a) 3.00 gr of PAN, (b) 30.333 gr of DMF, (c) Steering of PAN/DMF mixture. (d) 30.640 gr of PAN/DMF solution after steering, (e) 0.918 gr of graphene NPs, (f) Mixture of PAN/DMF/graphene NPs after steering process

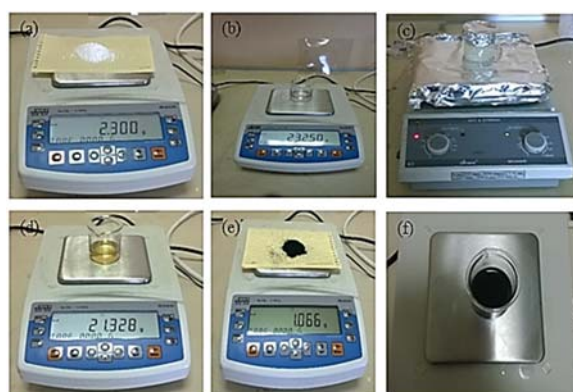


Figure 4.23. Weighing of chemicals and preparation of electrospinning solution containing 5 wt. % of graphene NPs. (a) 2.300 gr of PAN, (b) 23.250 gr of DMF, (c) Steering of PAN/DMF mixture. (d) 21.328 gr of PAN/DMF solution after steering, (e) 1.066 gr of graphene NPs, (f) Mixture of PAN/DMF/graphene NPs after steering process

For each copper content in solutions two samples of nanofibers were produced at two different applied voltage (15 kV and 20 kV) other parameters considered constant. The electrospinning process was conducted under even conditions as it was done for copper nanoparticles. Electrospinning process was conducted under the conditions specified in the Table 4.5 and the obtained samples of electrospun nanofibers are shown in the Figure 4.24 below.

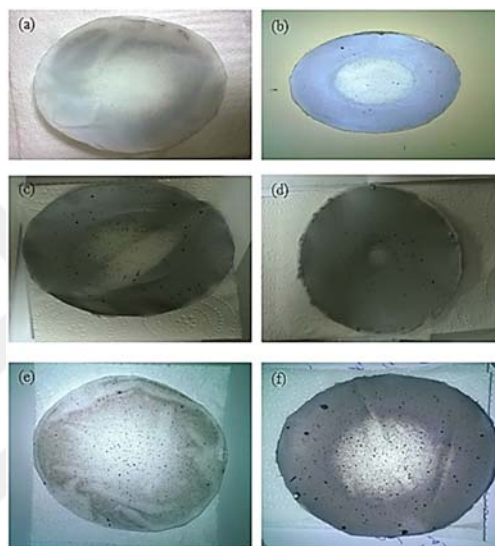


Figure 4.24. Pictures of pure PAN/DMF/GrapheneNPs electrospun nanofibers. (a) 1 wt. % Graphene NPs and 15 kV, (b) 1 wt. % Graphene NPs and 20 kV, (c) 3 wt. % Graphene NPs and 15 kV, (d) 3 wt. % Graphene NPs and 20 kV, (e) 5 wt. % Graphene NPs and 15 kV, (f) 5 wt. % Graphene NPs and 20 kV. All the other variables remained constant

4.2.3.3. Fabrication of PAN/Silica NPs nanofibers

This section reports the solution preparation and fabrication of nanofibers containing silica nanoparticles. In Accordance with the procedure used in the first two sections, three different samples of solutions containing silica nanoparticles (1 %, 3 % and 5 wt. %) have been prepared.

The Table 4.7 summarizes the composition of chemicals in terms of mass in each solution sample. All steps involved in the preparation of solutions are illustrated from the Figure 4.25 to Figure 4.27.

Table 4.7. Composition of PAN/DMF/Silica NPs solution samples

Sample		9wt. % of PAN (gr)	DMF(gr)	(DMF+PAN)(gr.) Before Stirring	(DMF+PAN) (gr.) After stirring	Silica NPs(gr)
N°	% of Silica					
1	1	3	30.333	33.333	31.546	0.315
2	3	3	30.333	33.333	31.914	0.957
3	5	3	30.333	33.333	31.987	1.599

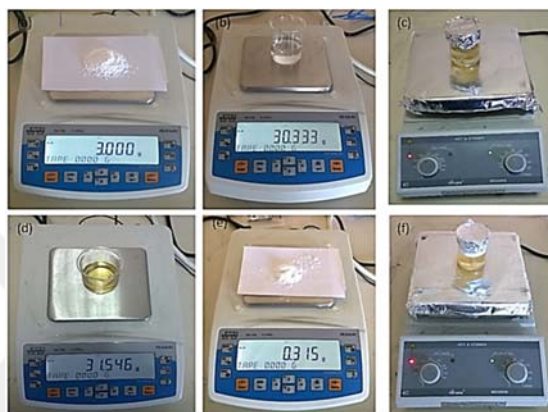


Figure 4. 25. Weighing of chemicals and preparation of electrospinning solution containing 1 wt. % of Silica NPs. (a) 3.000 gr of PAN, (b) 30.333 gr of DMF, (c) Steering of PAN/DMF mixture. (d) 31.546 gr of PAN/DMF solution after steering, (e) 0.315 gr of Silica NPs, (f) Mixture of PAN/DMF/Silica NPs on the stirrer

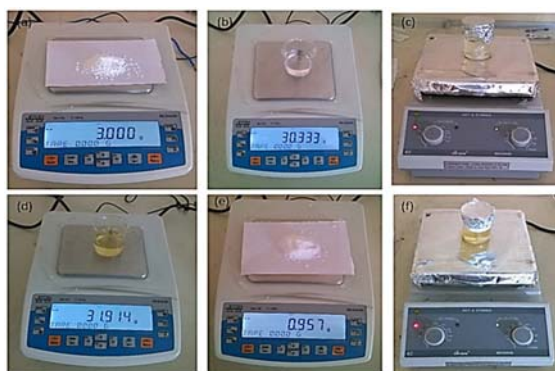


Figure 4. 26. Figure 4.21. Weighing of chemicals and preparation of electrospinning solution containing 3 wt. % of Silica NPs. (a) 3.000 gr of PAN, (b) 30.333 gr of DMF, (c) Steering of PAN/DMF mixture. (d) 31.914 gr of PAN/DMF solution after steering, (e) 0.957 gr of Silica NPs, (f) Mixture of PAN/DMF/Silica NPs on the stirrer

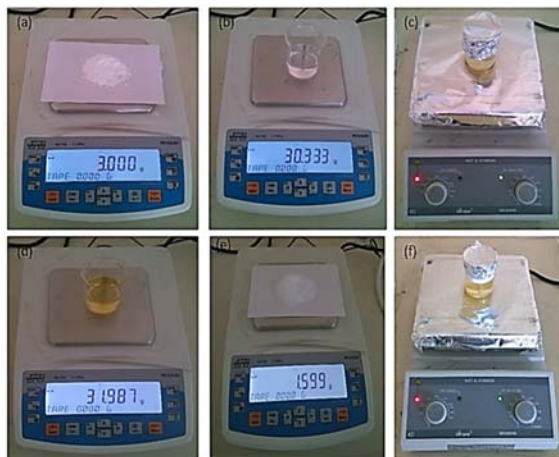


Figure 4.27. Weighing of chemicals and preparation of electrospinning solution containing 5 wt. % of Silica NPs. (a) 3.000 gr of PAN, (b) 30.333 gr of DMF, (c) Steering of PAN/DMF mixture. (d) 31.987 gr of PAN/DMF solution after steering, (e) 1.599 gr of Silica NPs, (f) Mixture of PAN/DMF/Silica NPs on the stirrer

The images of the resultant PAN/DMF/SiO₂ nanofibers are presented in the Figure 4.28 below.



Figure 4.28. Pictures of pure PAN/DMF/Silica NPs electrospun nanofibers. (a) 1 wt. % Silica NPs and 15 kV, (b) 1 wt. % Silica NPs and 20 kV, (c) 3 wt. % Silica NPs and 15 kV, (d) 3 wt. % Silica NPs and 20 kV, (e) 5 wt. % Silica NPs and 15 kV, (f) 5 wt. % Silica NPs and 20 kV. All the other variables remained constant

4.3. Viscosity of Electrospinning Solutions

In this section, dynamic viscosity of different electrospinning solutions was investigated. To do so, a rotational viscometer (JK-RV-1) was used in this research. The main technical indicators of the used viscometer are:

- Measuring range : 10 ~ 100000 mPa.s;
- Rotor specifications: 1,2,3,4 kinds of rotor;
- Speed: 6rpm, 12rpm, 30 rpm and 60 rpm;
- Measurement error : plus or minus 5%
- Power supply: 220V, 50 Hz;
- Dimension 300*300*300 (mm);
- Net weight : 1.5 kg (not including stent)



Figure 4. 29. Viscometer (JK-RV-1)

Viscosities of pure PAN and PAN/nanoparticles based solutions were investigated at room temperature at least five times for each solutions. The obtained average values are presented in Table 4.8.

Table 4. 8. Dynamic viscosity of electrospinning solutions at room temperature

Solutions	Dynamic viscosity (mPa.s)
9 wt. % PAN/DMF	462.5
PAN/DMF/1 wt. % Cu	577.7
PAN/DMF/3 wt. % Cu	3160.25
PAN/DMF/5 wt. % Cu	11526.66
PAN/DMF/1 wt. % Graphene	470
PAN/DMF/3 wt. % Graphene	713.8
PAN/DMF/5 wt. % Graphene	1139.6
PAN/DMF/1 wt. % SiO ₂	484.72
PAN/DMF/3 wt. % SiO ₂	872.375
PAN/DMF/5 wt. % SiO ₂	1348

4.4. Characterization Techniques

In this section, technical specifications of different devices and their setting parameters used in this work will be presented.

4.4.1. Scanning electron microscopy

Scanning electron microscopy (SEM, Zeiss Evo LS10) was used to evaluate the morphology and observe the dispersion of nanoparticles. Zeiss Evo LS10 SEM has specifications such as:

- Stage movement of 80x100x35 mm (X,Y,Z);
- Maximum specimen height of 100 mm;
- Reduce 400 manual steps to only 15, imaging four points of interest on nine specimens at three different magnifications.

Since a conductive coating is recommended to prevent charging of specimen with an electron beam in conventional scanning electron microscopy technique, the obtained electrospun nanofibers were brought in a sputter machine (Cressington Sputter Coater) in order to cover specimens with a thin layer of conducting material. Then, the coated nanofibers were characterized using SEM. The SEM device is presented in the Figure 4.30.

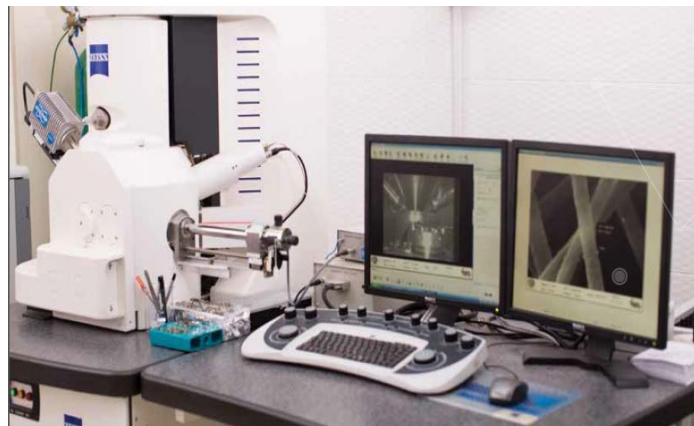


Figure 4. 30. SEM, Zeiss Evo LS10 Setup (SU, Iltek)

4.4.2. X-rays diffraction

Detailed insight into the relationship between structure, function, and reactivity is crucial for the success of modern science. X-ray Diffraction is one of the most powerful methods for generating this vital information and has thus become an essential tool for new discovery. In this work, we have used D8 ADVANCE. The D8 ADVANCE is the benchmark when it comes to extracting structural information from X-Ray Powder Diffraction (XRPD) including Rietveld (TOPAS) analysis, "total" scattering and Small Angle X-Ray Scattering (SAXS) (www.bruker.com). Figure 4.24 shows the XRD device used to investigate the crystallinity of the materials in this work.



Figure 4. 31. XRD, Bruker advanced X-ray solutions D8 (S.U, Iltek)

The crystallinity of synthesized pure PAN and composite nanofibers was further investigated by X-ray diffraction (XRD, Bruker advanced X-ray solutions D8). The XRD operating with a $\text{CuK}\alpha$ radiation source (wavelength $\lambda = 0.15406$ nm) was used. The X-ray beam were generated at 40 kV and 40 mA power. The XRD profiles were recorded from 10° to 90° for 2θ and at the scanning speed of $5^\circ/\text{min}$.

4.4.3. Contact angle setup

The hydrophobicity of pure PAN and nanocomposites fibers were investigated using the contact angle measurement device (Dataphysics instruments GmbH, model OCA15EC, version 1.3). The OCA 15EC is the entry level measuring device for professional contact angle measurements and drop shape analysis. The package consists

in addition to the base unit of a single direct dosing system SD-DM, one electronic syringe unit ESr-N and the software module SCA 20 (<http://www.dataphysics.de>).



Figure 4.32. OCA15EC with single-direct dosing system (<http://www.dataphysics.de>)

In this study, in order to study the hydrophobicity of the as-spun nanofibers a dosing volume of 2 μL of water was used at 0.5 $\mu\text{L/s}$ as dosing rate.

4.4.4. Four-point probe device

A four-point probe device (ENTEK Elk. FPP-460 with Pt probes) was used to measure the electrical conductivity of nanofibers at room temperature. The used four point probe device is illustrated in Figure 4.33 and present many features such as:

- The mechanical structure of the four point contact conductivity measurement system is mobile and adjustable;
- The distance can be adjusted so that samples of different thicknesses can be measured;
- The probe measuring points consist of four needles with a diameter of 0.5 mm, the needles moving inward according to the material geometry. The needles are made of platinum material. The cap is made of high-temperature resistant and highly insulating Teflon material;
- The inter-distance between points is 1mm, as the standard construction;
- The system is microprocessor controlled and can select both automatic and manual steps;

- To eliminate ambient noises, the data from the sample is taken in a selectable format from 1 to 999, and the average of these data is found to be the most accurate and noise-free value;
- The measurement is automatically determined by the built-in microprocessor (autorange) by scanning the device at a low ohmic value;
- LCD displays conductivity value both in Ohm and Siemens cm.



Figure 4. 33. Four-point probe device (ENTEK Elk. FPP-460)

4.4.5. TGA and DSC setup

DSC is used to examine the endothermic or exothermic energy changes that occur during the temperature increase of the materials. The DSC used in this work has some features such as:

- The nitrogen is used as gas in the analyses;
- Solid, semi-solid, liquid and dust samples can be analyzed;
- Thanks to the hub TC100 cooler, the DSC1 allows analysis in the temperature range -85°C ~ 700°C ;
- Transformations such as glass transition and crystallization can be analyzed;
- Information such as specific heat capacity (glass transition temperature (T_g), and enthalpy (H) can be obtained.

TGA is used to study changes in the mass of materials during temperature increase. The features for the used TGA device are:

- Gases such as Argon, nitrogen, dry air, oxygen and carbon dioxide can be used to analyze samples;
- Solid, semi-solid, liquid and dust samples can be analyzed;
- Thanks to the unchilling cooler, the TGA/DSC2 system allows analysis at temperatures range from 25 °C to 1600 °C.

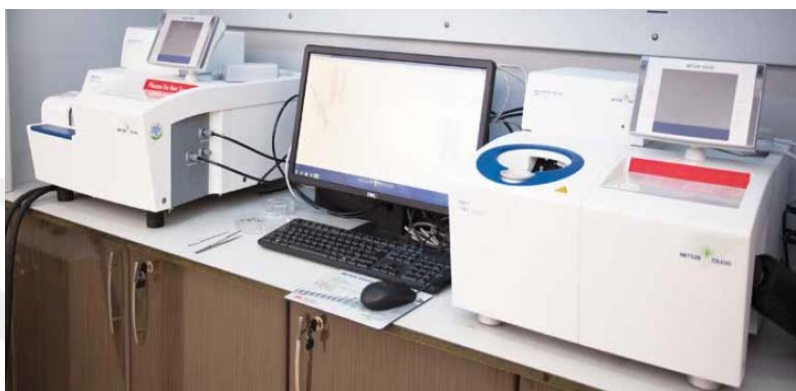


Figure 4. 34. TGA + DSC setup (S.U, Iltek)

In this study, samples of pure PAN nanofibers and PAN composite nanofibers with their respective mass were analyzed. The samples were heated from 0 - 900°C with heating rate of 10°C/min in Nitrogen atmosphere with a pure rate of 20 mL/min.

5. RESULTS AND DISCUSSION

In this study, pure PAN nanofibers and PAN composite nanofibers containing nanoparticles (copper, silica, and graphene) were fabricated by electrospinning technique. The nanoparticles were added in the PAN/DMF electrospinning solution at different rates (1, 3, 5 wt. %). According to the targeted objectives, the obtained nanofibers were characterized by different techniques used currently. The outcomes and conclusions are presented in the followings sections.

5.1. Morphology and Diameters of Nanofibers

It has been reported that morphology such as fiber diameter and its uniformity of the as-pun polymer fibers are linked to many processing parameters (Haghi, 2011). However, many researchers have highlighted that under certain conditions, not only uniform fibers but also beads-free fibers could be fabricated (Haghi, 2011). Therefore, in this study so as to obtain beads-free and uniform PAN nanofibers, different electrospinning solutions with different PAN contents (8, 9, 10 and 11 wt.% by mass) were prepared and electrospun at 15 kV and 20 kV, respectively.

5.1.1. Morphology and diameters of pure PAN nanofibers

The morphology of the as-fabricated PAN nanofibers was characterized by SEM and their respective results were displayed from Figure 4.8 to Figure 4.11. It was observed that even though at 8 wt. % of PAN, nanofibers with smaller average diameters were obtained but an important number of spindle-like beads were visible as well. The electrospinning of solutions containing a PAN content higher than 8 wt. % led to the fabrication of fibers without beads. It is worth to say that at 11 wt. % of PAN, branched fibers were observed. The formation of branched fibers can be justified by the instability of the jet due to the discrepancy between the electrical forces and surface tension. It was reported that such instability can decrease its local charge per unit surface area by ejecting a smaller jet from the surface of the primary jet or by splitting apart into two smaller jets. In 9 and 10 wt. % of PAN uniform nanofibers without any spindle-like beads were obtained. In addition, it was observed that increasing the PAN concentration, generally led to the increase of the fibers average diameter in both 15kV

and 20kV. By keeping the concentration constant and changing the applied voltage, it was observed an increase in nanofibers diameter with the increase of the applied voltage except for 11 wt. % at 20 kV wherein the average diameter where smaller than those performed at 15 kV. By keeping the applied voltage constant and changing the concentration of the PAN, it has been observed that thin nanofibers were obtained with a decrease in PAN concentration. Figure 5.1. Shows the variation of the average diameter respect to the PAN concentration and the applied voltage.

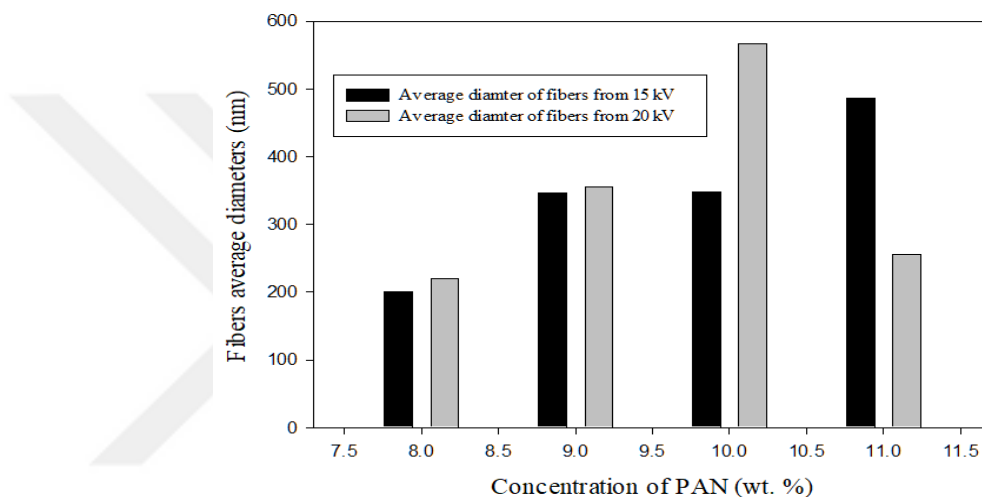


Figure 5. 1. Average diameter of the as-fabricated pure PAN nanofibers at different PAN contents and applied voltages

The average diameters of electrospun PAN nanofibers at 15 kV were 200.15 nm, 347 nm, 347.75 nm and 486.4 nm for electrospinning solution containing 8, 9, 10 and 11 wt. % of PAN content, respectively. However, nanofibers fabricated at 20 kV presented average diameters of 220.35 nm, 355.9 nm, 567.05 nm and 256.1 nm for the same PAN concentration range. According to all highlighted observations, the electrospinning solution containing 9 wt. % of PAN was selected for the continuation of this thesis.

5.1.2. Morphology and diameters of composite nanofibers

In this section different results in terms of morphology and average diameters of composite nanofibers consisting of 9 wt. % of PAN polymer, DMF and inorganic nanoparticles (silica, copper, graphene) will be presented and discussed.

5.1.2.1. Morphology and diameters of PAN/CuNPs composite nanofibers

Figure 5.2 and Figure 5.3 show the SEM images of the fabricated PAN/Cu composite nanofibers with different copper nanoparticles concentration (1, 3 and 5wt. %) performed at 15 kV and 20 kV, respectively. As can be seen from Figures below adding copper nanoparticles in the electrospinning solution did not generally affect negatively the morphology of the as-spun composite nanofibers. Most electrospinning solutions led to the fabrication of beads-free and uniform composite fibers. In addition, no agglomeration of copper nanoparticles was observed on the surface of the nanofibers. However, it is worth to mention that at 20 kV the electrospinning solution containing 1 wt. % Cu led to nanofibers with a number of spindle-like beads.

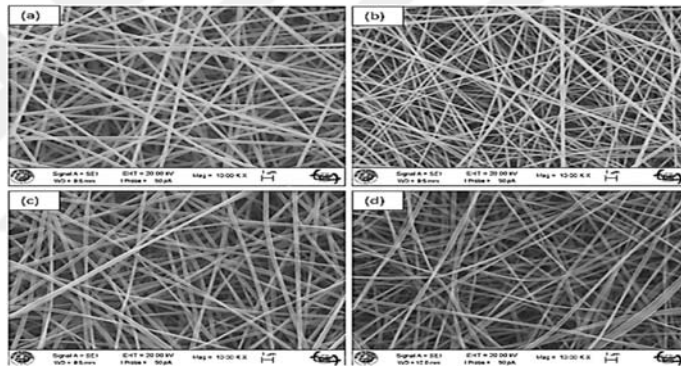


Figure 5. 2. SEM images of as-spun PAN and PAN/Cu nanofibers from 9 wt. % of PAN solution containing different Copper contents performed at 15 kV: (a) 9 wt.% PAN, (b) 1 wt.% Cu, (c) 3 wt. % Cu, (d) 5 wt.% Cu. All other processing parameters held constant

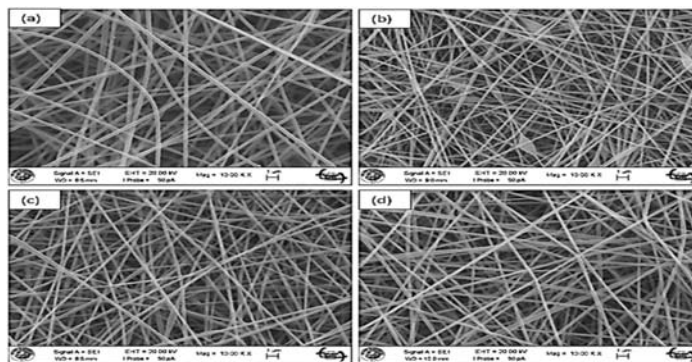


Figure 5. 3. SEM images of as-spun PAN and PAN/Cu nanofibers from 9 wt. % of PAN solution containing different Copper contents performed at 20 kV: (a) 9 wt.% PAN, (b) 1 wt.% Cu, (c) 3 wt. % Cu, (d) 5 wt.% Cu. All other processing parameters held constant

Figure 5.4 shows the variation of the average diameter of composite nanofibers compared to pure PAN nanofibers in terms of copper nanoparticles and applied voltage. It was observed that even if diameters of copper composite nanofibers were smaller than those of pure PAN nanofibers, but it is important to mention that the average diameters of composite nanofibers increased with the copper nanoparticles concentration in the electrospinning solution. The average diameters of fibers performed at 15 kV were 217.92 nm, 330.77 nm and 301.26 nm for PAN/Cu composite nanofibers containing 1, 3, and 5 wt. % of copper nanoparticles, respectively. However, at 20 kV the diameters of the as-spun composite fibers were 229.91 nm, 282.76 nm and 307.53 nm for PAN/Cu composite nanofibers containing 1, 3, and 5 wt. % of copper nanoparticles, respectively.

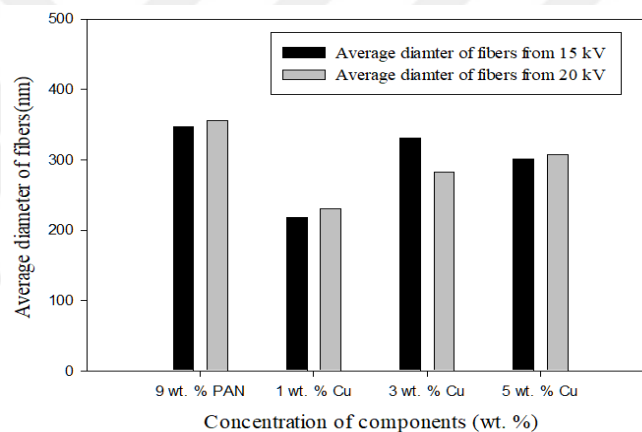


Figure 5.4. Comparison of average diameter of the as-fabricated pure pan nanofibers and PAN/Cu composite nanofibers with different Cu nanoparticles contents and applied voltages

5.1.2.2. Morphology and diameters of PAN/Graphene NPs composite nanofibers

Figure 5.5 and Figure 5.6 show the SEM images of the fabricated PAN/Gr. composite nanofibers with different graphene nanoparticles concentration (1, 3 and 5wt. %) performed at 15 kV and 20 kV, respectively. Agglomeration of graphene nanoparticles was observed on the surface of the as-spun nanofibers. It was observed that some spindle-like beads nanofibers were obtained in both 15 kV and 20 kV. Hence, compared to the pure PAN nanofibers, all the SEM images indicate that the morphology of the resultant composite nanofibers were affected by the addition of graphene nanoparticles in the solutions.

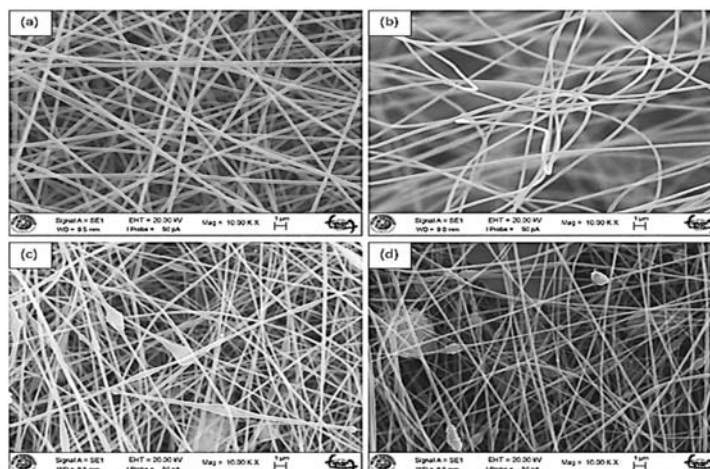


Figure 5. 5. SEM images of as-spun PAN and PAN/Gr nanofibers from 9 wt. % of PAN solution containing different Copper contents performed at 15 kV: (a) 9 wt.% PAN, (b) 1 wt.% Gr, (c) 3 wt. % Gr, (d) 5 wt.% Gr. All other processing parameters held constant

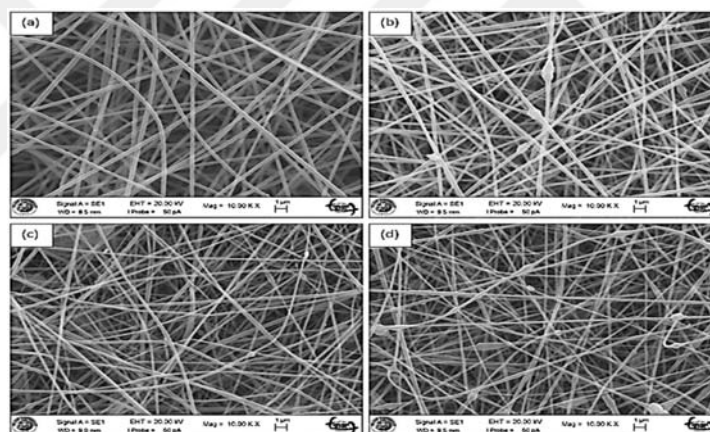


Figure 5. 6. SEM images of as-spun PAN and PAN/Gr nanofibers from 9 wt. % of PAN solution containing different copper contents performed at 20 kV: (a) 9 wt.% PAN, (b) 1 wt.% Gr, (c) 3 wt. % Gr, (d) 5 wt.% Gr. All other processing parameters held constant

The results on nanofibers diameters are compared in Figure 5.7. From the histogram we can see that independently of the applied voltage during electrospinning process, all the graphene based composite nanofibers presented smaller diameters than those of pure PAN nanofibers. As shown in Figure 5.7, it's generally observed that the diameters of composite nanofibers decreased with the increase of graphene nanoparticles in the electrospinning solutions. For nanofibers electrospun at 15 kV, the fibers diameters were 295.73 nm, 225.09 nm and 202.01 nm for PAN/Gr. composite nanofibers containing 1, 3, and 5 wt. % of graphene nanoparticles, respectively. However, at 20 kV as applied voltage, the fibers diameters were 268.1 nm, 224.61 nm

and 205.89 nm for PAN/Gr. composite nanofibers containing 1, 3, and 5 wt. % of graphene nanoparticles, respectively.

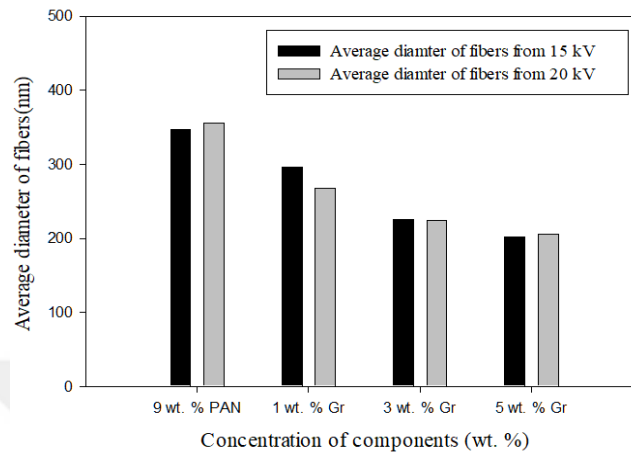


Figure 5. 7. Comparison of average diameter of the as-fabricated pure pan nanofibers and PAN/Gr. composite nanofibers with different graphene nanoparticles contents and applied voltages

5.1.2.3. Morphology and diameters of PAN/Silica NPs composite nanofibers

Figure 5.8 and Figure 5.9 show the SEM images of the as-spun PAN/SiO₂ composite nanofibers which contain different SiO₂ concentration (1, 3 and 5 wt. %) performed at 15 kV and 20 kV, respectively. The pure PAN nanofibers from 9 wt. % of PAN appear in both cases (15 kV and 20 kV) to be very uniform, smooth and without any beads compared to silica based composite nanofibers. Furthermore, although all the fabricated nanocomposites were beads-free, but all the SEM images indicate that the agglomeration of the silicon dioxide nanoparticles on the surface was obviously observed. Therefore, no-one would dispute that the addition of SiO₂ nanoparticles in the electrospinning solution has effected the morphology of the electrospun composite nanofibers. The change in morphology of silica based nanofibers with high silica contents are caused by the high solution viscosity, which must be overcome during electrospinning (Ji et al., 2008).

Figure 5.10 compares the diameters of pure PAN nanofibers to PAN/SiO₂ nanocomposites fabricated with different concentration of silicon dioxide nanoparticles. All the evidence suggests that the pure PAN nanofibers diameters were found to be smaller than any diameter of PAN/SiO₂ nanocomposites fabricated at 15 kV and 20 kV, respectively.

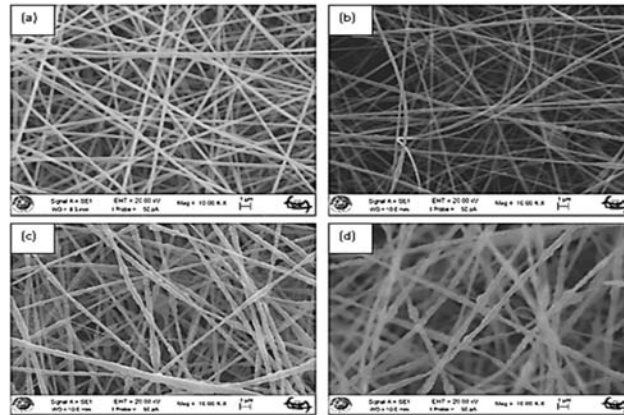


Figure 5. 8. SEM images of as-spun PAN and PAN/SiO₂ nanofibers from 9 wt. % of PAN solution containing different silica contents performed at 15 kV: (a) 9 wt.% PAN, (b) 1 wt.% SiO₂, (c) 3 wt. % SiO₂, (d) 5 wt.% SiO₂. All other processing parameters held constant

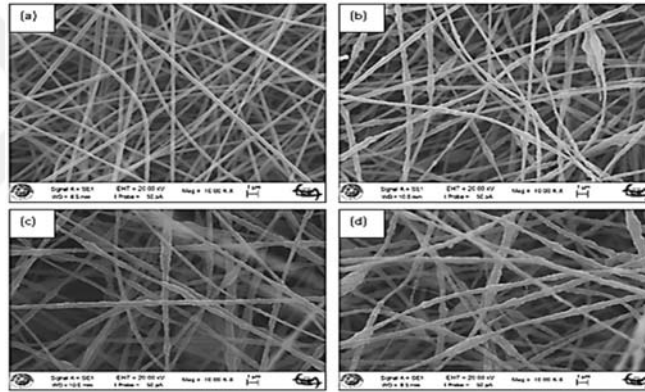


Figure 5. 9. SEM images of as-spun PAN and PAN/SiO₂ nanofibers from 9 wt. % of PAN solution containing different silica contents performed at 20 kV: (a) 9 wt.% PAN, (b) 1 wt.% SiO₂, (c) 3 wt. % SiO₂, (d) 5 wt.% SiO₂. All other processing parameters held constant

The average diameters of composite nanofibers performed at 15 kV increased with the SiO₂ nanoparticles concentration in the electrospinning solution. The fibers diameter increased from 347 nm for pure PAN fibers to 398.66 nm, 443.54 nm and 557.88 nm for PAN/SiO₂ composite nanofibers containing 1, 3, and 5 wt. % of silica nanoparticles, respectively. On the other hand, at 20 kV as applied voltage, fibers diameters increased from 355.94 nm for pure PAN fibers to 436.16 nm, 484.38 nm, and 513.81 nm for PAN/SiO₂ composite nanofibers containing 1, 3, and 5 wt. % of silica nanoparticles, respectively. The experiment results revealed that increasing the silica contents led to an increase of the average diameters of the fibers.

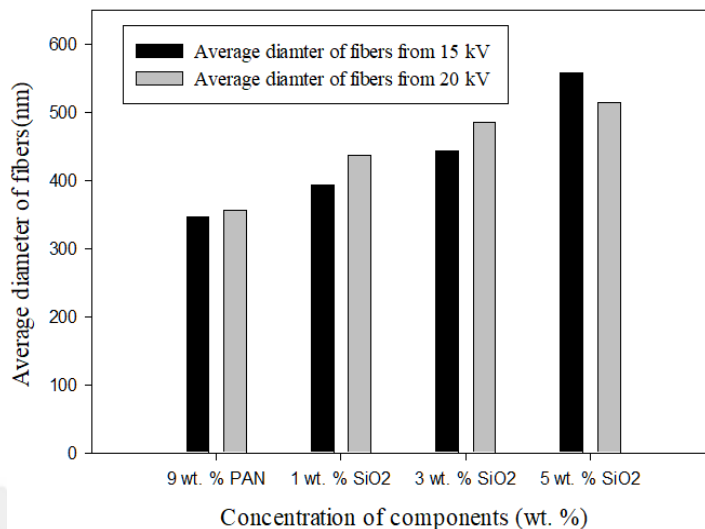


Figure 5. 10. Comparison of average diameter of the as-fabricated pure PAN nanofibers and PAN/SiO₂ composite nanofibers with different silica nanoparticles contents and applied voltages

5.1.2.4. Comparison of nanofibers diameters of various materials

The comparison of diameters of composite nanofibers reinforced with various inorganic nanoparticles contents (copper, graphene or silica) is presented in Figure 5.11 and Figure 5.12 for 15 kV and 20 kV as applied voltages, respectively.

The most remarkable result to emerge from the data is that average diameter of nanofibers containing silica nanoparticles was found to be higher than any other types of composite nanofibers (PAN/DMF/ CuNPs and PAN/DMF/ Gr.NPs). Furthermore, it is important to note that the average diameter of silica based nanofibers increased with the increase of silica nanoparticles contents in the electrospinning solution. This is in good agreement with Tański et al. (2016) findings. However, as can be seen from the Figure 5.11 and Figure 5.12 that adding graphene nanoparticles in the PAN/DMF solution tends to reduce the average diameter of the resultant composite nanofibers when the graphene content increases. For copper based composite nanofibers, even though no significant differences were found in terms of average diameters, it was observed that nanofibers with small diameters were obtained at low copper contents.

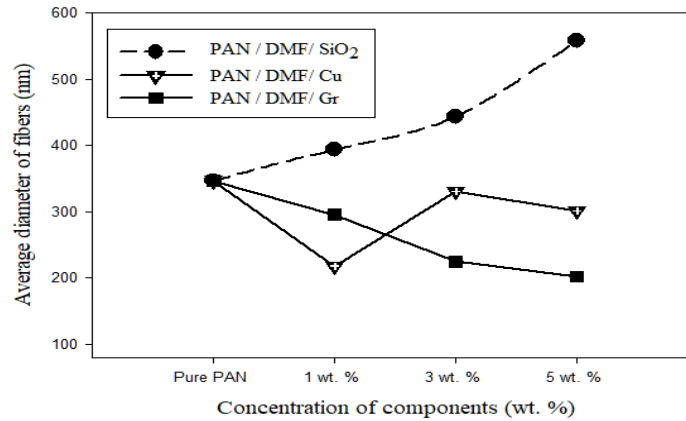


Figure 5.11. Comparison of average diameter of the as-fabricated composites nanofibers at 15 kV

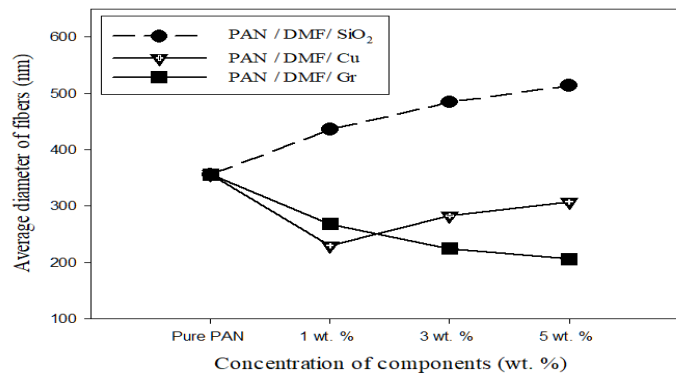


Figure 5.12. Comparison of average diameter of the as-fabricated composites nanofibers at 20 kV

5.2. Effect of Viscosity on Diameters of Electrospun Nanofibers

The fiber diameter is recognized as one of the most important quantities related with electrospinning. It has been reported that many parameters could influence the transformation of polymers solutions into nanofibers by the mean of electrospinning process. But as long as no splitting is involved, one of the most important parameters influencing the as-spun fiber diameter is the solution viscosity (Huang et al., 2003). So, in this research its effect on the as-spun nanofibers diameter was investigated.

Figure 5.13 shows a clear trend of nanofibers diameters with the change of copper solutions viscosity. Generally speaking, we have found that the fibers diameters increased with the increase of solutions viscosity. That's, fibers with smaller diameter were obtained at lower viscosity. This is in good agreement with the literature, a higher viscosity results in a large fiber diameter (Haghi, 2011). It is also important to point out

that at higher viscosity only a few fibers were obtained on the collector, due to the fact that the viscosity tended to prevent the motion of polymer solution induced by electric field (Frenot and Chronakis, 2003).

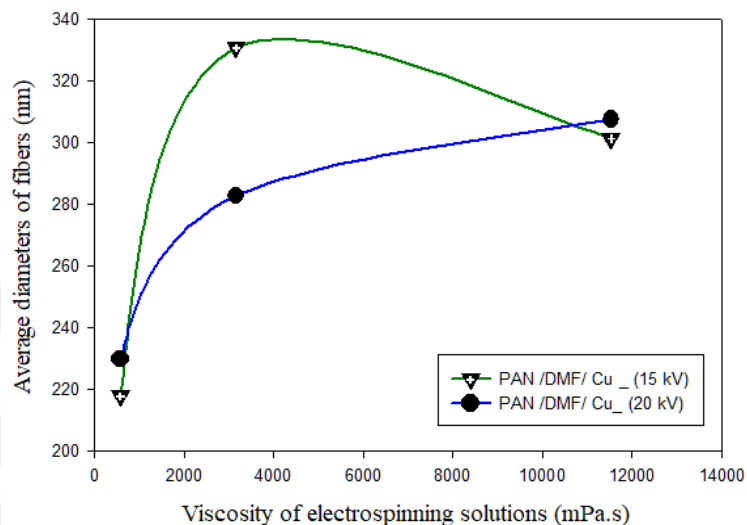


Figure 5.13. Variation of copper based fibers diameters in function of the solutions viscosity

Figure 5.14 reports the variation of electrospun fibers diameters in terms of the change of the viscosity of the graphene based solutions. With a closer inspection, our experiments reveals that the diameter of the graphene based fibers decreased with the increase of the viscosity of the electrospinning solutions.

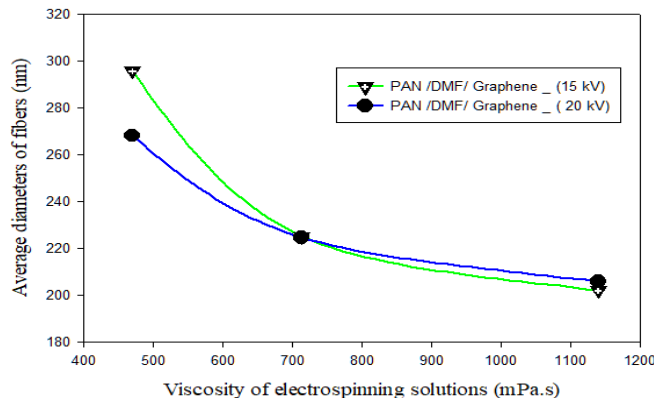


Figure 5.14. Variation of graphene based fibers diameter in function of the solutions viscosity

Figure 5.15 presents the data on the change of fibers diameters in terms of the variation of silica based solutions viscosity. As can be observed, the increase of the

viscosity of the electrospinning solutions led to the increase of fibers diameter. Our findings appear to be well supported by the fact that an increase in concentration corresponds to an increase in viscosity of the solution.

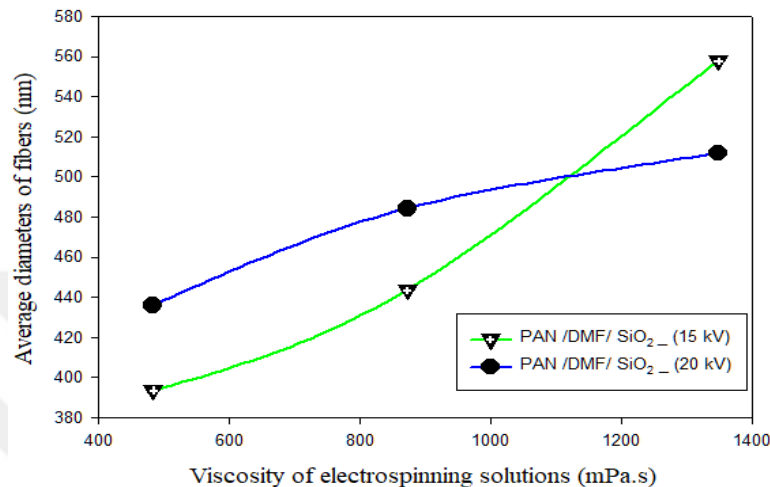


Figure 5.15. Variation of silica based fibers diameters in function of solutions viscosity

The Table 5.1 summarizes the data on the effect of solution viscosity of different materials on the diameter of their respective fibers.

Table 5.1. Fibers diameters in function of solution viscosity

Solutions	Dynamic viscosity mPa.s	Average fibers diameters	
		At 15kV as applied voltage	At 20 kV as applied voltage
PAN/DMF	462.5	347	355.9
PAN/DMF/ 1 wt.% Cu	577.7	217.9	229.9
PAN/DMF/ 3 wt.% Cu	3160.25	330.8	282.8
PAN/DMF/ 5 wt.% Cu	11526.66	301.3	307.5
PAN/DMF/ 1 wt.% Gr	470	295.73	268.1
PAN/DMF/ 3 wt.% Gr	713.8	225.09	224.61
PAN/DMF/ 5 wt.% Gr	1139.6	202.01	205.89
PAN/DMF/1 wt.% SiO ₂	484.72	393.66	436.16
PAN/DMF/3 wt.% SiO ₂	872.375	443.53	484.38
PAN/DMF/ 5 wt.% SiO ₂	1348	557.88	511.81

5.3. Electrical Conductivity of Nanofibers

In this section, the results on electrical conductivity of nanofibers containing nanoparticles will be presented as function of nanoparticles contents, nanofibers diameters, and solutions viscosity, respectively.

5.3.1. Electrical conductivity of nanofibers containing copper nanoparticles

The results on electrical conductivity of nanofibers containing different copper nanoparticles contents are compared in Figure 5.16. At 15 kV as applied voltage, electrical conductivity values found from the four-point probe technique were $5.81 \times 10^{-3} \text{S/cm}$ for pure PAN nanofibers and 1.38×10^{-2} , 8.69×10^{-3} and $4.43 \times 10^{-3} \text{S/cm}$ for nanofibers containing 1, 3 and 5 wt.% of copper nanoparticles contents, respectively. As can be seen from the Figure below, higher electrical conductivity were obtained at low copper nanoparticles contents (1 and 3wt. %). It is interesting to note that electrospun PAN nanofibers reinforced with 1 wt. % of copper performed at 15 kV present a 137.52 % increase in the value of electrical conductivity compared to pure PAN nanofibers. However, in 5 wt. % of copper nanoparticles contents, nanofibers presented an electrical conductivity lower than that of pure PAN nanofibers.

At 20 kV as applied voltage, electrical conductivity values of nanofibers were $1.63 \times 10^{-3} \text{S/cm}$ for pure PAN nanofibers and 2.83×10^{-2} , 2.85×10^{-3} and $3.88 \times 10^{-3} \text{S/cm}$ for nanofibers containing 1, 3 and 5 wt. % of copper nanoparticles contents, respectively. It is clear from the Figure 5.16 that all electrical conductivity values of the resultant composite nanofibers were higher than that of its respective pure PAN nanofibers. In 1 wt. % of copper nanoparticles contents, an increase of 1636.19 % in the value of electrical conductivity of the resultant fibers was observed compared to its pure PAN nanofibers. Even though, the values of electrical conductivity of copper based nanofibers were found to be higher than that of pure PAN nanofibers, the experiment results revealed that electrical conductivity of electrospun nanocomposites fibers decreased with the increase of copper nanoparticles contents in the solution.

The dispersion of small amount (1 wt. %) of copper nanoparticles in the electrospinning solution not only has led to a decrease of the average diameter of the as prepared nanofibers but also to the highest value of electrical conductivity in both cases of applied voltage (15 kV and 20 kV).

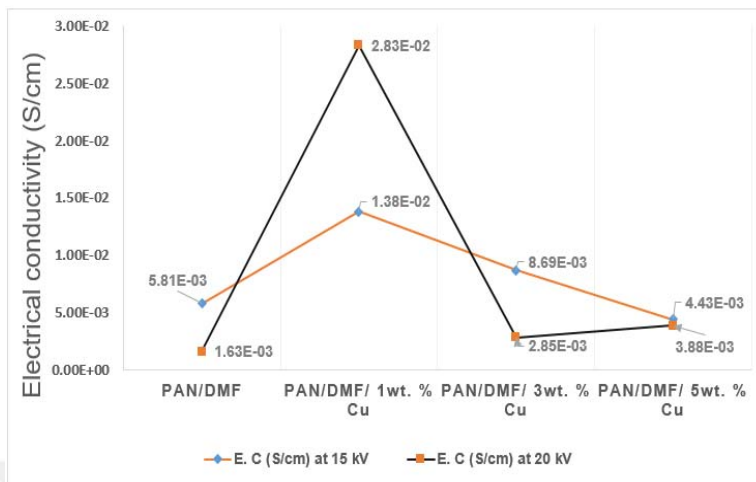


Figure 5. 16. Comparison of electrical conductivity of nanofibers containing different copper contents (1, 3 and 5 wt. %) for various applied voltages (15 kV and 20 kV)

5.3.2. Electrical conductivity of nanofibers containing graphene nanoparticles

Figure 5.17 shows the variation of electrical conductivity of the as-spun composite nanofibers in terms of graphene nanoparticles contents in the electrospinning solutions and applied voltage during electrospinning process. At 15 kV as applied voltage, electrical conductivity values of the as-spun composite nanofibers were 8.85×10^{-3} , 5.78×10^{-3} and 1.38×10^{-3} S/cm for nanofibers containing 1, 3 and 5 wt. % of graphene nanoparticles contents, respectively. As shown in Figure 5.17, higher values of electrical conductivity were found at low graphene nanoparticles contents (1 wt. %). In 1 wt. %, an increase of 52.32% in the value of electrical conductivity was observed compared to its respective pure PAN (PAN nanofibers fabricated at 15 kV). It is interesting to note that at 15 kV, increasing the content of graphene nanoparticles (3 wt. % and 5 wt. %) led to a diminution of values of electrical conductivity, as can be seen in Figure 5.17.

However, at 20 kV as applied voltage, electrical conductivity values of composite nanofibers were 2.79×10^{-3} , 2.64×10^{-3} and 5.01×10^{-3} S/cm for nanofibers containing 1, 3 and 5 wt. % of graphene nanoparticles contents, respectively. It has been observed that nanofibers reinforced with 5 wt. % of graphene at 20 kV present a 207.36% increase in the value of electrical conductivity compared to its pure PAN nanofibers. Unlike nanofibers fabricated at 15 kV as applied voltage, electrical

conductivity of nanofibers fabricated at 20 kV were found to increase with an increase of graphene contents in the electrospinning solution.

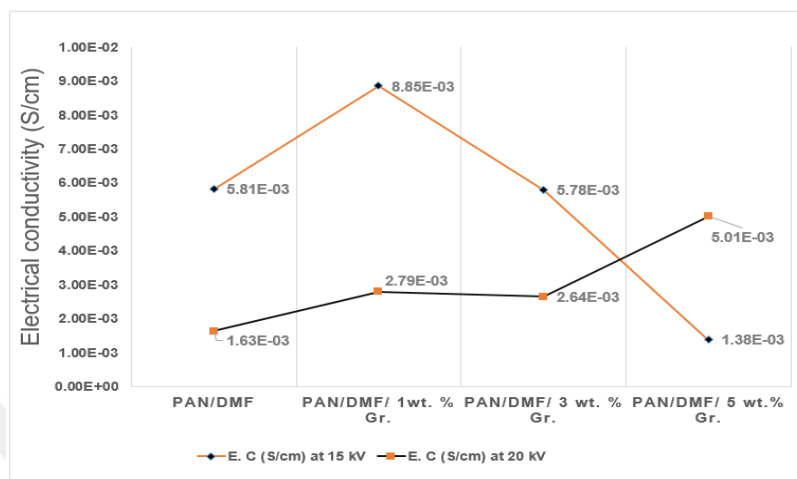


Figure 5. 17. Comparison of electrical conductivity of nanofibers containing different Graphene nanoparticles contents (1, 3 and 5 wt. %) for various applied voltages (15 kV and 20 kV)

The most striking result to emerge from the experiment is how the percolation threshold was affected by the applied voltage. As can be seen from Figure 5.17, at 15 kV the electrical conductivity increased suddenly (In 1 wt. % of graphene contents) and then started to decrease when the graphene content was higher than 1 wt. %. However, at 20 kV, even if the as-spun composite nanofibers did not exhibit a linear increase of electrical conductivity as a function of graphene nanoparticles contents, it is worth to say that the percolation threshold was beyond of 5 wt. %.

5.3.3. Electrical conductivity of nanofibers containing silica nanoparticles

The results on electrical conductivity of nanofibers containing different silica nanoparticles contents are compared in Figure 5.18. For nanocomposites fibers based SiO₂ nanoparticles electrospun at 15 kV, the conductivity of nanofibers containing 1, 3 and 5 wt. % SiO₂ was 7.10×10^{-3} , 8.26×10^{-3} and 4.19×10^{-3} S/cm, respectively. As can be observed the electrospun PAN nanofibers reinforced with 3 wt. % of silica performed at 15 kV present a 42.16 % increase in the value of electrical conductivity compared to its pure PAN nanofibers. However, it has been observed that the nanofibers reinforced with 5 wt. % of silica have presented an electrical conductivity lower than

that of pure PAN nanofibers. Hence, we believe that the percolation threshold was beyond of 3 wt. %.

However, for nanocomposites fibers based SiO₂ nanoparticles electrospun at 20 kV, the conductivity of nanofibers containing 1, 3 and 5 wt. % SiO₂ was 8.11×10^{-3} , 5.96×10^{-3} and 2.08×10^{-3} S/cm, respectively. It was found that even though the values of electrical conductivity of composite nanofibers were higher than that of pure PAN nanofibers, the electrical conductivity of fibers decreased with an increase of silica nanoparticles contents in the electrospinning solution. The electrospun PAN nanofibers reinforced with 1 wt. % of silica performed at 20 kV present a 397.54 % increase in the value of electrical conductivity compared to pure PAN nanofibers. Whereas, only a 27.6 % increase in the value of electrical conductivity was observed at 5 wt. % of silica contents.

From experimentation results, all the evidence suggested that independently of the applied voltage during the electrospinning process, the addition of silica nanoparticles up to a certain amount in PAN/DMF solution could improve the electrical conductivity of the resultant nanocomposites. Furthermore, higher values of electrical conductivity were found at low silica nanoparticles contents (1 and 3 wt. %).

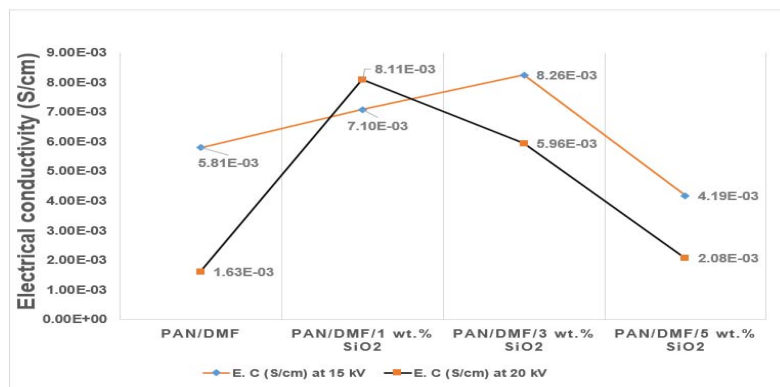


Figure 5. 18. Comparison of electrical conductivity of nanofibers containing different silica nanoparticles contents (1, 3 and 5wt. %) for various applied voltages (15 kV and 20 kV)

5.3.4. Comparison of electrical conductivity of various composite nanofibers

Figure 5.19 shows the variation of electrical conductivity of composite nanofibers fabricated at 15 kV as applied voltage in terms of inorganic nanoparticles contents. Generally speaking, our results show that the dispersion of a small amount of inorganic nanoparticles (copper, graphene or silica) in the electrospinning solution led

to higher values of electrical conductivity of the resultant nanofibers. The experiment results revealed that by further increasing nanoparticles contents up to a certain level in the electrospinning solution could affect negatively the electrical conductivity of the resultant nanofibers.

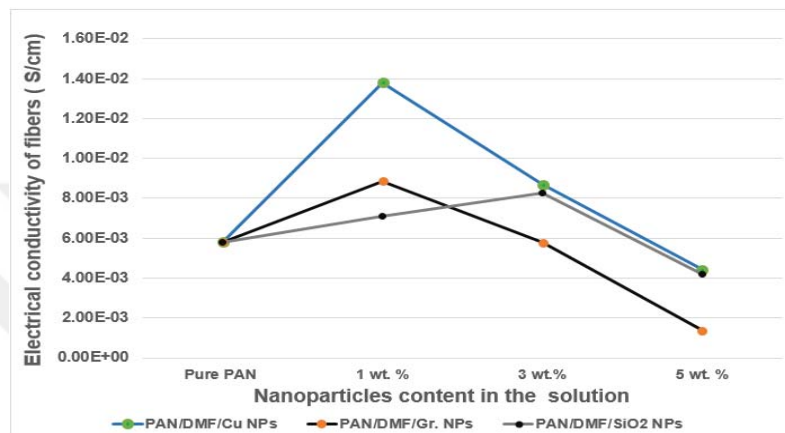


Figure 5. 19. Comparison of electrical conductivity (S/cm) of the as-fabricated composites nanofibers at 15 kV

As can be seen from Figure 5.19, at around 3 wt. % of graphene, the electrical conductivity of its resultant nanofibers started to become lower (5.78×10^{-3} S/cm) compared to that of pure PAN nanofibers (5.81×10^{-3} S/cm). However, at 5 wt. % of nanoparticles contents it was observed that all nanocomposites fabricated at 15 kV as applied voltage presented electrical conductivities lower than that of pure PAN nanofibers. The single most marked observation to emerge from the data comparison was nanofibers containing copper nanoparticles presented highest values of electrical conductivity in all cases.

The influence of nanoparticles contents on the electrical conductivity of composite nanofibers fabricated at 20 kV as applied voltage is presented on Figure 5.20. The four-point probe results revealed that copper and silica nanofibers presented their highest values of electrical conductivity at 1 wt.% of their respective nanoparticles contents. In addition, increasing the nanoparticles (copper and silica) concentration in their respective electrospinning solutions led to the decrease of electrical conductivity of their resultant composite nanofibers. However, the most striking results to emerge from the data comparison was how the percolation threshold was beyond of 5 wt. % of

graphene contents in nanofibers. As shown in Figure 5.20, electrical conductivity of composite nanofibers increased with the increase of graphene nanoparticles in the solutions.

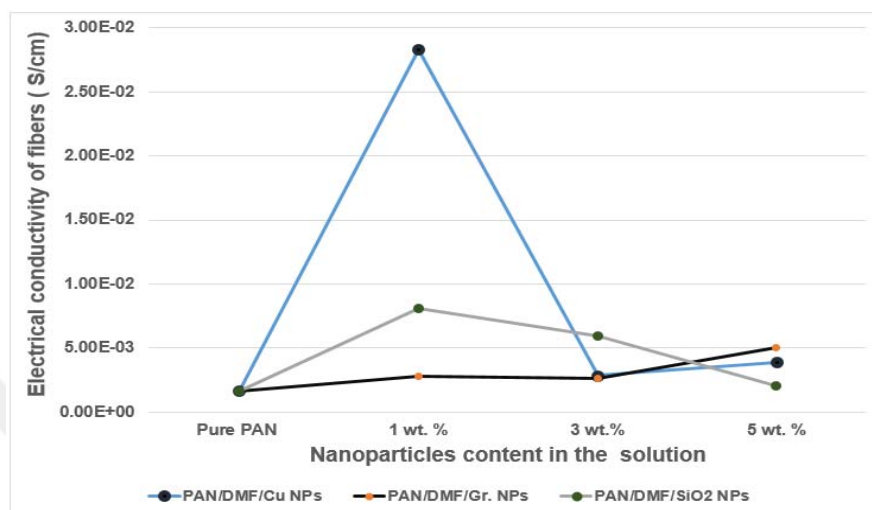


Figure 5. 20. Comparison of electrical conductivity(S/cm) of the as-fabricated composites nanofibers at 20 kV

Table 5.2. summarizes the data on the electrical conductivity of different as-spun nanofibers. As can be observed, in both applied voltage (15kV and 20kV) the highest values were obtained with nanofibers containing 1wt. % of copper nanoparticles. In addition, it is clear that the majority of nanofibers samples fabricated at 15 kV presented higher electrical conductivity than their homologues fabricated at 20 kV. According to the obtained results, we believe that not only the amount of nanoparticles contents in the electrospinning solution could affect the electrical conductivity of the resultant nanofibers but also the applied voltage during electrospinning process.

Table 5. 2. Comparison of electrical conductivity of different nanofibers at different applied voltages

Types of nanofibers	Electrical conductivity of nanofibers (S/cm)	
	At 15kV as applied voltage	At 20 kV as applied voltage
PAN/DMF	5.81E ⁻⁰³	1.63E ⁻⁰³
PAN/DMF/ 1 wt.% Cu	1.38E ⁻⁰²	2.83E ⁻⁰²
PAN/DMF/ 3 wt.% Cu	8.69E ⁻⁰³	2.85E ⁻⁰³
PAN/DMF/ 5 wt.% Cu	4.43E ⁻⁰³	3.88E ⁻⁰³
PAN/DMF/ 1 wt.% Gr	8.85E ⁻⁰³	2.79E ⁻⁰³
PAN/DMF/ 3 wt.% Gr	5.78E ⁻⁰³	2.64E ⁻⁰³
PAN/DMF/ 5 wt.% Gr	1.38E ⁻⁰³	5.01E ⁻⁰³
PAN/DMF/ 1 wt.% SiO ₂	7.10E ⁻⁰³	8.11E ⁻⁰³
PAN/DMF/ 3 wt.% SiO ₂	8.26E ⁻⁰³	5.96E ⁻⁰³
PAN/DMF/ 5 wt.% SiO ₂	4.19E ⁻⁰³	2.08E ⁻⁰³

5.3.5. Effect of fibers diameter on electrical conductivity

The properties of as-spun nanofibers depend not only on the nature of the chemicals of the electrospinning solutions but also on its structural characteristics such as fiber diameter, pore size, uniformity and fiber orientation (Haghi, 2011). Since, it has been reported by many researchers that the fiber diameter is a paramount structural characteristic for the resultant nanofibers, in this section the influence of fiber diameter on electrical conductivity was investigated.

As can be seen in Figure 5.21, nanofibers produced at 15 kV as applied voltage, presented controversial results due to the fact that each type of composite materials showed different results based on its respective diameters. Notably, PAN/DMF/Cu and PAN/DMF/SiO₂ fibers presented at least higher electrical conductivity when the diameter of the fibers were found to be small in their respective ranges. However, the results for PAN/DMF/graphene fibers were completely different compared to the previous ones. In fact, it was found that the electrical conductivity increased with the fiber diameter.

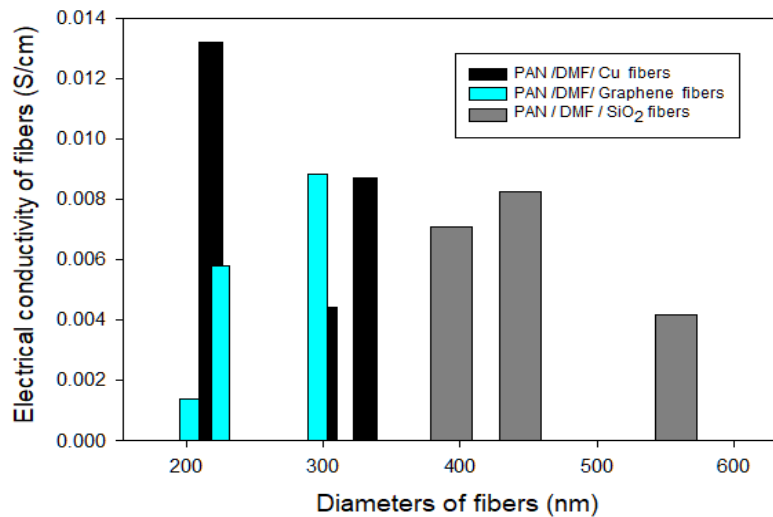


Figure 5. 21. Variation of electrical conductivity in function of fibers diameter (15 kV)

The Figure 5.22 outlines the results obtained from fibers performed at 20 kV, the correlation between the fiber diameter and the electrical conductivity is noteworthy because for each type of composite materials we have found that fibers with small diameter led to the highest electrical conductivity values.

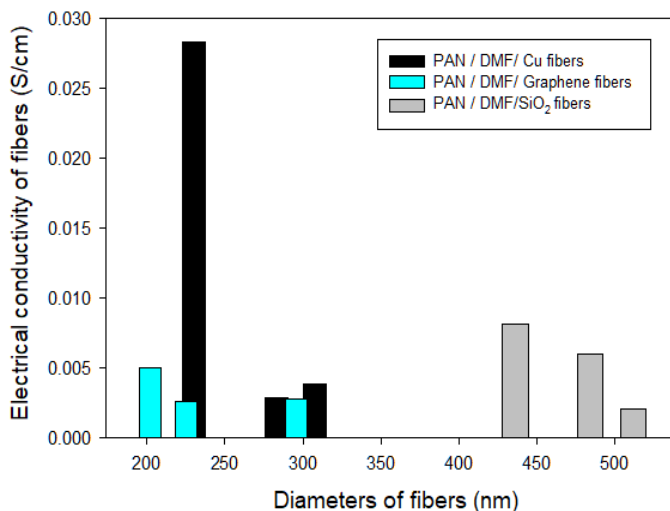


Figure 5. 22. Variation of electrical conductivity in function of fibers diameter (20 kV)

5.3.6. Effect of solution viscosity on electrical conductivity

In this section the influence of solution viscosity on electrical conductivity was investigated and the resultant variations were plotted and discussed below.

As can be seen in Figure 5.23, for PAN/DMF/Cu solutions, higher solution viscosity led to fibers with lower electrical conductivity. In other words, independently of the applied voltage (15 kV or 20 kV), our findings have shown that increasing solution viscosity could affect negatively the electrical properties of the resultant fibers.

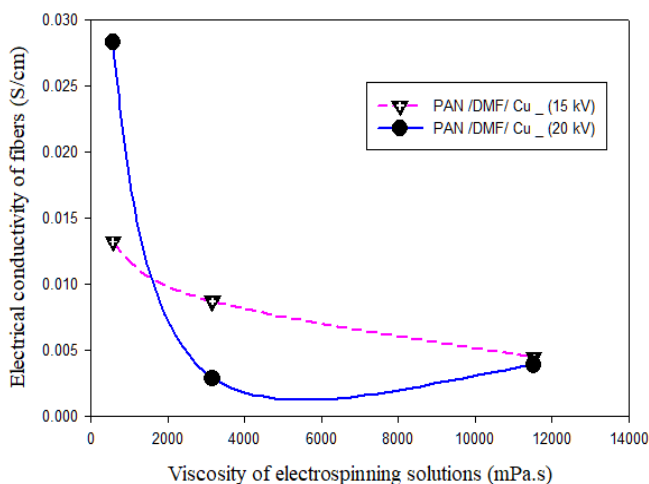


Figure 5. 23. Variation of electrical conductivity of PAN/DMF/ Cu fibers in function of solutions viscosity

Figure 5.24 shows the changes in electrical conductivity of PAN/DMF/ graphene fibers in terms of the solution viscosity. The conspicuous observation to emerge from the graph is that there was a remarkable difference between fibers produced at 15 kV and those performed at 20 kV. Nanofibers obtained at 15 kV presented higher electrical conductivity at low viscosity range. However, nanofibers obtained at 20 kV showed higher electrical conductivity at higher viscosity values. This can be attributed by the change in the percolation threshold observed when nanofibers were produced at 20 kV. An outstanding electrically conductive PAN/graphene composite was expected to have lower percolation threshold and higher conductivity at a lower graphene loading, which leads to a low solution viscosity as preconized by Stankovich et al. (2006).

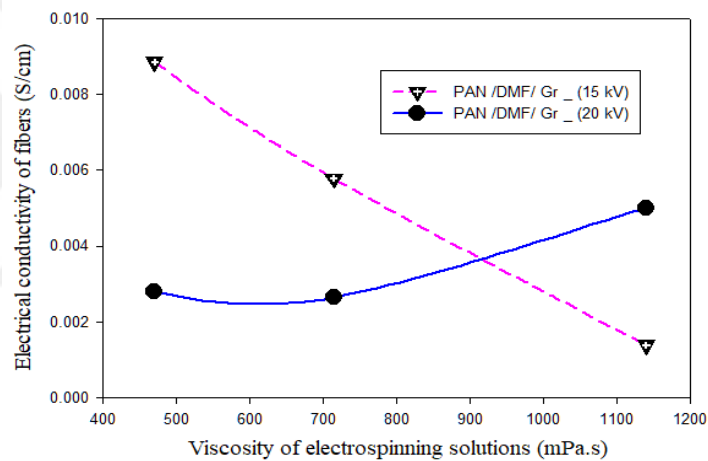


Figure 5. 24. Variation of electrical conductivity of PAN/DMF/ graphene fibers in function of solutions viscosity

Figure 5.25 presents the variation of electrical conductivity of PAN /DMF/ SiO₂ fibers in function of the solution viscosity changes. As expected, independently of the applied voltage during electrospinning process, fibers with higher electrical conductivity were obtained at low viscosity ranges. Therefore, it can be stated that increasing the viscosity of the solution has affected negatively the electrical conductivity of PAN /DMF/ SiO₂ composite materials.

By analyzing all the results plotted above, we are of the opinion that the viscosity of the electrospinning solution can affect the electrical properties of the resultant nanofibers, especially its electrical conductivity.

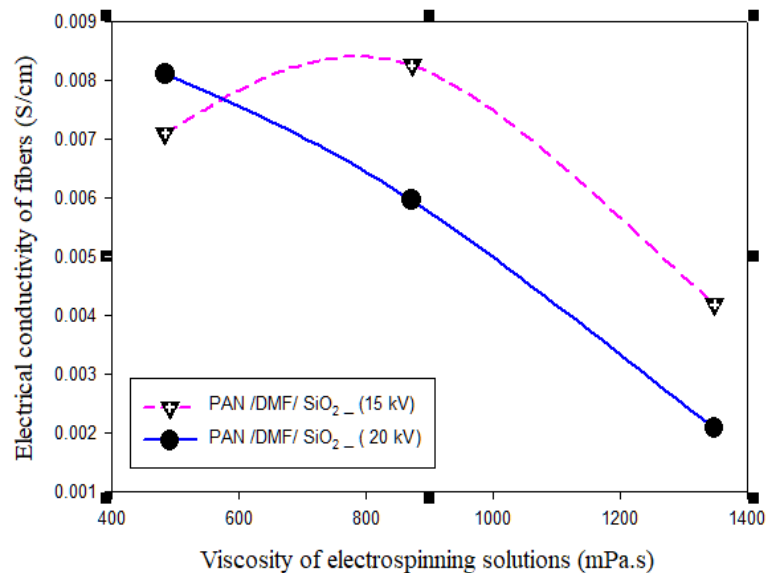


Figure 5. 25. Variation of electrical conductivity of PAN/DMF/ SiO₂ fibers in function of solutions viscosity

5.3.7. Comparison of electrical conductivity values to the literature studies

In order to have an idea of the range of our results, in the following Table, different results of this study were compared to the literature ones. To the best of our knowledge, the investigation of electrical conductivity of PAN polymer containing graphene, copper and silica have not yet been examined before.

Table 5. 3. Comparison of electrical conductivity values

Chemicals	Electrical conductivity (S/cm)	References	Comments
Pure PAN in DMF	5.81E ⁻⁰³	This study	Nanofibers produced at 15 kV
Pure PAN in DMF	1.63E ⁻⁰³	This study	Nanofibers produced at 20 kV
PAN/DMF/ Cu	1.38E ⁻⁰²	This study	Nanofibers produced at 15 kV
PAN/DMF/ Cu	2.83E ⁻⁰²	This study	Nanofibers produced at 20 kV
PAN/DMF/ Graphene	8.85E ⁻⁰³	This study	Nanofibers produced at 15 kV
PAN/DMF/ Graphene	5.01E ⁻⁰³	This study	Nanofibers produced at 20 kV
PAN/DMF/ SiO ₂	8.26E ⁻⁰³	This study	Nanofibers produced at 15 kV
PAN/DMF/ SiO ₂	8.11E ⁻⁰³	This study	Nanofibers produced at 20 kV
Pure PAN in DMF	0.2 – 0.5	Ra et al. (2005)	The electrical conductivity of the pure PAN nanofiber changed with the carbonization temperature. Aligned nanofiber membrane
Pure PAN in DMF	6.8 E ⁻⁰³ and 1.96	Kim et al. (2002)	Carbonized at 700 and 1000°C, respectively
PVA/MWCNT-MnO ₂	6.99 E ⁻⁰⁶	Zamri et al. (2011)	
PVA/MWCNT	5.263 E ⁻⁰⁶	Zamri et al. (2011)	
Neat PVA	1.25 E ⁻¹⁵	Zamri et al. (2011)	
PAN/Ag/ DMSO	1 E ⁻⁰⁸	Demirsoy et al. (2015)	
Pure PAN in DMF	1.42	Panapoy et al. (2008)	Carbonized at 1000°C
Gold	1.2 E ⁻⁰⁴	Pol et al (2008)	Single nanofiber Fiber
Nylon-6 with polyaniline	1.3	Hong et al (2005)	Polymerization technique. Randomly oriented nanofiber membrane fiber
Polypyrrole [PPy(SO ₃ H)-DEHS]	2.7 E ⁻⁰²	Chronakis et al (2006)	Not blending. Randomly oriented nanofiber membrane fiber.
Poly(L-lactide) with polyaniline	0.3	Dong et al (2004)	Randomly oriented nanofiber membrane fiber
Polyvinyl alcohol with Nafion (1:5)	1.7 E ⁻⁰²	Laforgue et al (2007)	Randomly oriented nanofiber membrane fiber
Poly(methyl methacrylate) with 2 wt% multi-walled carbon nanotube	5.3 E ⁻⁰⁴	Sundaray et al (2006)	Blending technique. Single fiber
Silk membrane coated with multi-walled carbon nanotube	2.4 E ⁻⁰⁴	Kang et al (2007)	Surface coating by dipping in carbon nanotube suspension. Randomly oriented nanofiber membrane fiber
Polyethylene oxide with polypyrrole coating	1 E ⁻⁰³	Nair et al (2005)	Surface polymerization. Randomly oriented nanofiber membrane fiber

5.3. Contact Angle Results

This section presents the results of the investigation on the hydrophobic behavior of the as-spun fibers in the presence or absence of nanoparticles such as copper, silica and graphene. As it was reported from the open literature, a hydrophilic surface is one on which a droplet of water forms a contact angle less than 90° , whereas a hydrophobic surface is one on which a droplet forms a contact angle greater than 90° (Alarifi et al. (2015); Groszek and Partyka (1993)). However, when a contact angle is between 150° and 180° , polymer surfaces are called superhydrophobic. The phenomenon is also known as the lotus effect, which exhibits self-cleaning and anti-contamination features, which means that contamination can be easily washed away by liquid (Nuraje et al. (2013); Dong et al. (2013)).

Since the main purpose of this study to investigate the effect of nanoparticles on the electrical conductivity of the electrospun composite nanofibers, in this section only nanocomposite samples which presented the highest electrical conductivity values were investigated and compared to pure PAN nanofibers results. To do so, the hydrophobicity of pure PAN and nanocomposites fibers were investigated using the contact angle measurement device (Dataphysics instruments GmbH, model OCA15 Pro, version 1.3) and a dosing volume of $2 \mu\text{L}$ of water at $0.5 \mu\text{L/s}$ as dosing rate was used. The thin film samples of nanocomposite fibers were placed on a glass plate and a single drop of water deposited on top of the films by a syringe. At least three static contact angles were measured at different positions and the obtained results were averaged for each sample.

5.3.1. Contact angle of graphene nanoparticles -based nanofibers

Graphene is a two-dimensional crystal of carbon, with many potential applications such as novel sensors, biomedical devices, efficient transistors and flexible electronics.

A number of graphene-based devices will have to operate in ambient conditions where humidity conditions is different to zero and not be controlled. Therefore, the performance of the graphene can be affected by the air humidity of the ambient conditions. Hence, it is necessary to pay attention to the hydrophobic behavior of graphene based nanofibers. Pristine graphene is usually a hydrophobic material. Contrary to widely- held beliefs, the findings indicate that the hydrophobic behavior of

graphene is highly thickness dependent. Researches revealed that single-layer graphene is more significantly hydrophilic than its thicker counterparts (<http://www.npl.co.uk/>).

Figure 5.26. presents the average static contact angles of pure PAN nanofibers and composite nanofibers containing 1 wt. % and 5 wt. % of graphene nanoparticles contents. The pure PAN nanofibers in both applied voltages (15 kV and 20 kV) showed a hydrophobic surfaces while the results for composite nanofibers were graphene contents dependent. The results revealed that the hydrophilicity of nanofibers surface increases with the amount of graphene nanoparticles in the electrospinning solution. As can be seen in Figure 5.26, the value of the average static contact angle of nanofibers with 1 wt. % of graphene was 115.3° whereas that of nanofibers with 5 wt. % decreased to 33.27°.

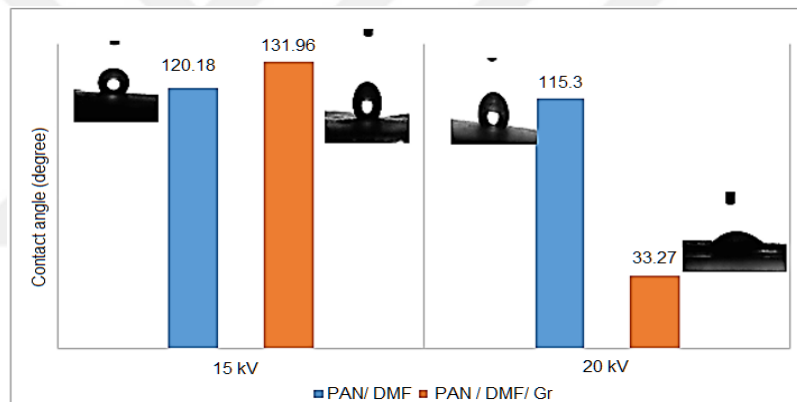


Figure 5. 26. Average static contact angles of the as-fabricated pure PAN and PAN/Gr. Nanofibers at different applied voltages

5.3.2. Contact angle of silica nanoparticles-based nanofibers

Figure 5.27. shows the average static water contact angles of pure PAN nanofibers and composite nanofibers containing 1 wt. % and 3 wt. % of SiO₂ nanoparticles concentration. As can be seen in Figure 5.27, the applied voltage during electrospinning process did not affect the hydrophobic behavior of nanofibers. The contact angles for pure PAN nanofibers were 120.8° and 115.3° for samples electrospun at 15 kV and 20 kV, respectively, and those of composite nanofibers were 123.06° and 125.42° for samples electrospun at 15 kV and 20 kV, respectively. For both applied voltages (15 kV and 20 kV) the contact angles were greater than 90°, hence, wetting of the surface of nanofibers is unfavorable so the liquid will bead on the surface. Although

the incorporation of silicon dioxide nanoparticles in the electrospinning solution led to an increase of contact angle values of the electrospun nanofibers, but did not change its hydrophobic state.

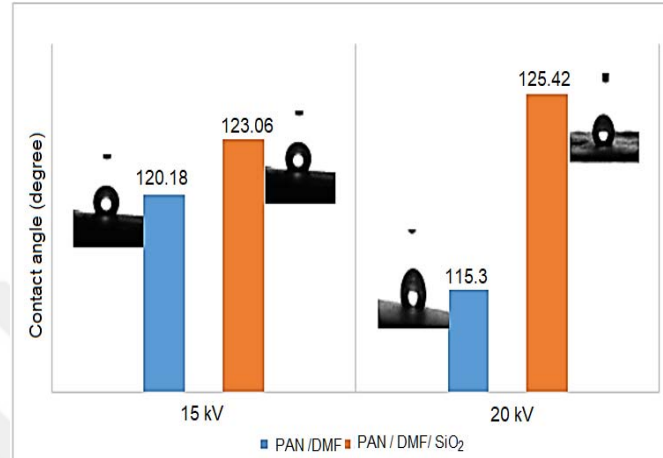


Figure 5. 27. Average static contact angles of the as-fabricated pure PAN and PAN/SiO₂ Nanofibers at different applied voltages

5.3.3. Contact angle of copper nanoparticles-based nanofibers

Since only nanofibers samples which presented the highest values of electrical conductivity were picked out for hydrophobicity investigation, in this section samples containing 1 wt. % of copper nanoparticles were investigated. The contact angle measurement results revealed that nanofibers containing 1 wt. % of copper nanoparticles showed an hydrophobic behavior. As illustrated in Figure 5.28, there was a slight difference between both contact angle values of composite nanofibers. It is important to note how the hydrophobic behavior of nanofibers surfaces was improved in both cases by adding 1 wt.% : from 120.18° to 124.93° and from 115.3° to 125.93° for nanofibers fabricated at 15 kV and 20 kV as applied voltage, respectively.

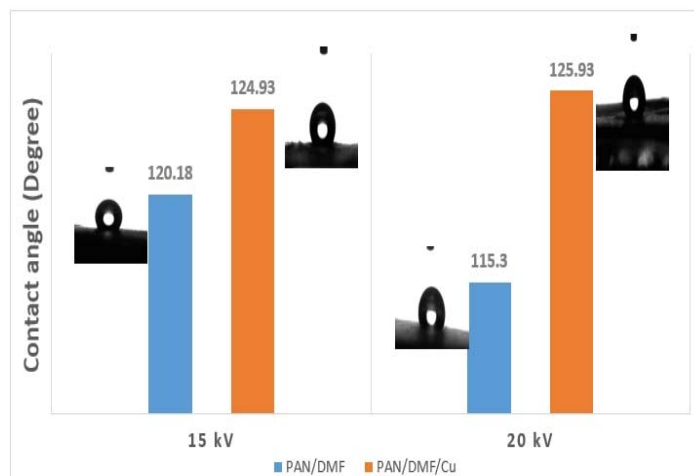


Figure 5. 28. Average static contact angles of the as-fabricated pure PAN and PAN/Cu. Nanofibers at different applied voltages

5.4. XRD- Results

XRD was performed to give detailed information on the structure of crystalline samples and to confirm the phase composition of the as-spun nanofibers. The respective results will be presented and discussed in the following sub-sections.

5.4.1. XRD patterns of pure PAN and Cu/PAN nanofibers

As can be seen in Figure 5.29 below, two broad peaks were found for either nanofibers sample. The first broad peak is located at around $2\theta = 16^\circ$, which represents the x-ray reflection of the (100) crystallographic plane in PAN (Zussman et al., 2005). The second peak which was sharper than the first one was found at around $2\theta = 23^\circ$ and reveals the crystalline structure of the materials. Furthermore, such a peak does not make any significant shifts but it was observed a decrease of the relative intensity of peaks when Cu nanoparticles were added in the electrospinning solution. Since a decrease in peak intensity was observed in either sample (sample performed at 15 kV or 20 kV), it can be said that there is an interaction between copper nanoparticles and PAN polymer. However, as is well known that XRD is not a trace analysis technique. Therefore, a component should be present at 3-5% by weight at a minimum in order for diffraction peaks to be detected (Robinson et al., 2014). The content of copper nanoparticles in the prepared solution was 1wt. %. Although two small peaks were found at around $2\theta = 36^\circ$ and $2\theta = 39^\circ$ for samples containing copper

nanoparticles, it can be attributed with reserve to copper nanoparticles due to the fact that a closer inspection revealed that the positions of these peaks are different to those of pure copper nanoparticles.

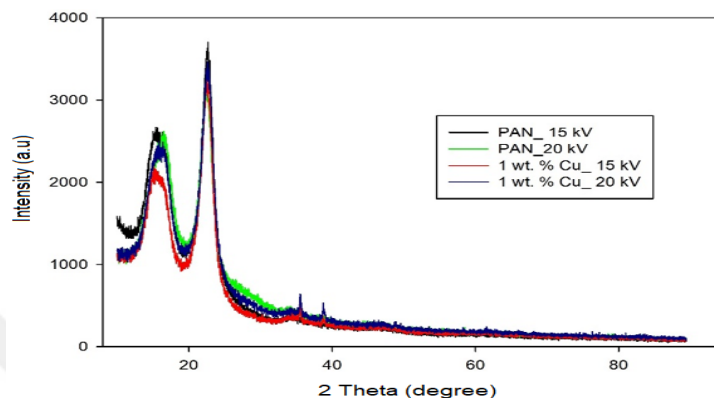


Figure 5. 29. XRD patterns of pure PAN and PAN/Cu NPs nanofibers

5.4.2. XRD patterns of pure PAN and graphene /PAN nanofibers

Even though the pure graphene nanoparticles have no diffraction peaks, XRD was used to further characterize the crystalline structure in the as-spun graphene based nanofibers. Figure 5.30 shows a significant difference in terms of diffraction peaks between pure PAN and graphene-based nanofibers. As highlighted in the previous section, the intensities of diffraction peaks of PAN were affected by the incorporation of graphene nanoparticles in the solution. A decrease in terms of diffraction peaks led to a decrease of the degree of crystallinity of PAN/Graphene nanofibers. The most part of materials was in the amorphous state. This can be justified by the existence of only broad peak of PAN without another one elsewhere.

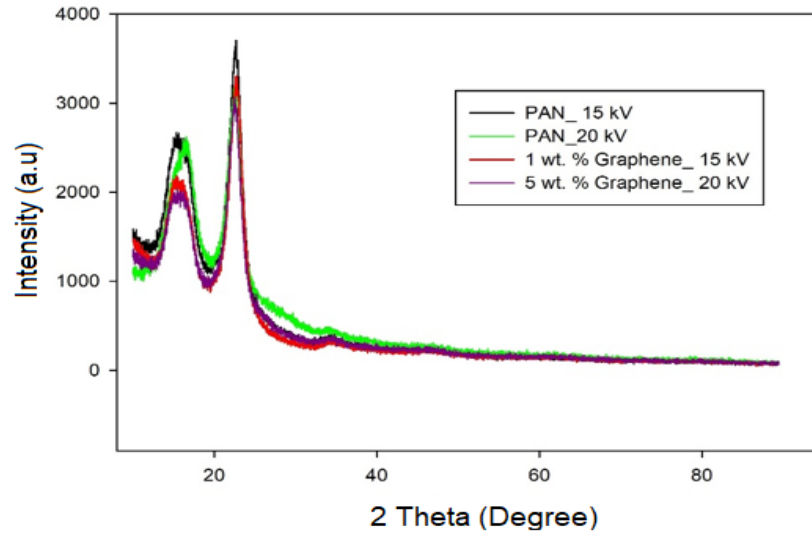


Figure 5. 30. XRD patterns of pure PAN and PAN/Graphene NPs nanofibers

5.4.3. XRD patterns of pure PAN and SiO₂/PAN nanofibers

The pure PAN and electrospun nanocomposites based silica nanoparticles were characterized by X-ray diffractometer (XRD) and the results were shown in Figure 5.31. As can be observed a difference in diffraction peaks between pure PAN and PAN/SiO₂ nanofibers patterns. It means that there is an interaction of silica nanoparticles with PAN in the resultant nanofibers. Broad diffraction peaks were found in either pattern, this means that a considerable parts of PAN and Silica were in the amorphous form, but a few of them were crystalline. In addition, the XRD results for both pure PAN and silica based nanofibers suggest that the full width at half the maximum (FWHM) of peaks are large and therefore correspond to smaller crystallites.

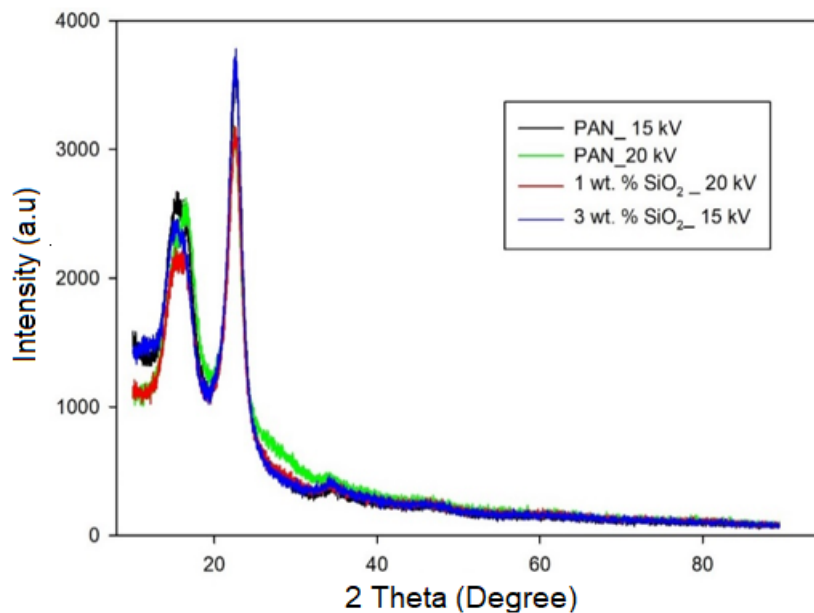


Figure 5. 31. XRD patterns of pure PAN and PAN/SiO₂ NPs nanofibers

In both cases (15 kV and 20 kV), it was observed that the values of peak intensity of Pure PAN nanofibers were higher than those of nanofibers containing silica nanoparticles. Therefore the degree of crystallization of nanocomposite fibers was lower than that of pure PAN. Respect to all observations made above, no-one would dispute that SiO₂ nanoparticles has affected the crystallinity of PAN nanofibers.

5.5. Thermal Analysis.

In this study, thermogravimetric analyzer (TGA) and differential scanning calorimetry were used in order to investigate the thermal behavior of the as-spun nanofibers. To do so, samples of pure PAN nanofibers and PAN composite nanofibers were analyzed. The samples were heated from 0 - 900°C with heating rate of 10°C/min in Nitrogen atmosphere with a pure rate of 20 mL/min. The results of the investigation are presented in the Table 5.4 below.

Table 5. 4. Thermal behavior of PAN/NPs composite nanofibers

Materials	Step		Residue		T _{onset} (°C)	C _p (mW/°C)	T _p (°C)	Comments (kV)
	(%)	(mg)	(%)	(mg)				
Pure PAN 15 kV	-77.1636	-0.8287	22.6765	0.2435	296.57	0.34	295	Nanofibers 15
Pure PAN 20 kV	-80.4830	-0.2974	21.0470	0.00077	291.27	0.12	296	Nanofibers 20
PAN/DMF/ 1wt % SiO ₂	-67.2862	-0.8498	32.3090	0.4080	298.39	0.57	298	Nanofibers 20
PAN/DMF/ 3wt % SiO ₂	-55.6038	-0.2419	44.3678	0.1930	292.33	0.22	298	Nanofibers 15
PAN/DMF/ 1wt % Cu	-74.1048	-2.444	26.0652	0.8596	298.11	-----	300	Nanofibers 15
PAN/DMF/ 1wt % Cu	-66.8569	-5.5705	33.1515	2.7622	301.05	-----	300	Nanofibers 20
PAN/DMF/ 1wt % Gr.	-90.653	-0.1824	8.8987	0.00017	253.98	0.00037	288	Nanofibers 15
PAN/DMF/ 5wt % Gr	-55.9963	-0.4752	43.7886	0.3718	260.93	0.00029	307	Nanofibers 20

The thermogravimetric analysis and corresponding DSC results for pure PAN nanofibers and PAN nanofibers containing nanoparticles are presented in annexes. The results revealed that most of the nanofibers samples decomposed in similar process. As can be seen in Table 5.4, the onset temperatures (T_{Onset} : temperature at which the weight loss begins) of the as-spun nanofibers are related to the type of incorporated nanoparticles. For instance, compared to pure PAN nanofibers, nanofibers containing graphene nanoparticles showed a decrease of the T_{Onset} , which means that graphene nanoparticles did not improve the thermal stability of its resultant nanofibers. However, samples containing copper nanoparticles and silica nanoparticles respectively, showed a slight enhancement of the thermal stability by increasing the T_{Onset} of their nanofibers.

The TGA thermograms of pure PAN nanofibers showed % 77.1636 and % 80.483 of weight loss for samples obtained from 15kV and 20kV as electrospinning voltage, respectively. And their respective residuals were % 22.6765 and % 21.0470 after reaching 900 °C. As can be seen in Table 5.4 (step column), most of weight loss values of composite fibers were less than those of pure PAN fibers. Therefore, their respective residuals values were higher than those of pure PAN fibers after reaching 900 °C. These results confirm the existence of nanoparticles in the as-spun nanofibers.

5.6. Transmission Electron Microscopy

Due to the fact that samples containing nanoparticles presented a higher electron movement during TEM analysis, it was pointed out that it was not possible to conduct an investigation on the nanoparticles diameters found in the electrospun fibers with the current TEM device of the Iltek laboratory. However, the existence of nanoparticles in the electrospun nanofibers were confirmed by the following TEM images.

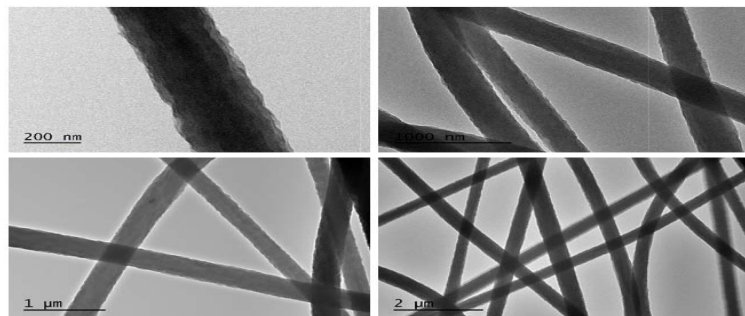


Figure 5. 32. TEM image of pure PAN fibers produced at 15 kV

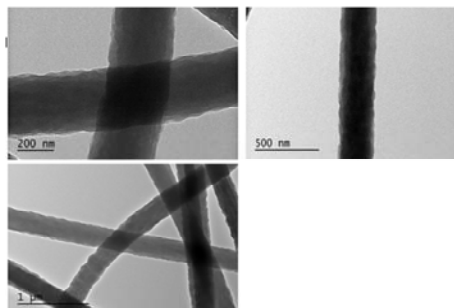


Figure 5.33. TEM image of pure PAN fibers produced at 20 kV

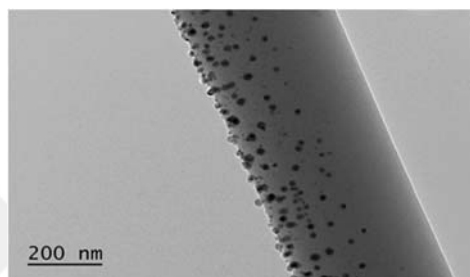


Figure 5.34. TEM image of PAN/DMF/ %1 wt. Copper fibers produced at 20 kV

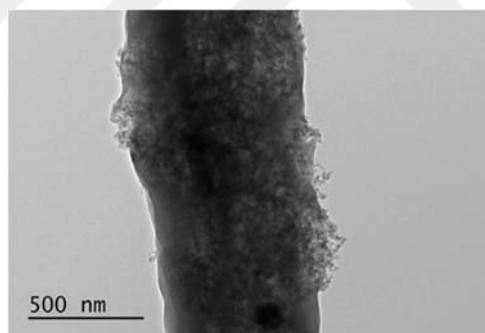


Figure 5.35. TEM image of PAN/DMF/ %3 wt. SiO₂ fibers produced at 15 kV

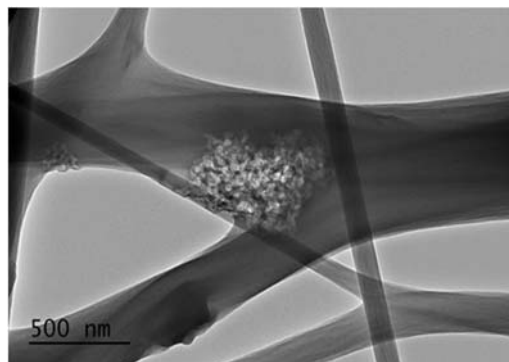


Figure 5.36. TEM image of PAN/DMF/ %1 wt. Graphene fibers produced at 15 kV

6. CONCLUSION AND RECOMMENDATIONS

6.1. Results

As stated in the Introduction, the research was undertaken in order to investigate the effect of the added nanoparticles in the solutions on the electrical conductivity of the as-spun fibers. To do so, in this thesis firstly, different pure PAN nanofibers from 8 to 11 wt. % of PAN concentration range were produced at 15 kV and 20 kV as electrospinning voltage, respectively. The obtained pure PAN fibers were investigated in terms of diameters, morphology and the presence or lack of beads. According to the results of the scanning electron microscopy, all the data indicated that the number of beads in the nanofibers decreased with an increase in PAN concentration. In other words, straight and bead-free fibers with a smooth surface were obtained when the concentration of the PAN polymer in the solution was brought from 8 to 11 wt. %. Referring to the SEM results, the solution containing 9 wt. % of PAN was picked out for the fabrication of composite fibers since its nanofibers were bead-free and in good diameter range compared to others.

Secondly, 1, 3 and 5 wt. % of each type of nanoparticles (copper, graphene or silica) was incorporated in the PAN/ DMF electrospinning solutions, separately. Then, nanofibers containing specific type of nanoparticles were produced at 15 kV and 20 kV as the electrospinning voltages. In addition the dynamic viscosities of the pure PAN, PAN/DMF/Cu, PAN/DMF/Graphene and PAN/DMF/SiO₂ solutions were also investigated. Different results of our investigation are presented below.

The dynamic viscosity of the pure PAN solution (with 9 wt. % of PAN) was 462.5 mPa.s while the those of different solutions containing nanoparticles increased with an increase in concentration. Copper-based solutions led to the highest values for each concentration level (1, 3 and 5 wt. %) compared to both graphene and silica-based solutions. The variation of fibers diameters as a function of their respective viscosities was analyzed. The results demonstrated that copper-based and silica-based solutions led to fibers with a higher diameter when the viscosity of the solutions increased. However, the graphene-based solutions led to fibers with smaller diameters with an increase in the solutions viscosity.

The SEM results revealed that adding copper nanoparticles in the PAN/DMF solutions did not affect negatively the morphology of the as-spun composite fibers.

Taken together, the findings highlighted that increasing the concentration of the copper nanoparticles led to an increase in fibers diameters. However, fibers with smaller diameter were obtained with an increase of the graphene concentration. In addition, adding graphene nanoparticles in the solutions tends to affect the morphology of the resultant fibers. Finally, average diameter of nanofibers containing silica nanoparticles was found to be higher than any other types of composite fibers produced in this thesis. It has been observed that fibers with smaller diameters were obtained at lower silica contents. According to all results highlighted above, we have obtained a comprehensive results showing that the incorporation of nanoparticles in PAN polymer generally affects the morphology and geometry properties of the resultant nanofibers.

Investigation on the electrical conductivity of the as-spun pure PAN fibers and fibers containing nanoparticles has been successfully conducted and the highest values are presented below.

- The pure PAN fibers exhibited electrical conductivity values 5.81×10^{-3} S/cm and 1.63×10^{-3} S/cm for fibers obtained at 15 kV and 20 kV, respectively.
- Copper-based nanofibers exhibited the highest values at 1 wt. % of copper contents. The electrical conductivity values were 1.38×10^{-2} S/cm and 2.83×10^{-2} S/cm for nanofibers produced at 15 kV and 20 kV, respectively.
- Graphene-based nanofibers exhibited the highest values at 1wt. % of silica contents for nanofibers produced at 15 kV and at 5 wt. % for those produced at 20 kV, and their respective electrical conductivity values are 8.85×10^{-3} S/cm and 5.01×10^{-3} S/cm.
- Silica-based nanofibers presented its highest electrical conductivity values at 3 wt. % and 1 wt. % of silica contents for nanofibers produced at 15 kV and 20 kV, respectively. Their respective electrical conductivity values were 8.26×10^{-3} S/cm and 8.11×10^{-3} S/cm.

In general, these results would seem to suggest that the dispersion of a small content of nanoparticles (copper, graphene or silica) in the electrospinning solution could lead to higher values of electrical conductivity of the as-spun fibers. In addition, according to the electrical conductivity values of this thesis, we believe that not only the

amount of nanoparticles contents in the solution could affect the conductivity of the produced fibers but also the applied voltage during the electrospinning process.

Table 6. 1. Increase and decrease in electrical conductivity of composite fibers respect to pure PAN fibers

Composite fibers	Increase and decrease in electrical conductivity (%) of fibers 15 kV	Increase and decrease in electrical conductivity (%) of fibers 20 kV
Pure PAN/DMF	-----	-----
PAN/DMF/ 1wt % SiO ₂	+ 22.2	+397.55
PAN/DMF/ 3wt % SiO ₂	+ 42.16	+265.64
PAN/DMF/ 5wt % SiO ₂	-27.88	+27.6
PAN/DMF/ 1wt % Cu	+137.52	+1636.19
PAN/DMF/ 3wt % Cu	+49.57	+74.85
PAN/DMF/ 5wt % Cu	-23.75	+138.04
PAN/DMF/ 1wt % Gr.	+52.32	+71.16
PAN/DMF/ 3wt % Gr.	-0.52	+61.96
PAN/DMF/ 5wt % Gr	-76.24	+207.36

The effect of fiber diameter on the electrical conductivity was also investigated, the findings slightly differ from an electrospinning voltage to another. Contrary to fibers fabricated at 15 kV, it has been found that those obtained from 20 kV presented the highest values of electrical conductivity at a small diameter.

Another aspect was the effect of the solution viscosity on the conductivity of the as-spun nanofibers. Taken together, higher values of electrical conductivity were obtained with lower solution viscosity. In other words, increasing solution viscosity trends to decrease the electrical conductivity of the fibers.

The hydrophobicity of the fibers with highest electrical conductivity was analyzed and compared to that of their respective pure PAN nanofibers. The results revealed that the hydrophilicity of graphene-based nanofibers surface increases with the amount of graphene nanoparticles in the electrospinning solution. The static contact angles were 131.96° and 33.27° for 1 wt. % at 15 kV and 5 wt. % at 20 kV, respectively.

The study showed that the incorporation of silica nanoparticles in the electrospinning solution led to an increase of contact angle values of the electrospun nanofibers. Notably, from 115.3° for pure PAN to 125.42° for 1 wt. % at 20 kV and from 120.18° for pure PAN to 123.06° for 3 wt. % at 20 kV. The same hydrophobic behavior was observed for copper-based nanofibers. An slight enhancement of hydrophobicity was observed by adding 1 wt. % of copper. Values were 120.18° for

pure PAN to 124.93° and from 115.3° for pure PAN to 125.93° for nanofibers fabricated at 15 kV and 20 kV as applied voltage, respectively.

The presence of nanoparticles in the fibers was confirmed by XRD investigation. In most cases, the existence of nanoparticles in the as-spun fibers was observed in terms of peaks variation, since most of the nanofibers analyzed had a low nanoparticles content.

Thermal stability of pure PAN nanofibers and PAN composite fibers was investigated using TGA and DSC, generally speaking it was found that pure PAN fibers, PAN/DMF/Cu and PAN/DMF/ SiO₂ started to decompose at 291.27 °C, 292.53 °C and 298.11 °C, respectively. However, fibers containing graphene nanoparticles started to decompose at 253.98 °C and its thermal stability was affected negatively compared to pure PAN fibers.

6.2. Recommendations

The findings suggest the following opportunities for future research:

- Investigation of the effect of different electrospinning voltages on the electrical conductivity of fibers containing nanoparticles,
- Electrical conductivity of carbonized PAN fibers containing nanoparticles (copper, silica or graphene),
- Hydrophobicity of the as-spun PAN fibers containing different graphene nanoparticles contents,
- Thermal stability of electrospun PAN fibers containing different graphene nanoparticles contents.

REFERENCES

- Alarifi, I. M., Alharbi, A., Khan, W. S., Swindle, A. and Asmatulu, R., 2015, Thermal, electrical and surface hydrophobic properties of electrospun polyacrylonitrile nanofibers for structural health monitoring, *Materials*, 8 (10), 7017-7031.
- Bai, J., Li, Y., Li, M., Wang, S., Zhang, C. and Yang, Q., 2008, Electrospinning method for the preparation of silver chloride nanoparticles in PVP nanofiber, *Applied Surface Science*, 254 (15), 4520-4523.
- Baumgarten, P. K., 1971, Electrostatic spinning of acrylic microfibers, *Journal of colloid and interface science*, 36 (1), 71-79.
- Bhardwaj, N. and Kundu, S. C., 2010, Electrospinning: a fascinating fiber fabrication technique, *Biotechnology advances*, 28 (3), 325-347.
- Buchko, C. J., Chen, L. C., Shen, Y. and Martin, D. C., 1999, Processing and microstructural characterization of porous biocompatible protein polymer thin films, *Polymer*, 40 (26), 7397-7407.
- Casper, C. L., Stephens, J. S., Tassi, N. G., Chase, D. B. and Rabolt, J. F., 2004, Controlling surface morphology of electrospun polystyrene fibers: effect of humidity and molecular weight in the electrospinning process, *Macromolecules*, 37 (2), 573-578.
- Cavaliere, S., 2015, Electrospinning for advanced energy and environmental applications, CRC Press, p.
- Cramariuc, B., Cramariuc, R., Scarlet, R., Manea, L. R., Lupu, I. G. and Cramariuc, O., 2013, Fiber diameter in electrospinning process, *Journal of Electrostatics*, 71 (3), 189-198.
- Deitzel, J. M., Kleinmeyer, J., Harris, D. and Tan, N. B., 2001, The effect of processing variables on the morphology of electrospun nanofibers and textiles, *Polymer*, 42 (1), 261-272.
- Demir, M. M., Yilgor, I., Yilgor, E. and Erman, B., 2002, Electrospinning of polyurethane fibers, *Polymer*, 43 (11), 3303-3309.
- Demirsoy, N., Nuray, U., Aysen, O. and KIZILDAG, N., 2015, Nanocomposite Nanofibers of Polyacrylonitrile (PAN) and Silver Nanoparticles (AgNPs) Electrospun from Dimethylsulfoxide, *Marmara Fen Bilimleri Dergisi*, 27, 16-18.
- Ding, B. and Yu, J., 2014, Electrospun nanofibers for energy and environmental applications, Springer Science & Business Media, p.
- Dong, J., Yao, Z., Yang, T., Jiang, L. and Shen, C., 2013, Control of superhydrophilic and superhydrophobic graphene interface, *Scientific reports*, 3.
- Doshi, J. and Reneker, D. H., 1995, Electrospinning process and applications of electrospun fibers, *Journal of Electrostatics*, 35 (2-3), 151-160.
- Dung, N. V., Le, D. T. T., Trung, N. D., Dung, H. N., Hung, N. M., Duy, N. V., Hoa, N. D. and Hieu, N. V., 2016, CuO Nanofibers Prepared by Electrospinning for Gas Sensing Application: Effect of Copper Salt Concentration, *Journal of Nanoscience and Nanotechnology*, 16 (8), 7910-7918.
- Fong, H., Chun, I. and Reneker, D., 1999, Beaded nanofibers formed during electrospinning, *Polymer*, 40 (16), 4585-4592.
- Frenot, A. and Chronakis, I. S., 2003, Polymer nanofibers assembled by electrospinning, *Current opinion in colloid & interface science*, 8 (1), 64-75.
- Groszek, A. and Partyka, S., 1993, Measurements of hydrophobic and hydrophilic surface sites by flow microcalorimetry, *Langmuir*, 9 (10), 2721-2725.

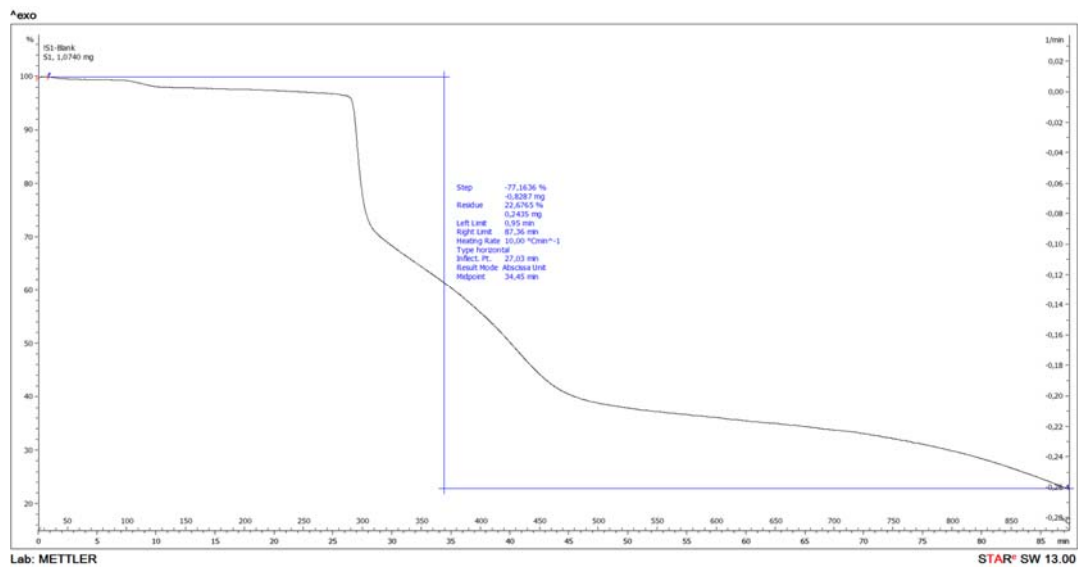
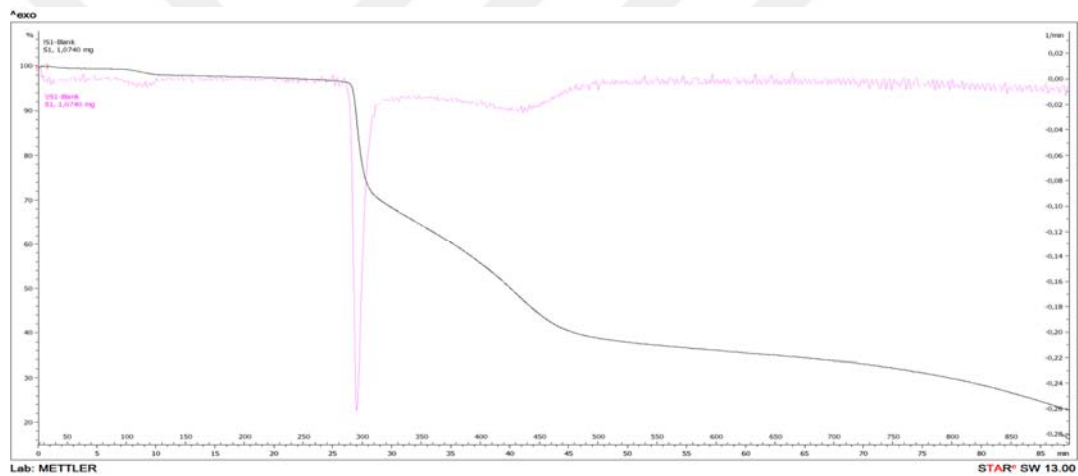
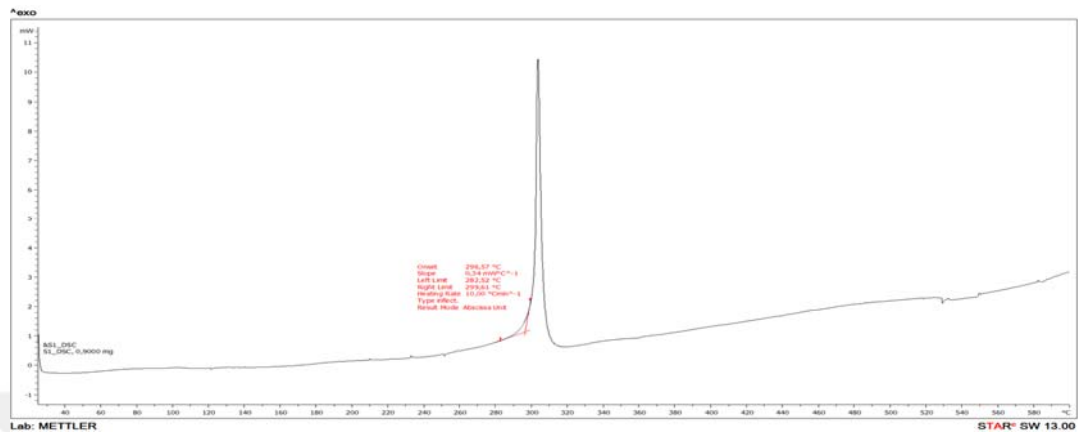
- Guclu, S., Pasaoglu, M. E. and Koyuncu, I., 2016, Membrane manufacturing via simultaneous electrospinning of PAN and PSU solutions, *Desalination and Water Treatment*, 57 (18), 8152-8160.
- Gupta, A., Paliwal, D. and Bajaj, P., 1998, Melting behavior of acrylonitrile polymers, *Journal of applied polymer science*, 70 (13), 2703-2709.
- Haghi, A., 2011, *Electrospinning of Nanofibers in Textiles*, CRC Press, p.
- Heikkilä, P. and Harlin, A., 2009, Electrospinning of polyacrylonitrile (PAN) solution: Effect of conductive additive and filler on the process, *Express Polymer Letters*, 3 (7), 437-445.
- Huang, Z.-M., Zhang, Y.-Z., Kotaki, M. and Ramakrishna, S., 2003, A review on polymer nanofibers by electrospinning and their applications in nanocomposites, *Composites science and technology*, 63 (15), 2223-2253.
- Jaeger, R., Schönherr, H. and Vancso, G. J., 1996, Chain packing in electro-spun poly (ethylene oxide) visualized by atomic force microscopy, *Macromolecules*, 29 (23), 7634-7636.
- Jeong, L. and Park, W. H., 2014, Preparation and characterization of gelatin nanofibers containing silver nanoparticles, *International journal of molecular sciences*, 15 (4), 6857-6879.
- Ji, L., Saquing, C., Khan, S. A. and Zhang, X., 2008, Preparation and characterization of silica nanoparticulate-polyacrylonitrile composite and porous nanofibers, *Nanotechnology*, 19 (8), 085605.
- Ji, L. and Zhang, X., 2008, Ultrafine polyacrylonitrile/silica composite fibers via electrospinning, *Materials Letters*, 62 (14), 2161-2164.
- Karakaş, H., 2015, *Electrospinning of Nanofibers and Their Applications*, Istanbul Technical University, Textile Technologies and Design Faculty.
- Khan, W., Ceylan, M., Jabarrania, A., Saeednia, L. and Asmatulu, R., 2017, Chemical And Thermal Investigations Of Electrospun Polyacrylonitrile Nanofibers Incorporated With Various Nanoscale Inclusions, *Journal Of Thermal Engineering*, 3 (4), 1374-1389.
- Kim, C., Kim, J.-S., Lee, W.-J., Kim, H.-S., Edie, D. D. and Yang, K.-S., 2002, Preparations of PAN-based Activated Carbon Nanofiber Web Electrode by Electrostatic Spinning and Their Applications to EDLC, *Journal of the Korean Electrochemical Society*, 5 (3), 117-124.
- Koski, A., Yim, K. and Shivkumar, S., 2004, Effect of molecular weight on fibrous PVA produced by electrospinning, *Materials Letters*, 58 (3), 493-497.
- Lafuma, A. and Quéré, D., 2003, Superhydrophobic states, *Nature materials*, 2 (7), 457-460.
- Levitt, A. S., Knittel, C. E., Vallett, R., Koerner, M., Dion, G. and Schauer, C. L., 2017, Investigation of nanoyarn preparation by modified electrospinning setup, *Journal of applied polymer science*, 134 (19).
- Liang, H., Li, C., Bai, J., Zhang, L., Guo, L. and Huang, Y., 2013, Synthesis and characterization of AgI nanoparticles in β -CD/PAN nanofibers by electrospinning method, *Applied Surface Science*, 270, 617-620.
- Liu, H. and Hsieh, Y. L., 2002, Ultrafine fibrous cellulose membranes from electrospinning of cellulose acetate, *Journal of Polymer Science Part B: Polymer Physics*, 40 (18), 2119-2129.
- Luo, C., Nangrejo, M. and Edirisinghe, M., 2010, A novel method of selecting solvents for polymer electrospinning, *Polymer*, 51 (7), 1654-1662.
- Luo, Z., 2015, *A Practical Guide to Transmission Electron Microscopy: Fundamentals*, Momentum Press, p.

- Megelski, S., Stephens, J. S., Chase, D. B. and Rabolt, J. F., 2002, Micro- and nanostructured surface morphology on electrospun polymer fibers, *Macromolecules*, 35 (22), 8456-8466.
- Min, B.-M., Lee, G., Kim, S. H., Nam, Y. S., Lee, T. S. and Park, W. H., 2004, Electrospinning of silk fibroin nanofibers and its effect on the adhesion and spreading of normal human keratinocytes and fibroblasts in vitro, *Biomaterials*, 25 (7), 1289-1297.
- Mittal, K. L., 2006, Contact angle, wettability and adhesion, CRC Press, p.
- Mo, X., Xu, C., Kotaki, M. and Ramakrishna, S., 2004, Electrospun P (LLA-CL) nanofiber: a biomimetic extracellular matrix for smooth muscle cell and endothelial cell proliferation, *Biomaterials*, 25 (10), 1883-1890.
- Norris, I. D., Shaker, M. M., Ko, F. K. and MacDiarmid, A. G., 2000, Electrostatic fabrication of ultrafine conducting fibers: polyaniline/polyethylene oxide blends, *Synthetic metals*, 114 (2), 109-114.
- Nuraje, N., Khan, W. S., Lei, Y., Ceylan, M. and Asmatulu, R., 2013, Superhydrophobic electrospun nanofibers, *Journal of Materials Chemistry A*, 1 (6), 1929-1946.
- Panapoy, M., Dankeaw, A. and Ksapabutr, B., 2008, Electrical conductivity of PAN-based carbon nanofibers prepared by electrospinning method, *Thammasat Int J Sc Tech*, 13, 11-17.
- Pant, H. R., Nam, K.-T., Oh, H.-J., Panthi, G., Kim, H.-D., Kim, B.-i. and Kim, H. Y., 2011, Effect of polymer molecular weight on the fiber morphology of electrospun mats, *Journal of colloid and interface science*, 364 (1), 107-111.
- Ra, E. J., An, K. H., Kim, K. K., Jeong, S. Y. and Lee, Y. H., 2005, Anisotropic electrical conductivity of MWCNT/PAN nanofiber paper, *Chemical Physics Letters*, 413 (1), 188-193.
- Ráčová, Z., Ryparová, P., Hlaváč, R., Tesárek, P. and Nežerka, V., 2014, Influence of copper ions on mechanical properties of PVA-based nanofiber textiles, *Applied Mechanics and Materials*, 201-204.
- Ramakrishna, S., 2005, An introduction to electrospinning and nanofibers, World Scientific, p.
- Rezaee, S. and Moghbeli, M., 2014, Crosslinked Electrospun Poly (Vinyl Alcohol) Nanofibers Coated by Antibacterial Copper Nanoparticles, *Iranian Journal of Chemical Engineering*, 11 (3).
- Robinson, J. W., Frame, E. S. and Frame II, G. M., 2014, Undergraduate instrumental analysis, CRC Press, p.
- Rujitanaroj, P. o., Pimpha, N. and Supaphol, P., 2010, Preparation, characterization, and antibacterial properties of electrospun polyacrylonitrile fibrous membranes containing silver nanoparticles, *Journal of applied polymer science*, 116 (4), 1967-1976.
- Rutledge, G. C., Li, Y., Fridrikh, S., Warner, S., Kalayci, V. and Patra, P., 2000, Electrostatic spinning and properties of ultrafine fibers, *National Textile Center, Technical Report (M98-D01)*.
- Savest, N., Plamus, T., Tarasova, E., Viirsalu, M., Krasnou, I., Gudkova, V., Küppar, K.-A. and Krumme, A., 2016, The effect of ionic liquids on the conductivity of electrospun polyacrylonitrile membranes, *Journal of Electrostatics*, 83, 63-68.
- Sichani, G. N., Morshed, M., Amirnasr, M. and Abedi, D., 2010, In situ preparation, electrospinning, and characterization of polyacrylonitrile nanofibers containing silver nanoparticles, *Journal of applied polymer science*, 116 (2), 1021-1029.

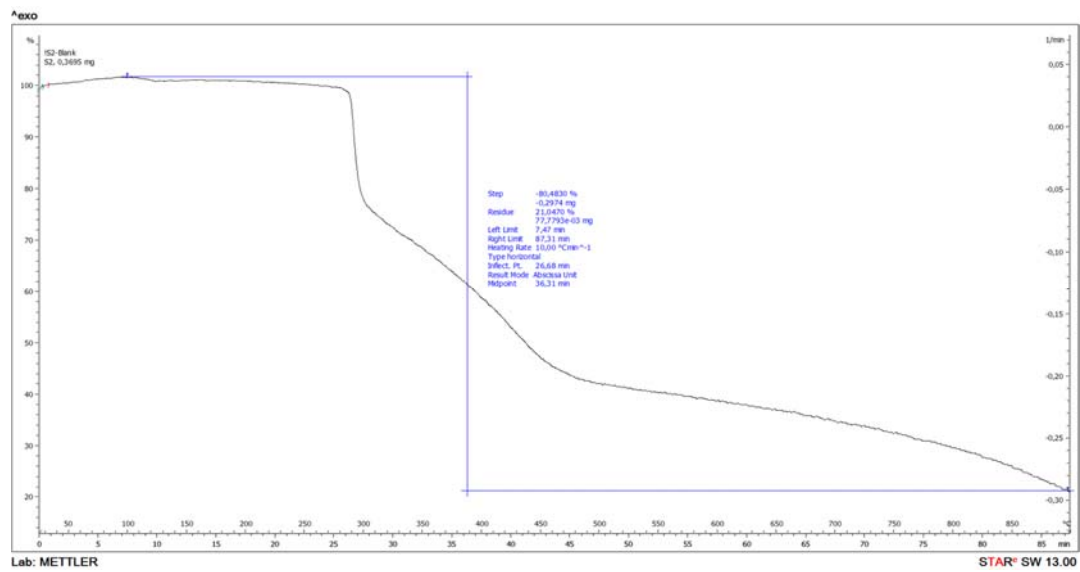
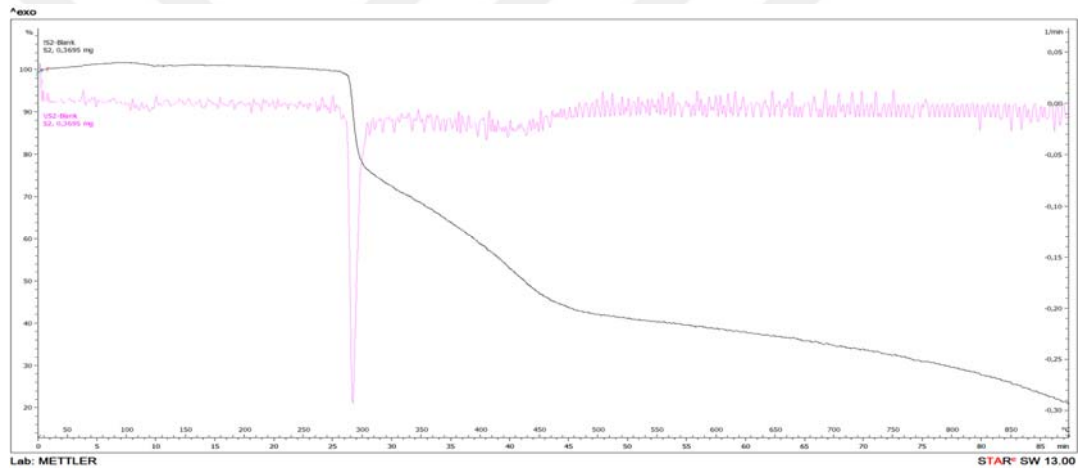
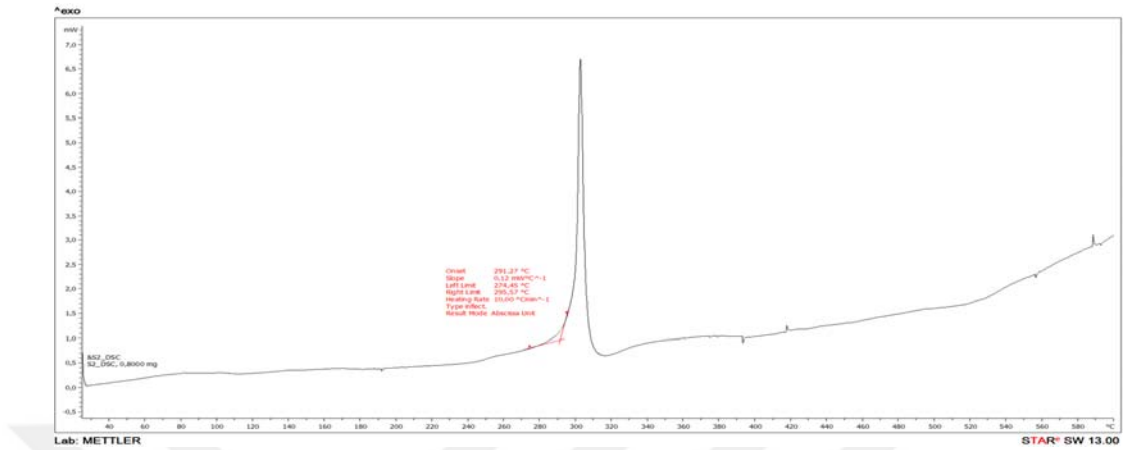
- Stankovich, S., Dikin, D. A., Dommett, G. H., Kohlhaas, K. M., Zimney, E. J., Stach, E. A., Piner, R. D., Nguyen, S. T. and Ruoff, R. S., 2006, Graphene-based composite materials, *nature*, 442 (7100), 282-286.
- Sundaray, B., Choi, A. and Park, Y. W., 2010, Highly conducting electrospun polyaniline-polyethylene oxide nanofibrous membranes filled with single-walled carbon nanotubes, *Synthetic metals*, 160 (9), 984-988.
- Tai, M. H., Tan, B. Y. L., Juay, J., Sun, D. D. and Leckie, J. O., 2015, A Self-Assembled Superhydrophobic Electrospun Carbon-Silica Nanofiber Sponge for Selective Removal and Recovery of Oils and Organic Solvents, *Chemistry-A European Journal*, 21 (14), 5395-5402.
- Tański, T., Matysiak, W. and Hajduk, B., 2016, Manufacturing and investigation of physical properties of polyacrylonitrile nanofibre composites with SiO₂, TiO₂ and Bi₂O₃ nanoparticles, *Beilstein journal of nanotechnology*, 7, 1141.
- Tapasztó, O., Tapasztó, L., Marko, M., Kern, F., Gadov, D. and Balázs, C., 2011, Dispersion patterns of graphene and carbon nanotubes in ceramic matrix composites, p.
- Wannatong, L., Sirivat, A. and Supaphol, P., 2004, Effects of solvents on electrospun polymeric fibers: preliminary study on polystyrene, *Polymer International*, 53 (11), 1851-1859.
- Yang, Q., Li, Z., Hong, Y., Zhao, Y., Qiu, S., Wang, C. and Wei, Y., 2004, Influence of solvents on the formation of ultrathin uniform poly (vinyl pyrrolidone) nanofibers with electrospinning, *Journal of Polymer Science Part B: Polymer Physics*, 42 (20), 3721-3726.
- Yu, Q.-Z., Shi, M.-M., Deng, M., Wang, M. and Chen, H.-Z., 2008, Morphology and conductivity of polyaniline sub-micron fibers prepared by electrospinning, *Materials Science and Engineering: B*, 150 (1), 70-76.
- Yu, X., Xiang, H., Long, Y., Zhao, N., Zhang, X. and Xu, J., 2010, Preparation of porous polyacrylonitrile fibers by electrospinning a ternary system of PAN/DMF/H₂O, *Materials Letters*, 64 (22), 2407-2409.
- Yuan, X., Zhang, Y., Dong, C. and Sheng, J., 2004, Morphology of ultrafine polysulfone fibers prepared by electrospinning, *Polymer International*, 53 (11), 1704-1710.
- Yuan, Y. and Lee, T. R., 2013, Contact angle and wetting properties, In: *Surface science techniques*, Eds: Springer, p. 3-34.
- Zamri, M., Zein, S. H. S., Abdullah, A. Z. and Basir, N. I., 2011, Improved electrical conductivity of polyvinyl alcohol/multiwalled carbon nanotube nanofibre composite films with MnO₂ as filler synthesised using the electrospinning process, *International Journal of Engineering & Technology IJET-IJENS*, 11 (06).
- Zhang, D., Karki, A. B., Rutman, D., Young, D. P., Wang, A., Cocke, D., Ho, T. H. and Guo, Z., 2009, Electrospun polyacrylonitrile nanocomposite fibers reinforced with Fe₃O₄ nanoparticles: fabrication and property analysis, *Polymer*, 50 (17), 4189-4198.
- Zhang, F., Zhang, Z., Liu, Y. and Leng, J., 2014, Electrospun nanofiber membranes for electrically activated shape memory nanocomposites, *Smart Materials and Structures*, 23 (6), 065020.
- Zhang, Y. and Rutledge, G. C., 2012, Electrical conductivity of electrospun polyaniline and polyaniline-blend fibers and mats, *Macromolecules*, 45 (10), 4238-4246.
- Zussman, E., Chen, X., Ding, W., Calabri, L., Dikin, D., Quintana, J. and Ruoff, R., 2005, Mechanical and structural characterization of electrospun PAN-derived carbon nanofibers, *Carbon*, 43 (10), 2175-2185.

ANNEXES

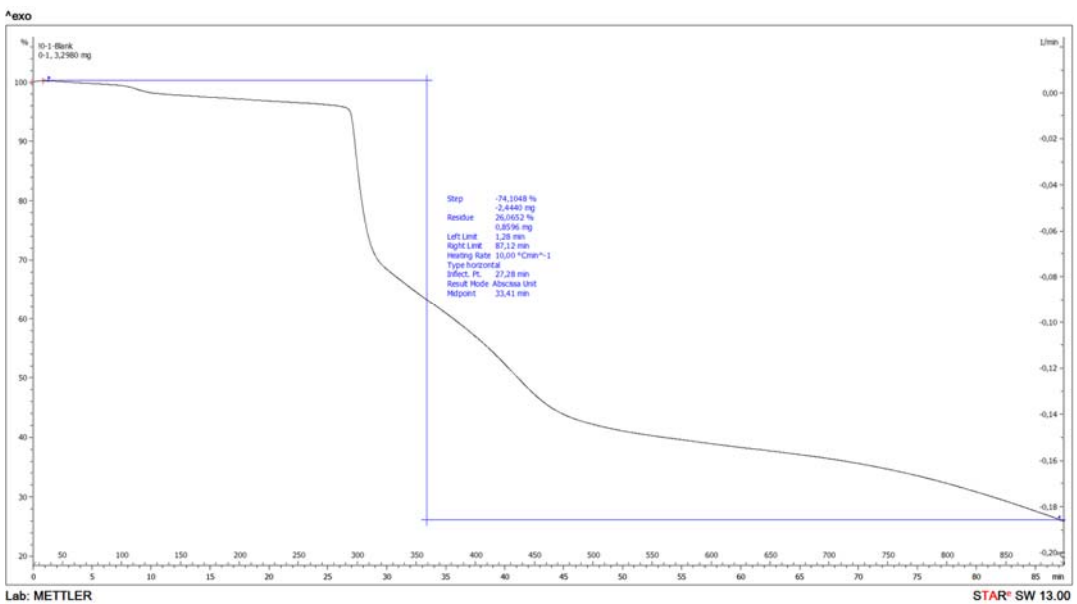
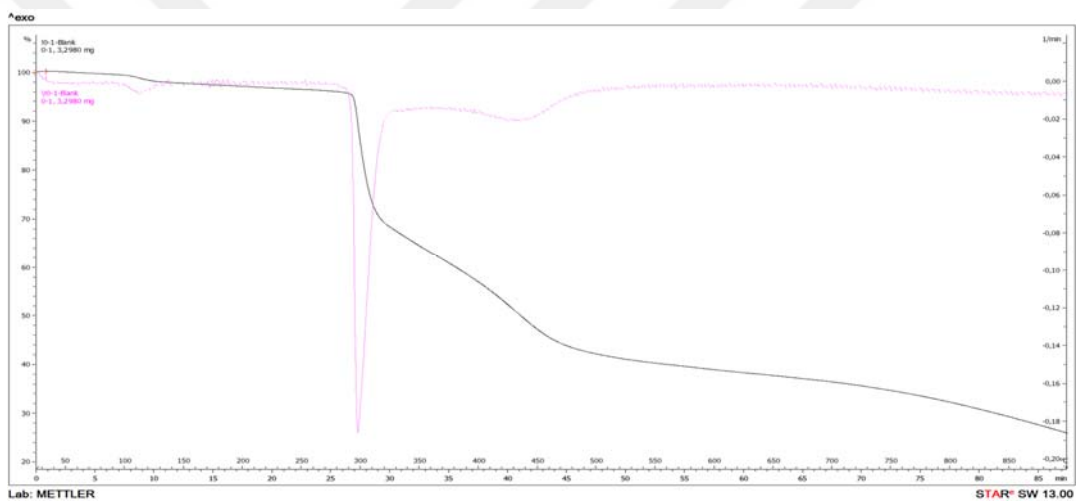
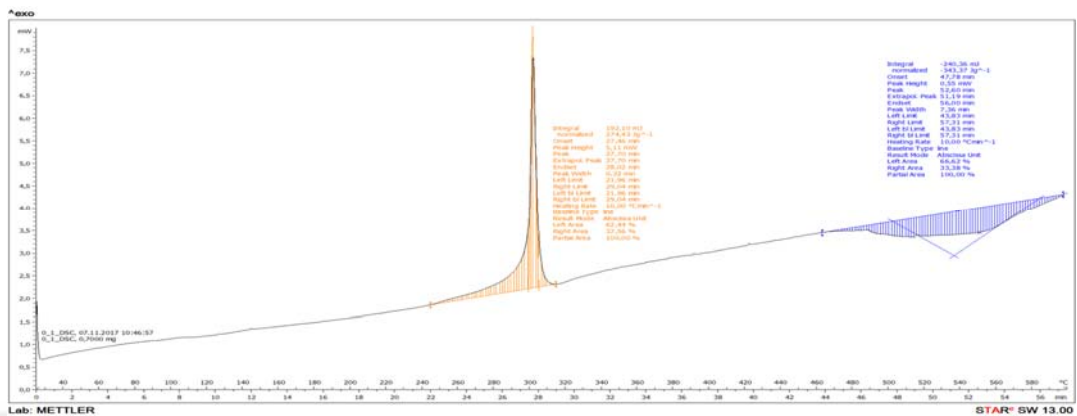
Annex-1 TGA+DTA+ DSC of Pure PAN (15kV)



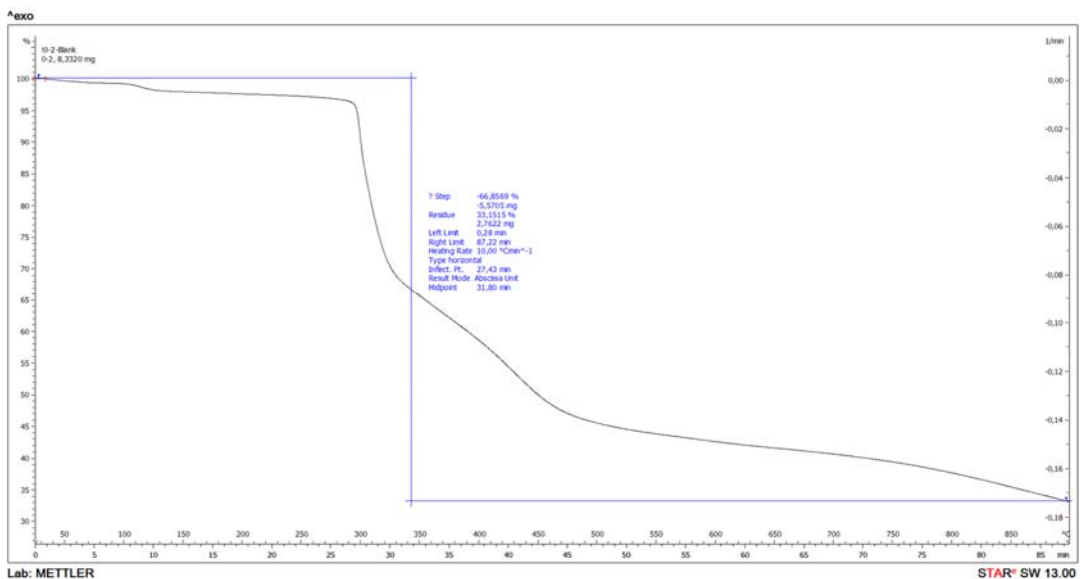
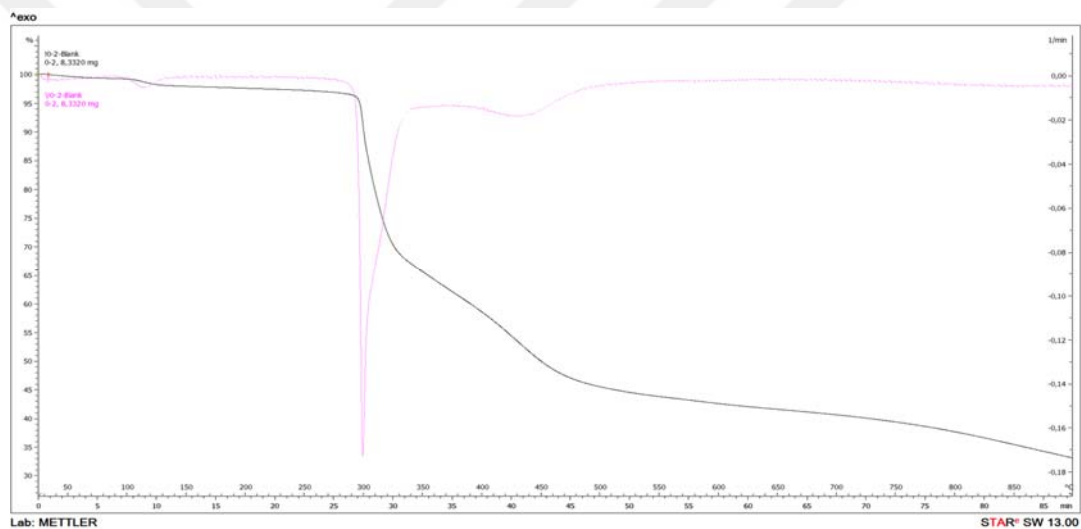
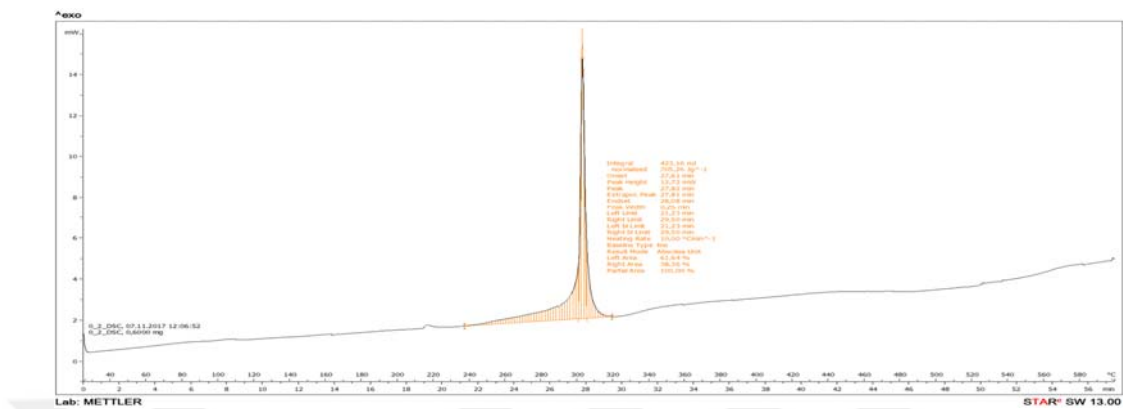
Annex-2 TGA+DTA+ DSC of Pure PAN (20 kV)



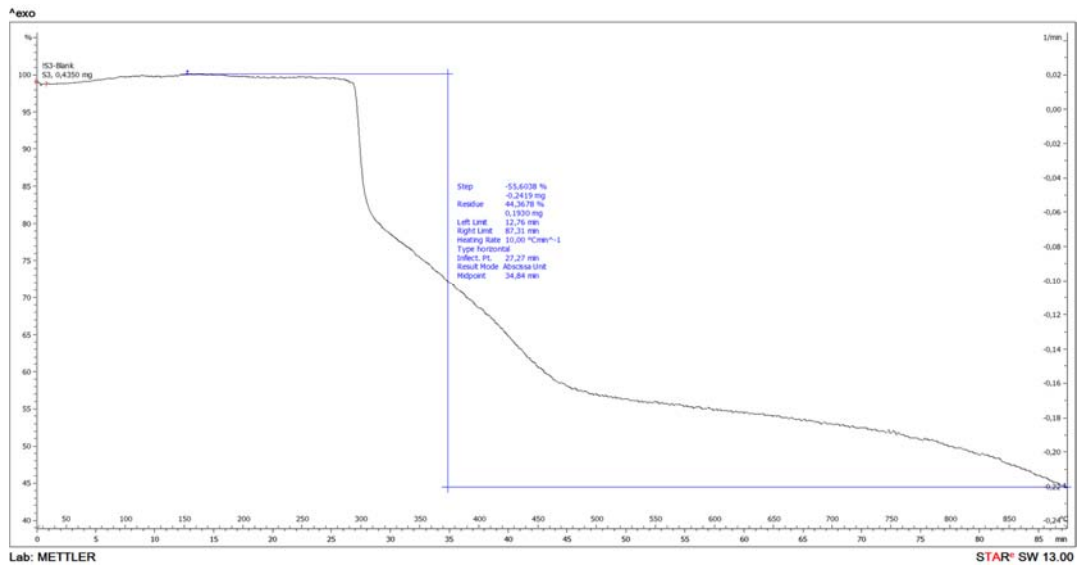
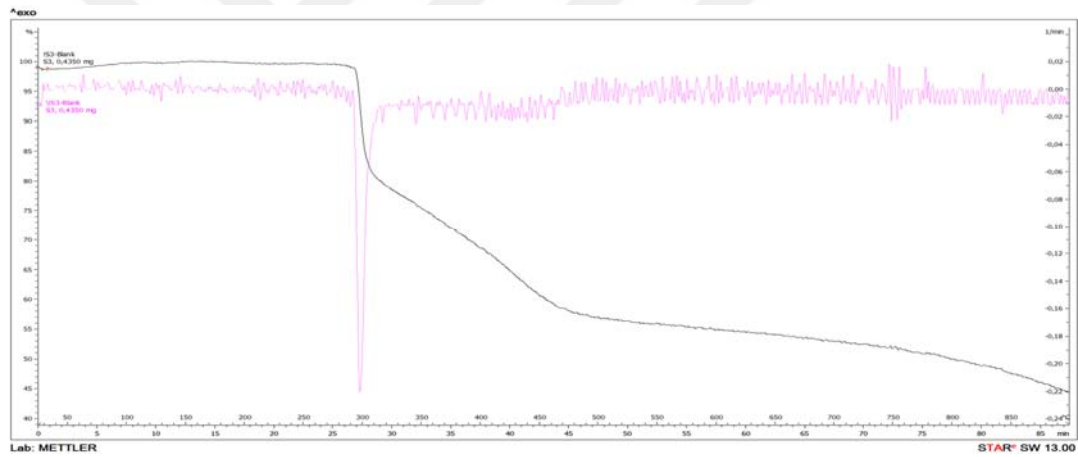
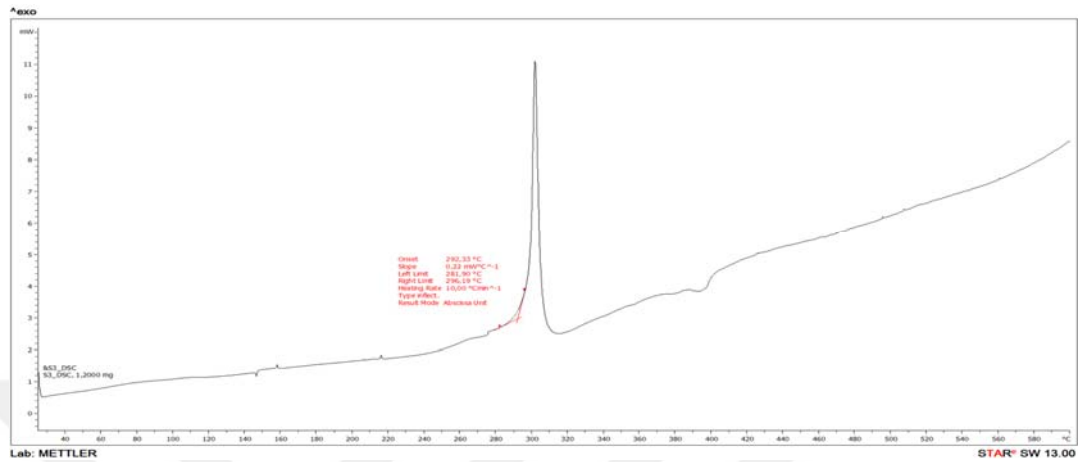
Annex-3 TGA+DTA+ DSC of PAN/DMF/Cu (15 kV)



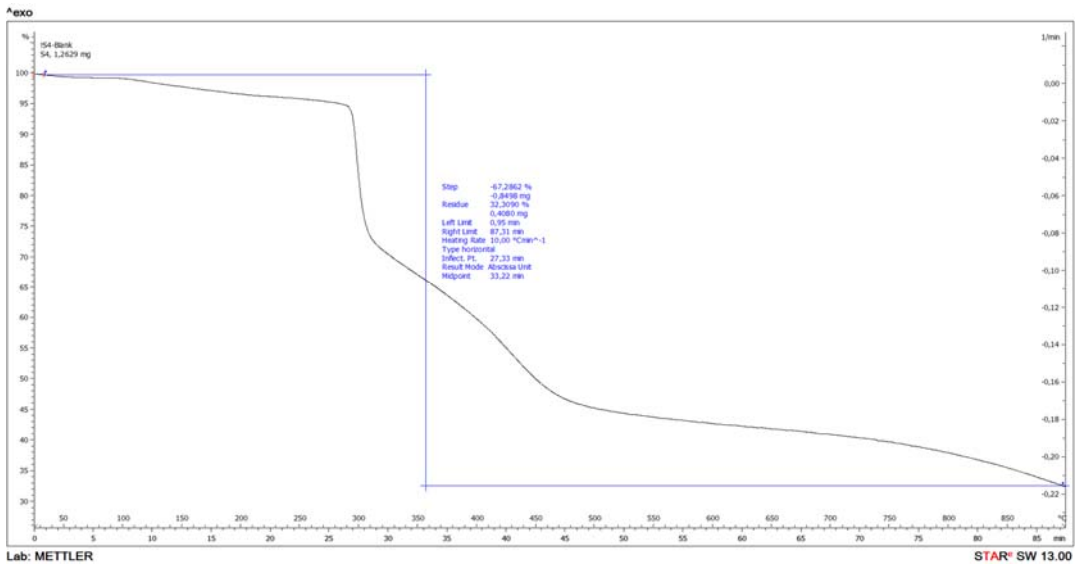
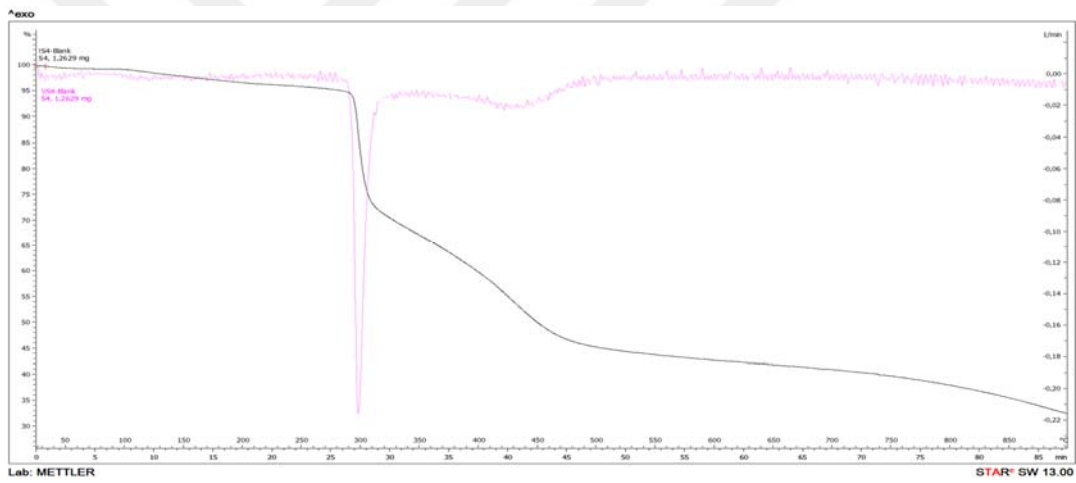
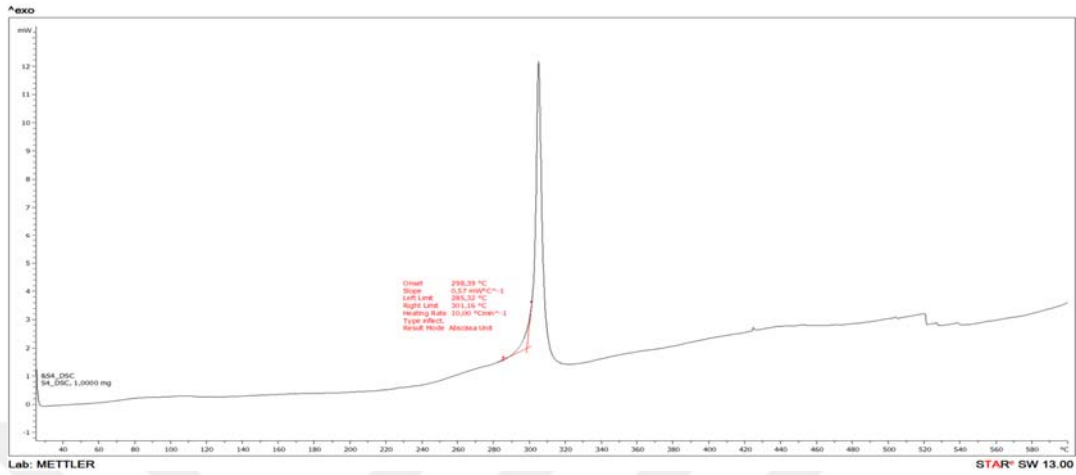
Annex-4 TGA+DTA+ DSC of PAN/DMF/Cu (20 kV)



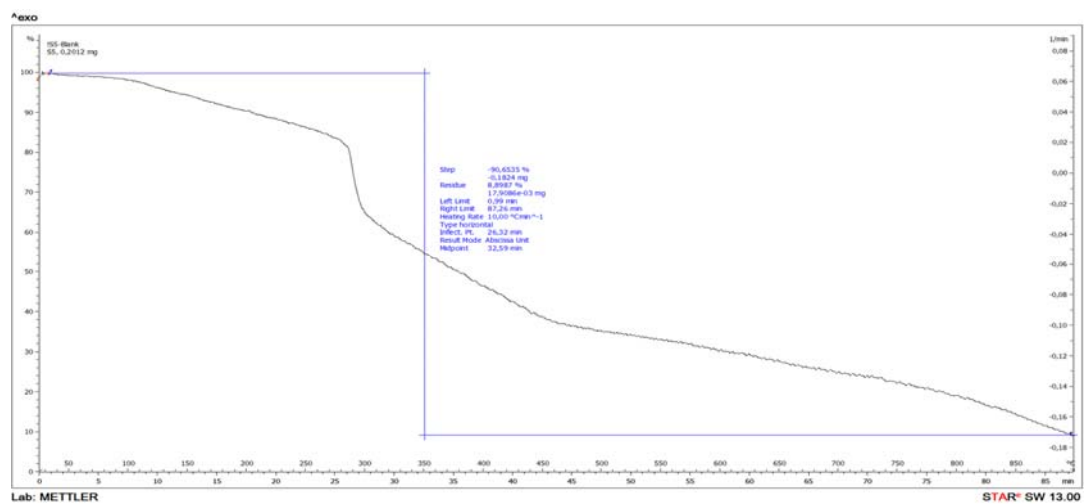
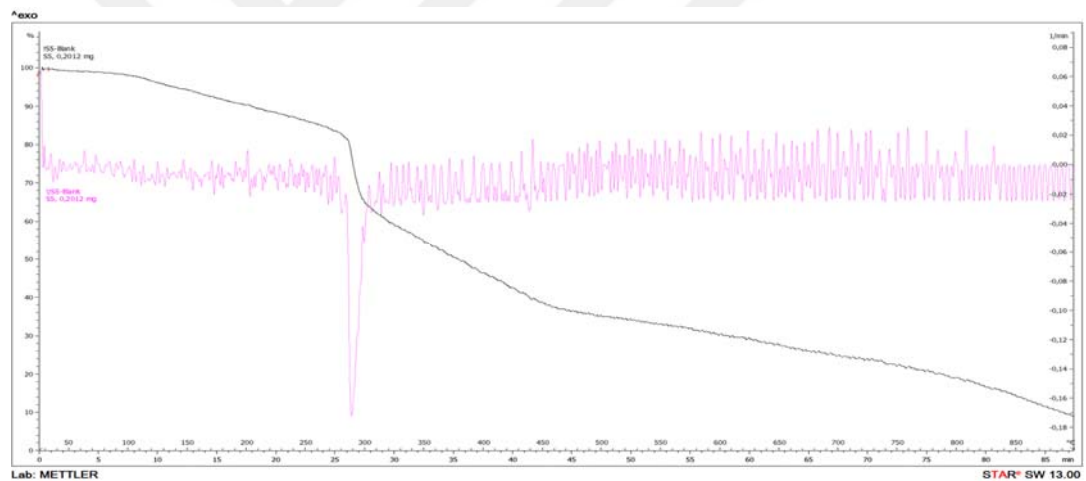
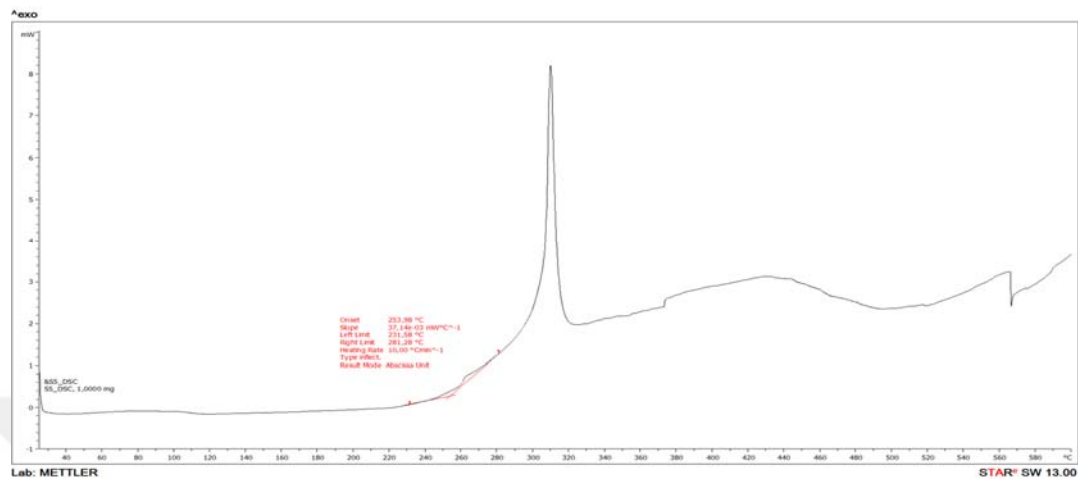
Annex-5 TGA+DTA+ DSC of PAN/DMF/SiO₂ (15 kV)



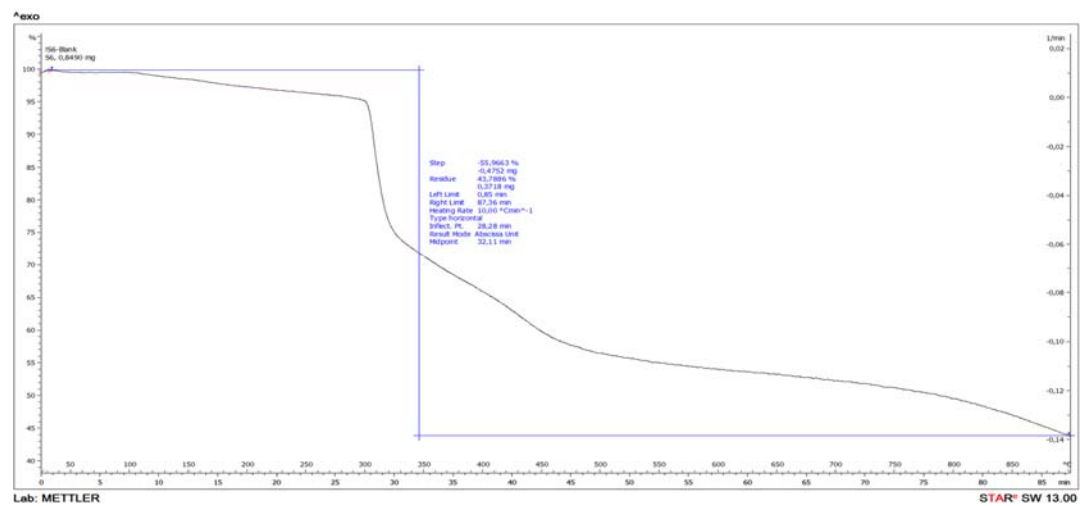
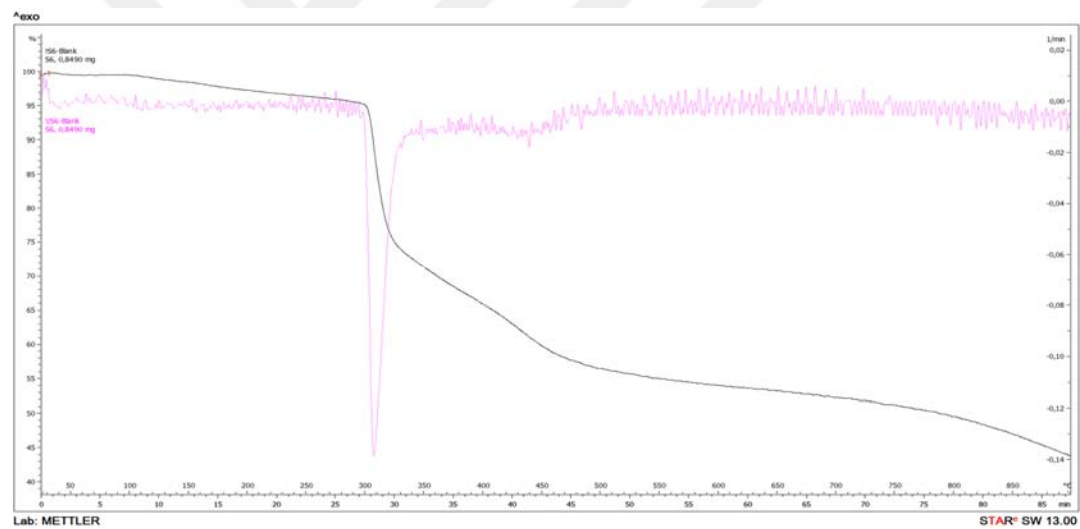
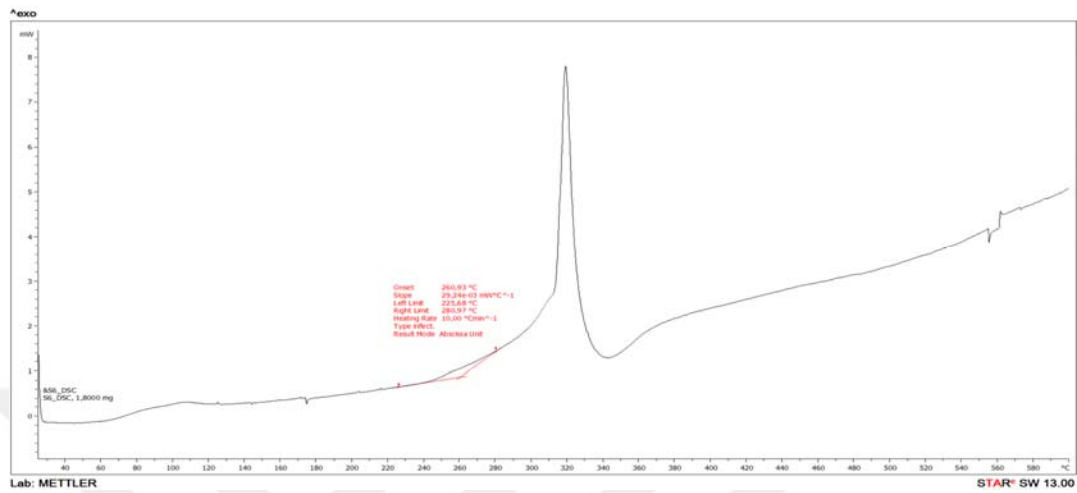
Annex-6 TGA+DTA+ DSC of PAN/DMF/SiO₂ (20 kV)



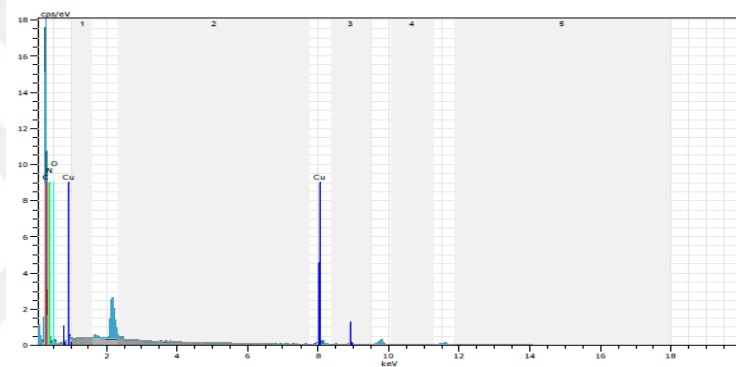
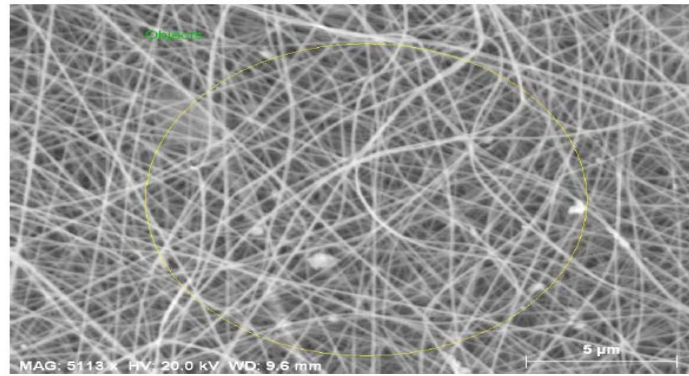
Annex-7 TGA+DTA+ DSC of PAN/DMF/Graphene (15 kV)



Annex-8 TGA+DTA+ DSC of PAN/DMF/Graphene (20 kV)



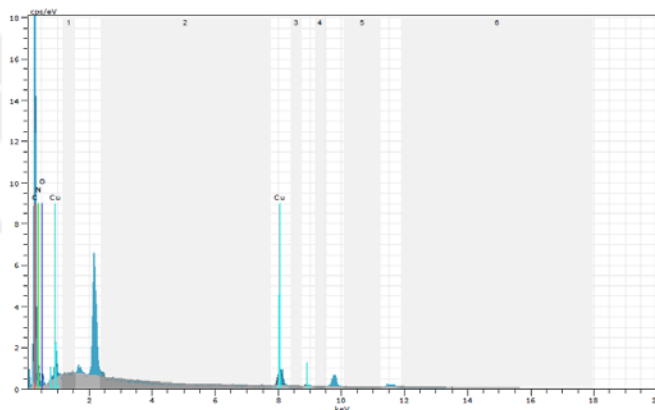
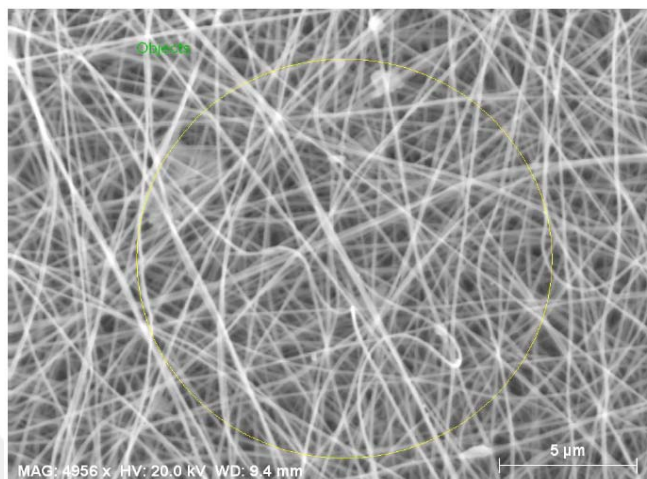
Annex-9 Energy Dispersive X-ray (EDX) of PAN/DMF/ %1wt. Copper (20 kV)



Spectrum: Objects

Element	Series	unn. C [wt.%]	norm. C [wt.%]	Atom. C [at.%]	Error [%]
Carbon	K-series	52.20	52.21	57.37	16.5
Nitrogen	K-series	34.15	34.15	32.18	12.9
Copper	K-series	1.31	1.31	0.27	0.1
Oxygen	K-series	12.34	12.34	10.18	5.2
Total:		100.00	100.00	100.00	

Annex-10 Energy Dispersive X-ray (EDX) of PAN/DMF/ % 3wt. Copper (20 kV)



Spectrum: Objects

Element	Series	unn. C [wt.%]	norm. C [wt.%]	Atom. C [at.%]	Error [%]
Carbon	K-series	48.26	48.26	54.15	15.3
Nitrogen	K-series	32.47	32.47	31.24	12.3
Oxygen	K-series	16.70	16.70	14.07	6.7
Copper	K-series	2.56	2.56	0.54	0.1
Total:		100.00	100.00	100.00	

CURRICULUM VITAE

Personal information

Name and Surname : Olivier Mukongo MPUKUTA
 Nationality : Congolese (DR Congo)
 E-mail : oliviermpukuta@gmail.com

Education

Degree	Name , City, province	Year of graduation
High school	: Institut de la Gombe, Kinshasa	2003
University	: University of Kinshasa	2010
M.Sc.	: Selcuk University	

Experience

Year	Institution	Tasks
2014	Total DRC	Maintenance Engineer
2013	UKV University	Research Assistant
2010	Sep - Congo	Projector Engineer

Profession: Mechanical Engineer

Foreign Languages: English, French, Turkish

Computer skills and MOOC courses: MS word, MS Excel, MS project, Outlook, Sigmplot, ImageJ, Epanet, SAP, AutoCAD, SolidWorks, Tekla Structures, Introduction to project management, Leadership, Industrial Maintenance (Minimaint), HSEQ and so on.

Papers and Congress Presentation:

Investigation of Electrical Conductivity of PAN Nanofibers Containing Silica Nanoparticles Produced by Electrospinning, O.M. Mpukuta, K. Dincer, M. O. Erdal; Materials Today (accepted).

Electrical Conductivity of Electrospun Polyacrylonitrile (PAN) fibers containing copper nanoparticles (CuNPs), Olivier M. Mpukuta, Kevser Dincer, Ilkay Özyaytekin; Applied Energy (Submitted).

Investigation of Electrical Conductivity of PAN Nanofibers Containing Silica Nanoparticles Produced by Electrospinning, O.M. Mpukuta, K. Dincer, M. O. Erdal, International Congress on Semiconductor Materials and Devices, Oral presentation. 17-19.08.2017.

Other Useful Information:

Bachelor in polytechnic faculty, especially in mechanical engineering. My skills are proven in research project areas, Computer aided design and simulation of mechanical structures, industrial mechanics, project management, maintenance of machines and in the field of scientific and industrial researches.